



the
abdus salam
international centre for theoretical physics

40th anniversary
1964
2004

H4.SMR/1586-13

**"7th Workshop on Three-Dimensional Modelling
of Seismic Waves Generation and their Propagation"**

25 October - 5 November 2004

GLOBAL SEISMOLOGY

**From Normal Modes to Surface and Body Waves
Application to Anisotropic Tomography**

*J.P. Montagner
Dept. Sismologie
I.P.G.
Paris, France*



Global Seismology

From normal modes to surface waves and body waves

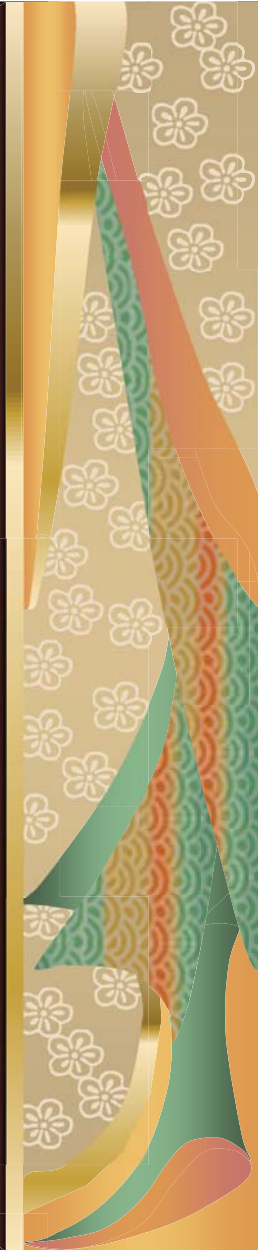
Jean-Paul Montagner

Dept. Sismologie, I.P.G., Paris; France

Overview

Large scale Seismology: an observational field

- Data (Seismic source) + Instrument (Seismometer) -> Observations (seismograms)
- Historical evolution: Ray theory, Normal mode theory, Numerical techniques (SEM, NM-SEM)
- Scientific Issues: earthquakes, structure of the Earth and planets
- Tomographic Technique
- Seismic Experiment: Plume detection
- NM-SEM and time reversal

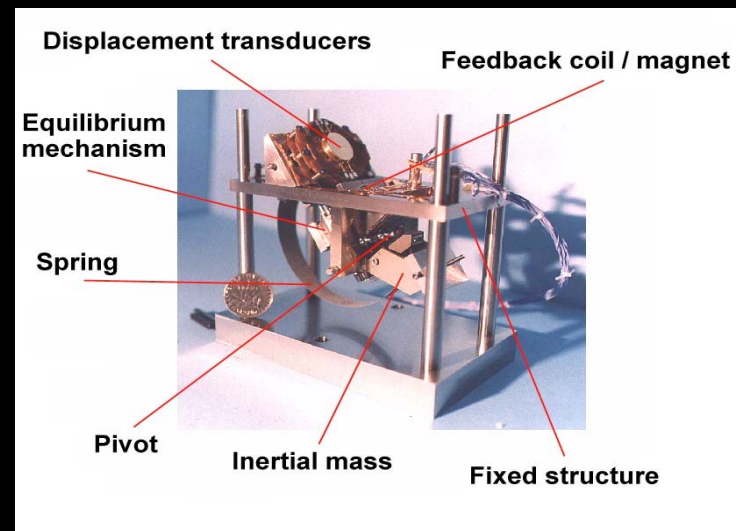


Seismic Instruments

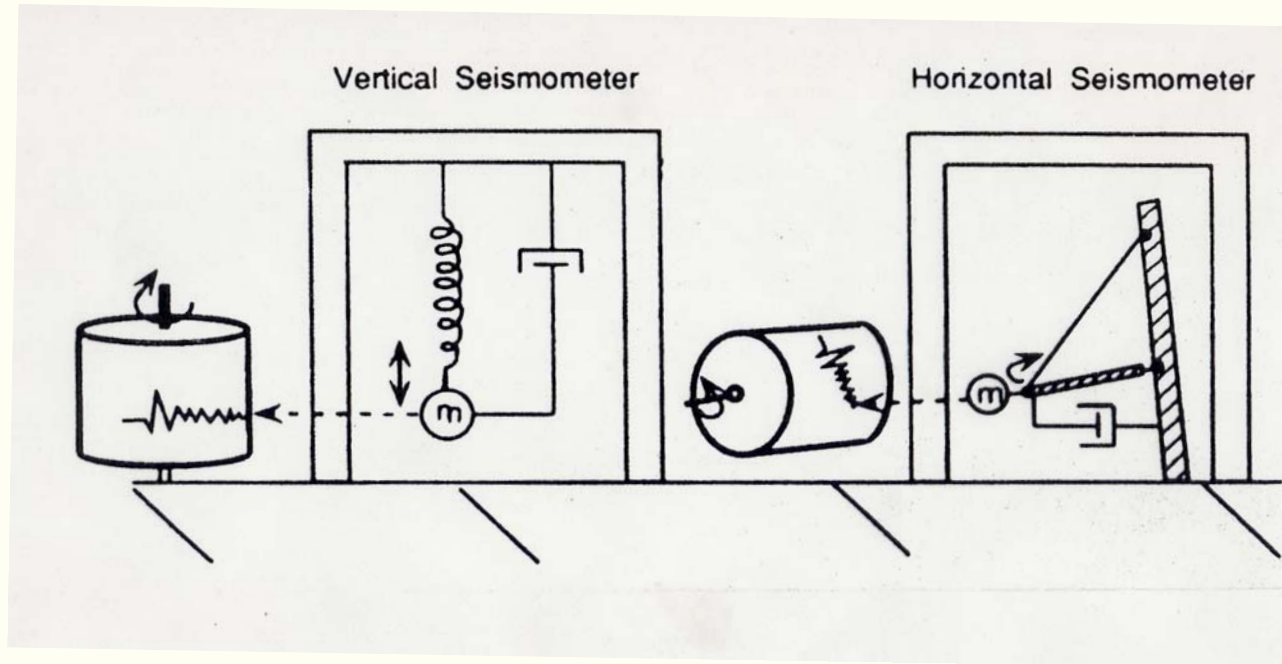
■ Seismoscope
(China -100BC)



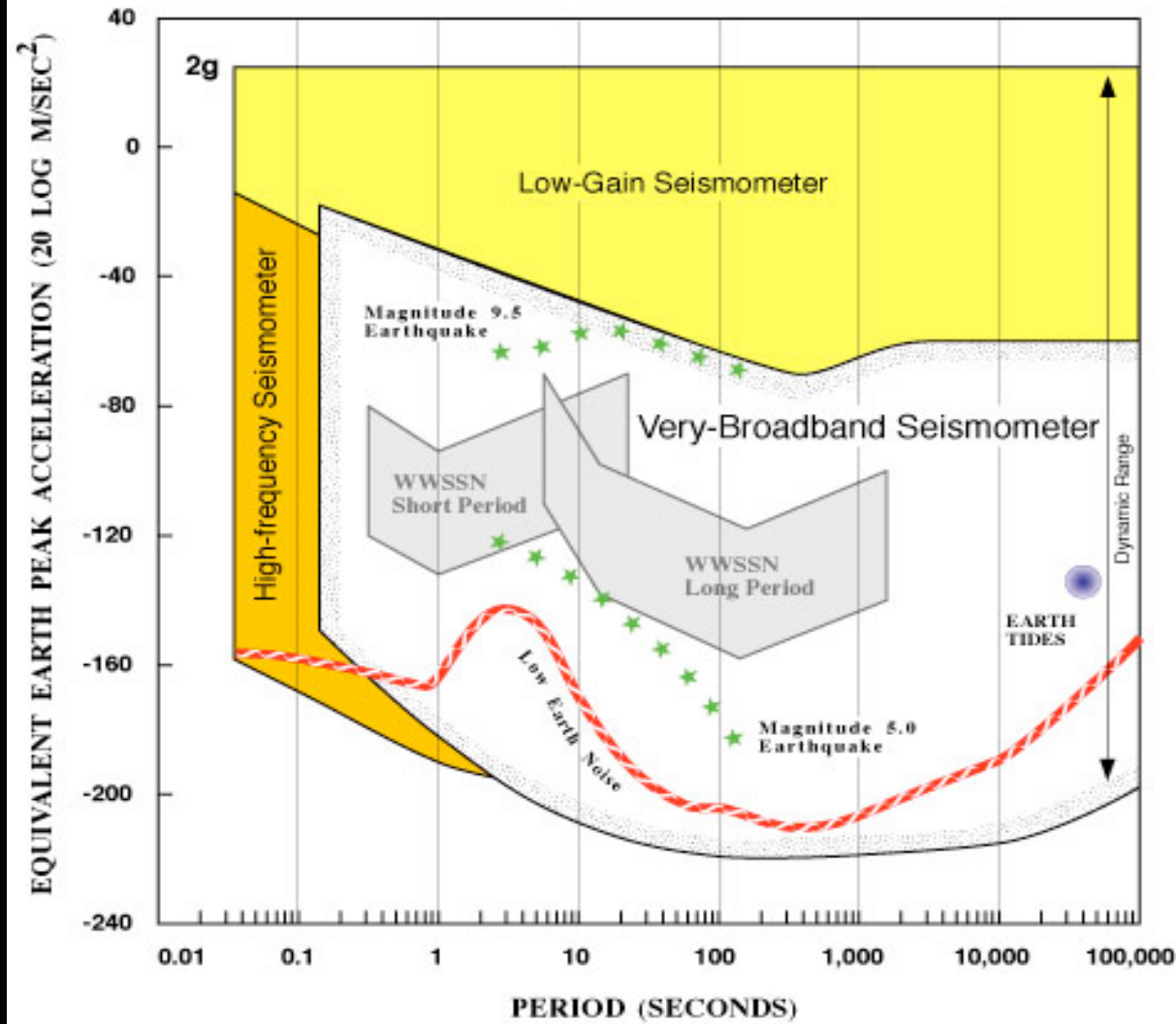
Broadband
Seismometer
(1mHz-20Hz)
(Cacho, 1998)



Principle of a Seismometer



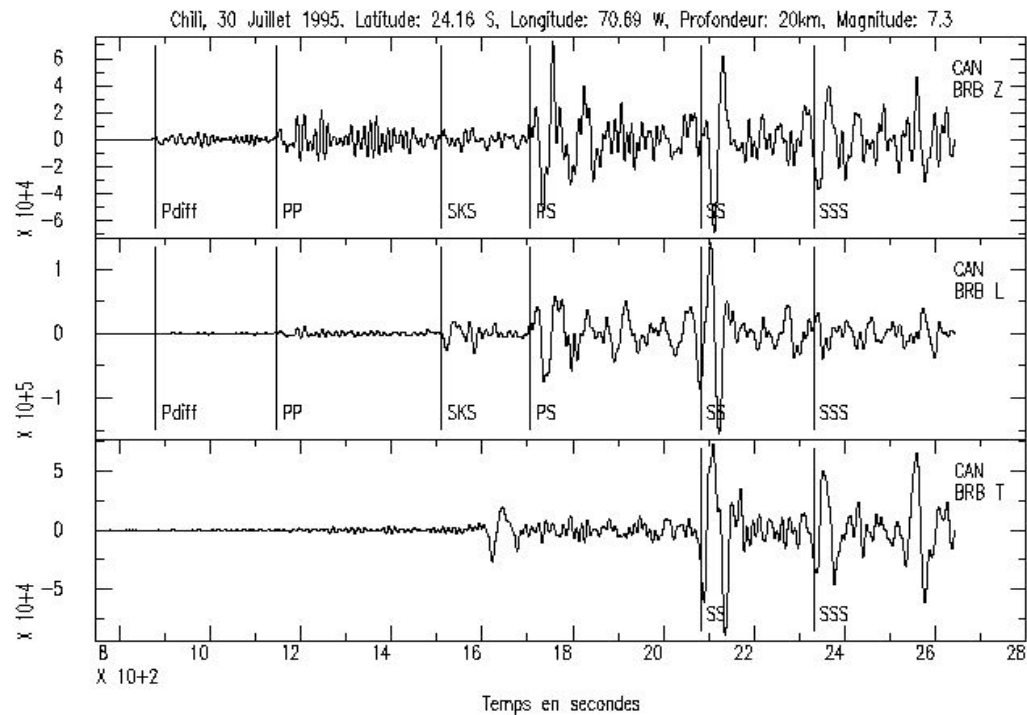
IRIS GSN SYSTEM



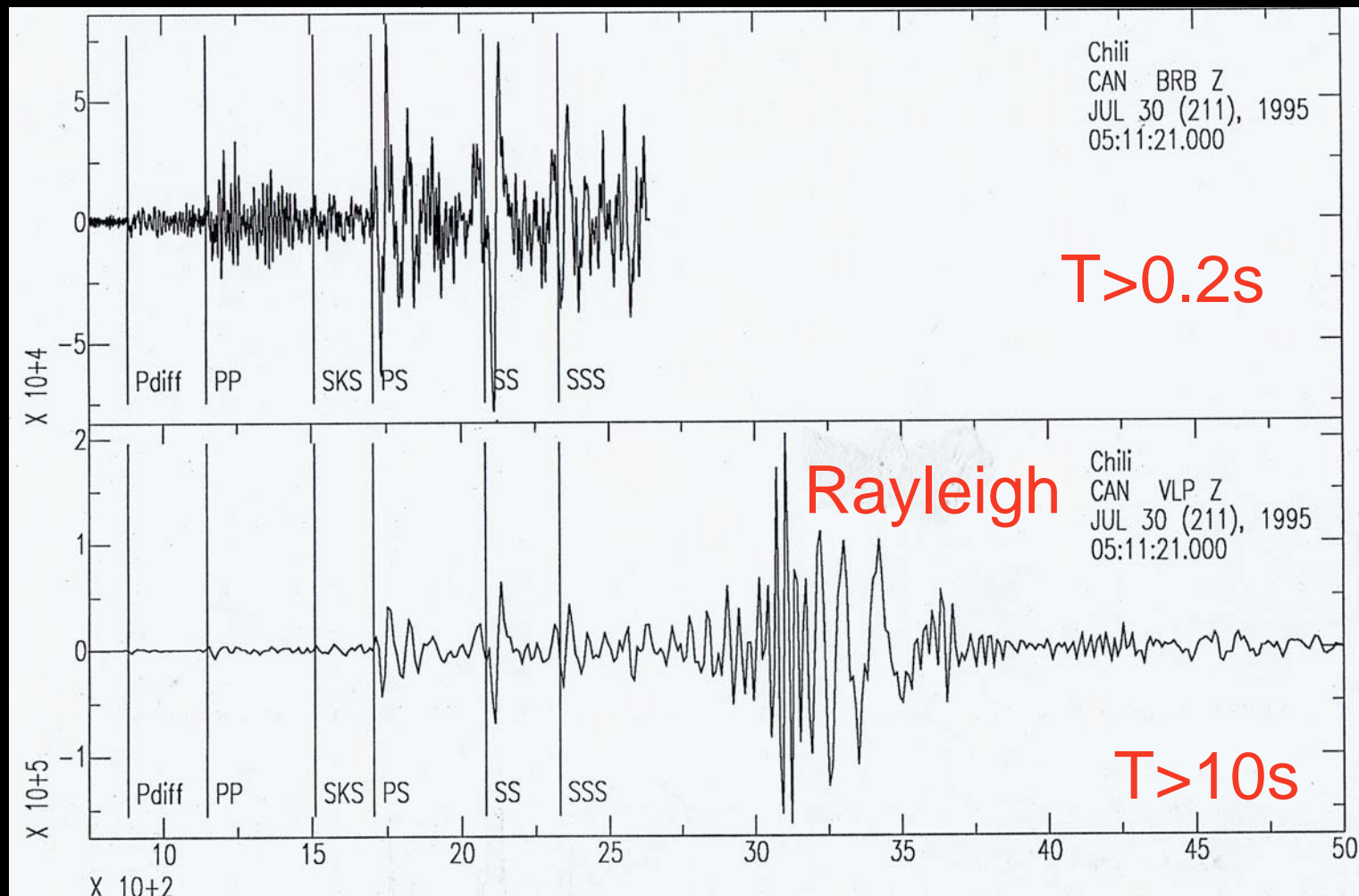
Butler et al., 2004

3 components
frequency range: 1mHz-20Hz
Period range: 0.05-1000s

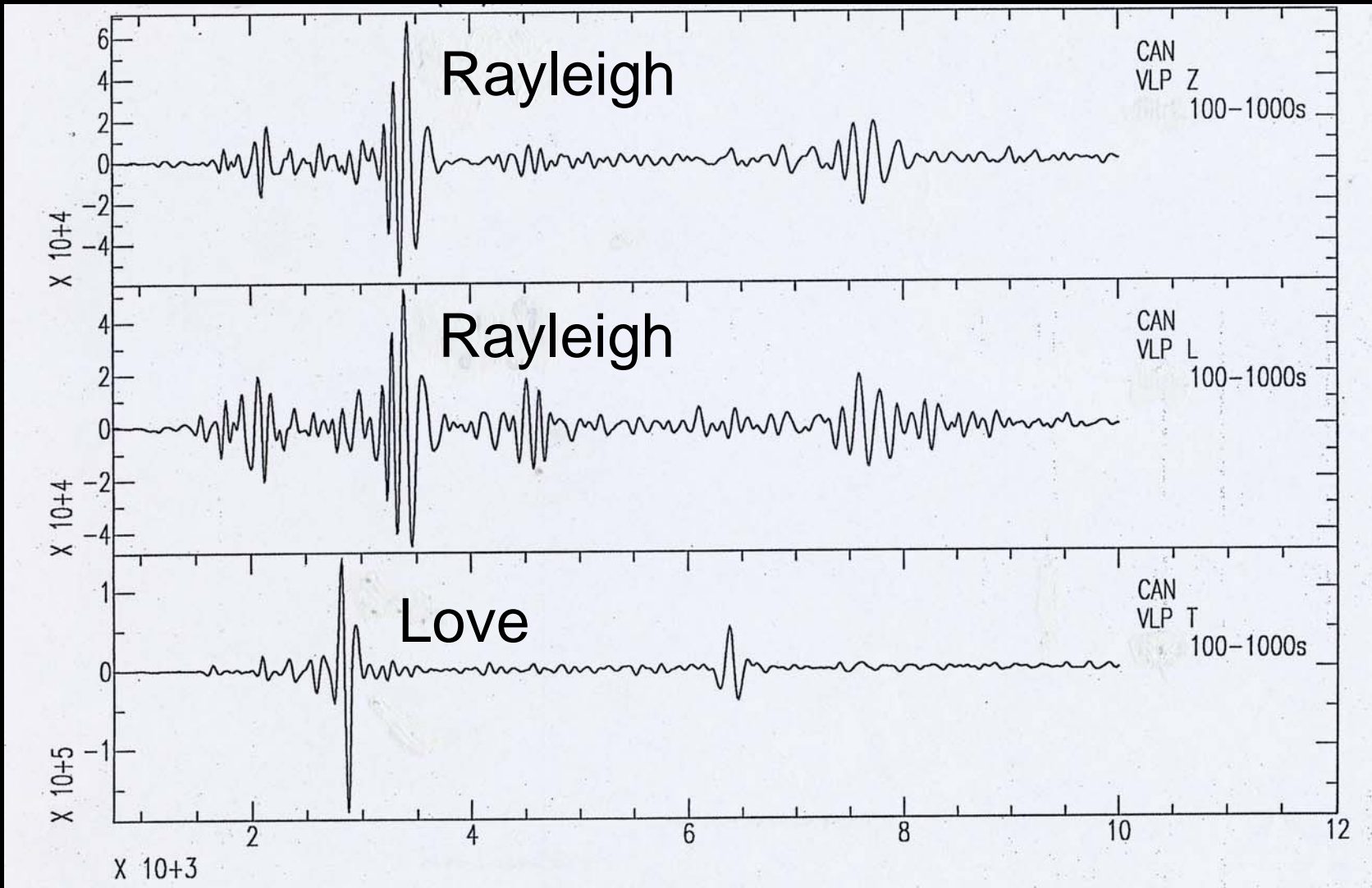
Chile July 30, 1995, Ms=8.3



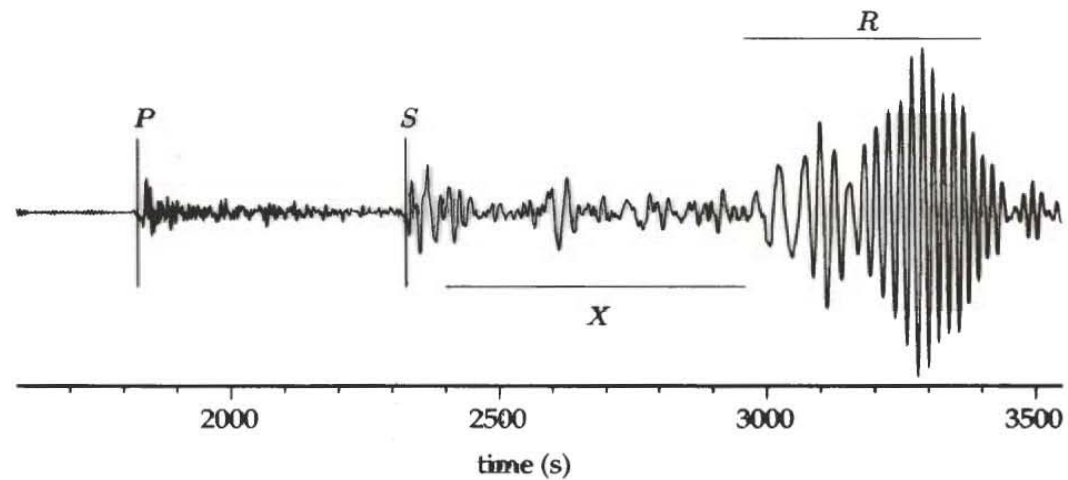
Chile earthquake magnitude= 7.3
Epicentral distance = 12,300km-depth 20km



Chile Earthquake Jul. 1995



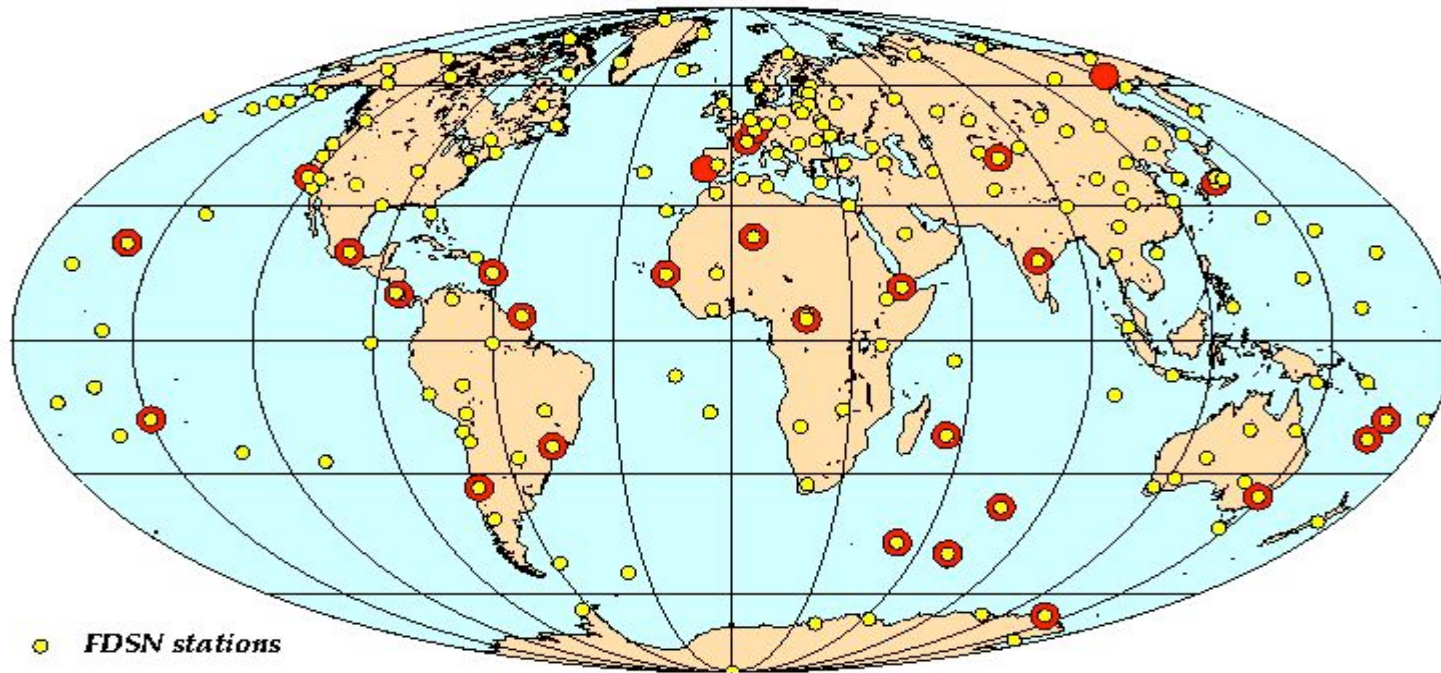
- Dispersive waves,
- Good global coverage,
- Large scale heterogeneities (min. 600 km).



Vertical component of displacement field recorded at DRV station corresponding to the New-Guinea 05/16/1999 earthquake.

Global Networks

GEOSCOPE stations and FDSN stations



● *FDSN stations*

● *Geoscope/FDSN stations*

Geoscope/G.Roult

Ocean Bottom Observatories

=> International Ocean network (I.O.N.)

- 2/3 of the Earth are covered by water.
- seafloor seismometers enable:
 - To investigate oceanic regions with a better resolution
 - To fill gaps in the global coverage

NERO (joint French-Japanese Project)



I.O.N.

International Ocean Network

ION (International Ocean network) France, Italy, Japan, UK, U.S.

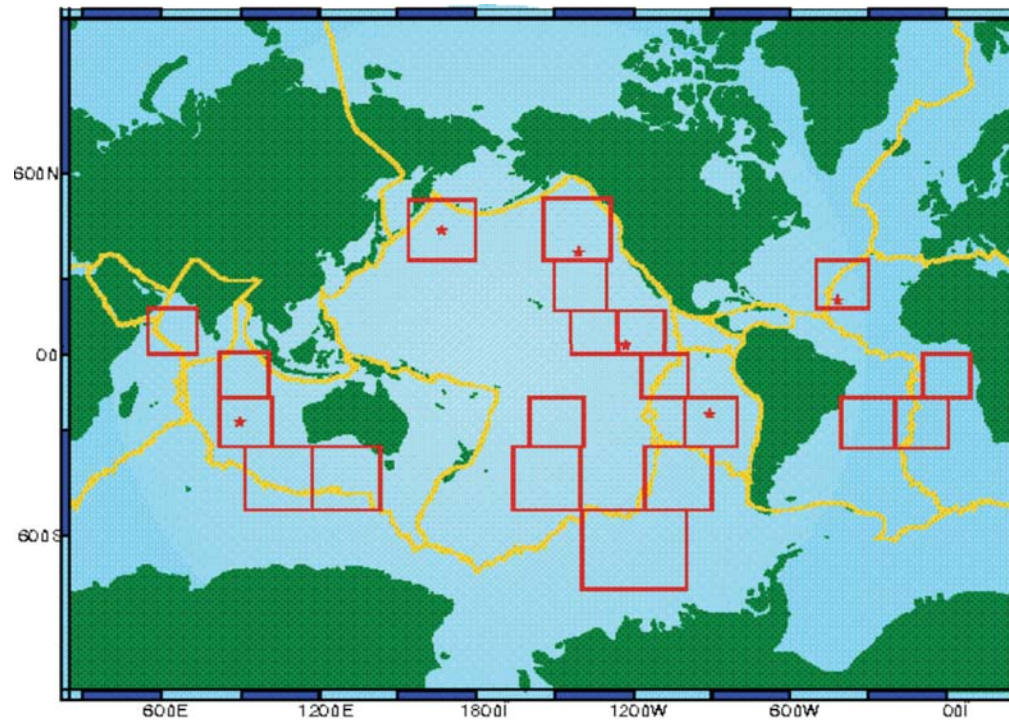
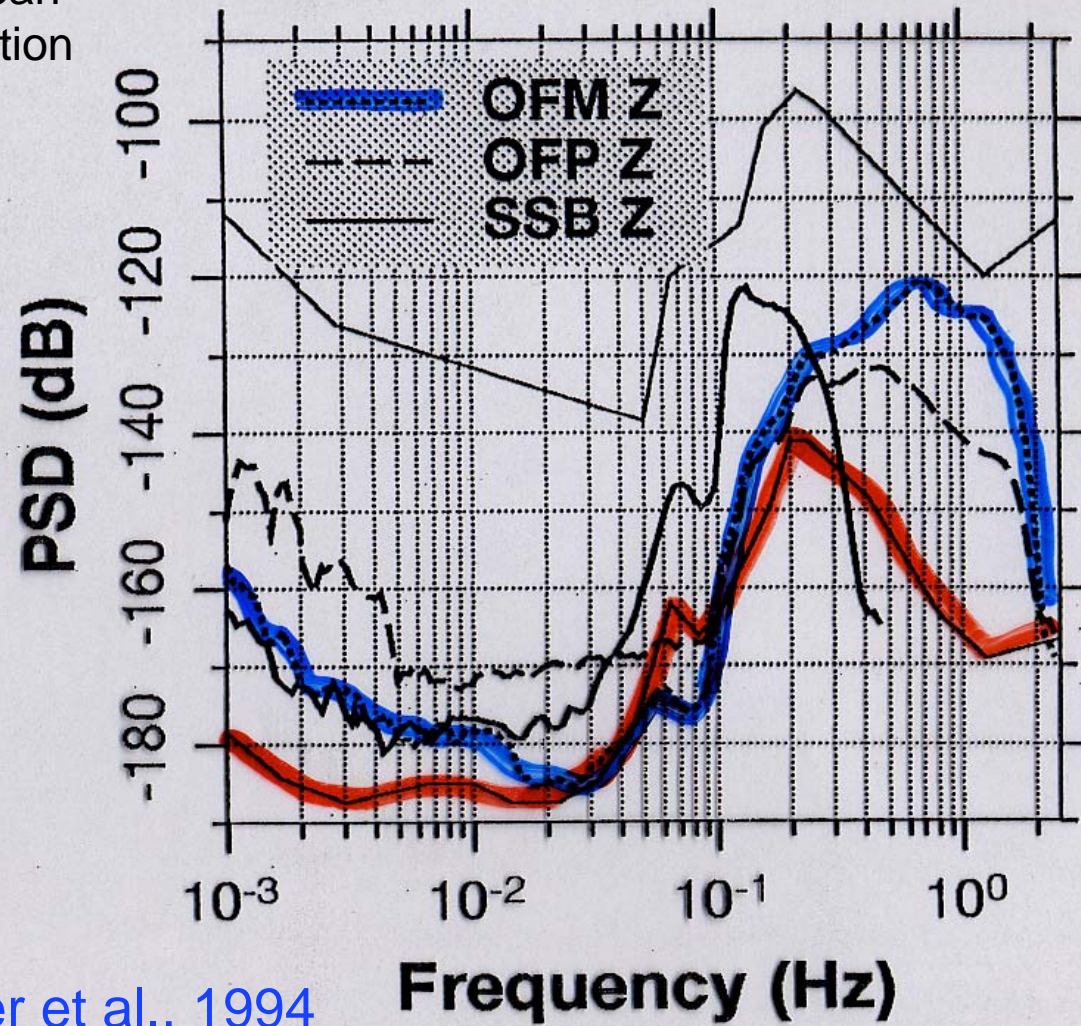


Figure 1: This map shows twenty regions which would require a seafloor seismic observatory in order to have 128 GSN stations evenly spaced around the globe (red boxes). The six starred boxes have been selected as preliminary test sites. The yellow lines mark plate boundaries.

OFM: Ocean
bottom station



Montagner et al., 1994





M.O.I.S.E (June-Sept. 1997)

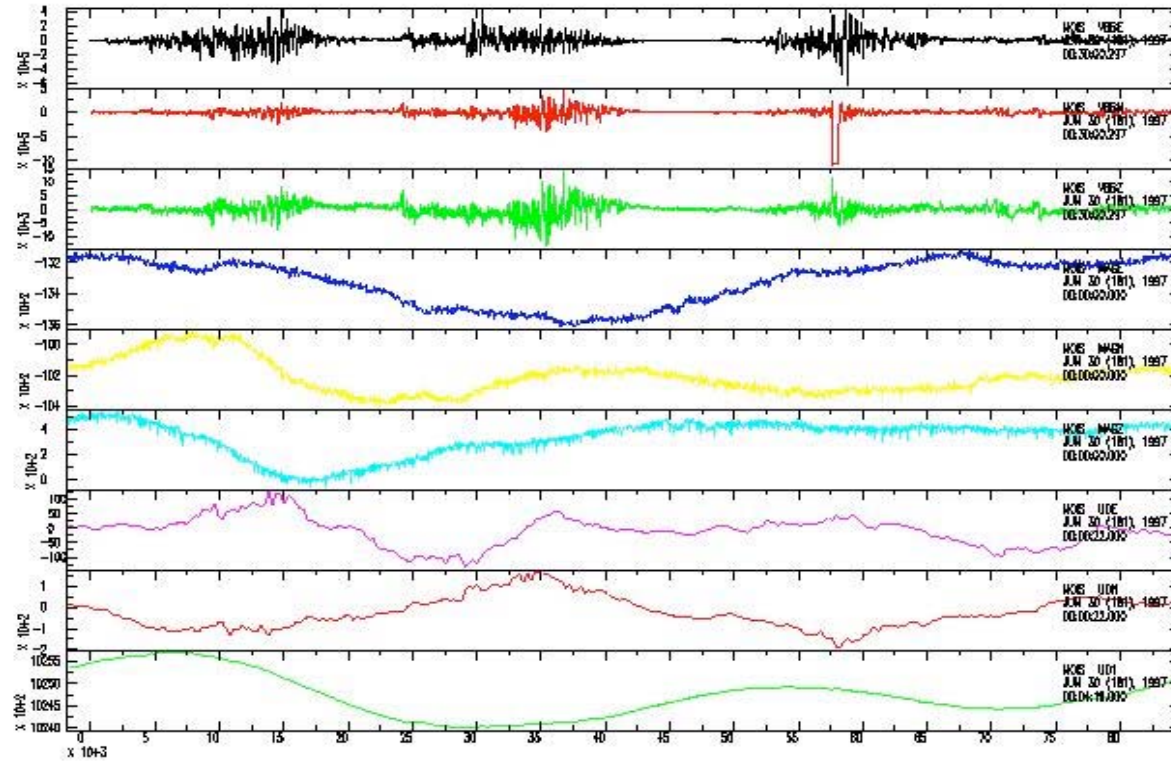
(Monterey bay Ocean bottom International Experiment)

MBARI, UC Berkeley, IPG-Paris, UBO-Brest

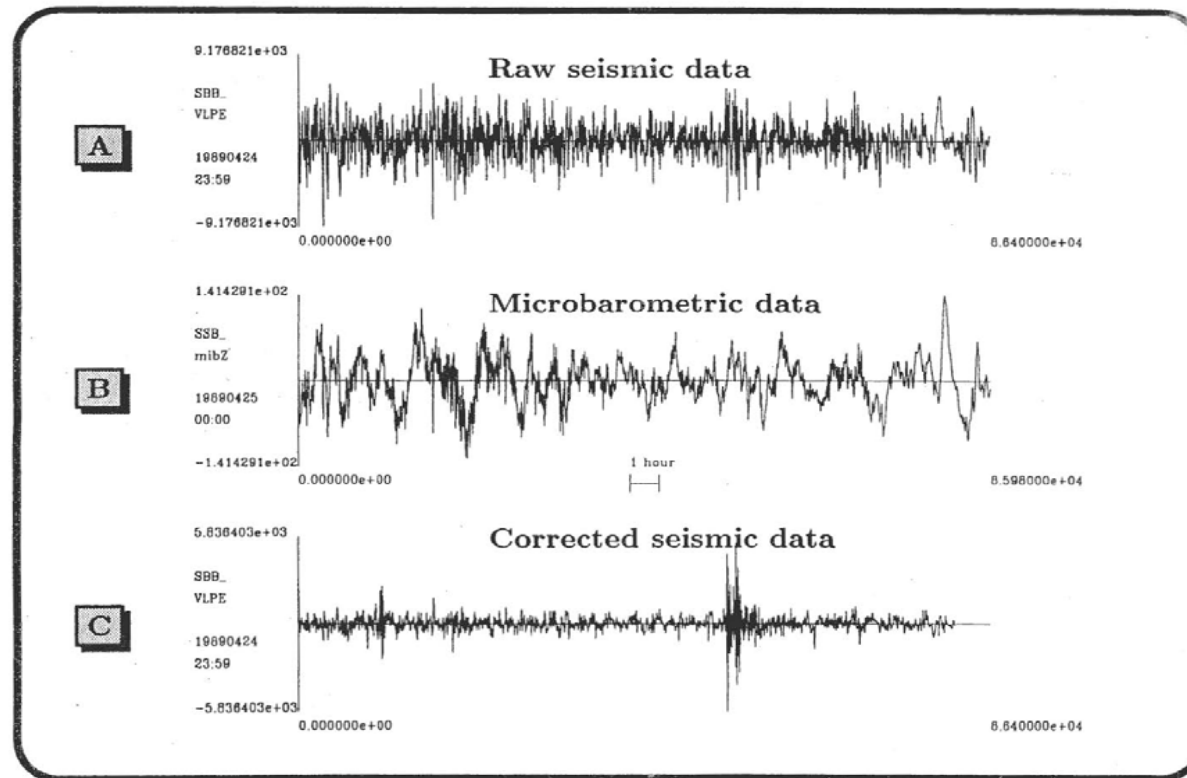




Multiparameter signals



Deconvolution of the seismic signal from the pressure influence

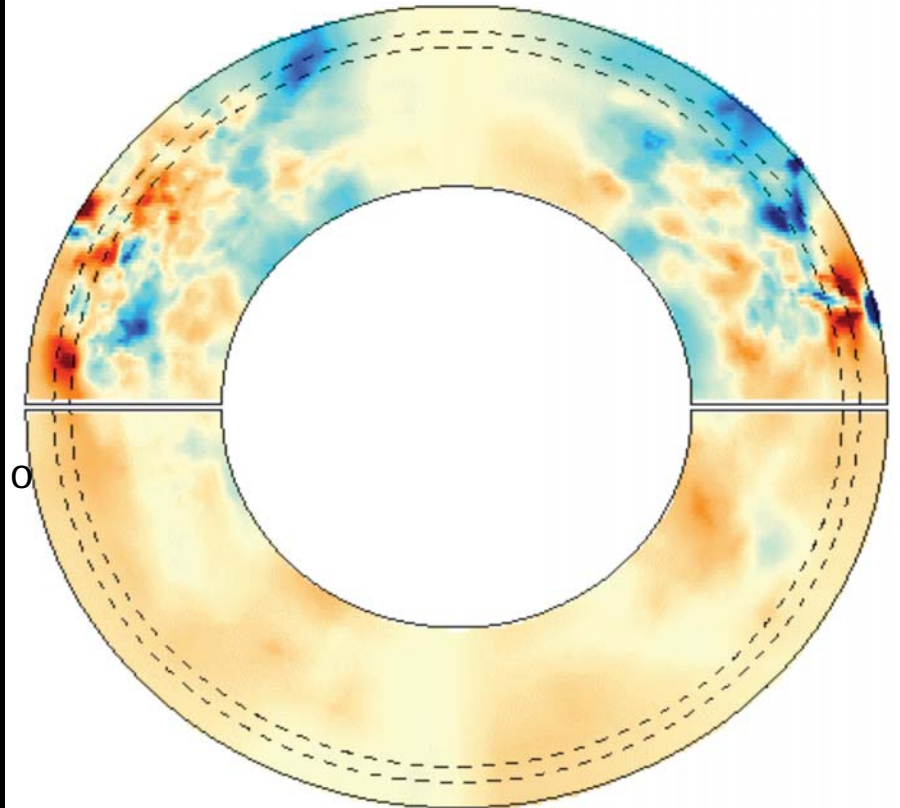
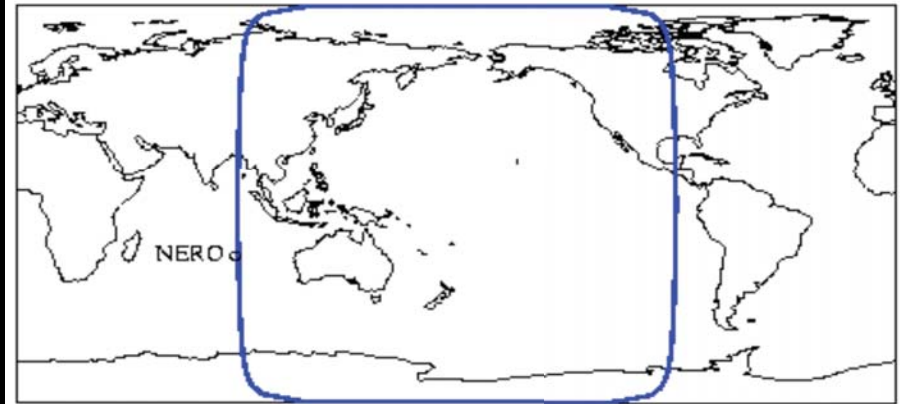


Beauduin et al., 1996



NERO:
Scientific Interest
Global scale

- To fill a gap in global station coverage
- To improve global tomographic model resolution
- To improve azimuthal distribution in determination of large earthquakes focal



Karason & van der Hilst, 2003



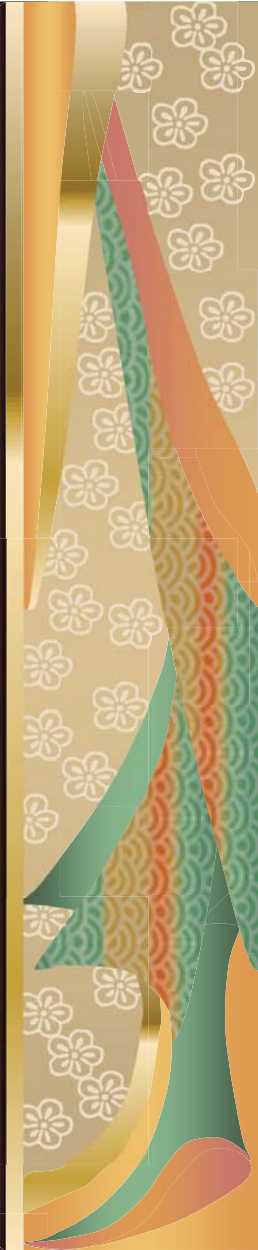
NERO observatory (in 2008)



Overview

Large scale Seismology: an observational field

- Data (Seismic source) + Instrument (Seismometer) -> Observations (seismograms)
- **Historical evolution: Ray theory, Normal mode theory, Numerical techniques (SEM, NM-SEM)**
- Scientific Issues: earthquakes, structure of the Earth and planets
- Seismic Experiment: Plume detection
- NM-SEM and time reversal



Hypothesis: Elastic Medium

$$s_{ij} = C_{ijkl} e_{kl}$$

Where e_{kl} is the strain tensor, s_{ij} the stress tensor

C_{ijkl} the elastic tensor: 81 elastic moduli

Symmetries of e_{kl} , s_{ij} and of the strain energy

$W = 1/2 s_{ij} e_{ij} \Rightarrow 21$ independent elements

Isotropic case:

$$C_{ijkl} = l d_{ij} d_{kl} + m(d_{ik} d_{jl} + d_{il} d_{jk})$$

l, m are Lamé parameters

Elastodynamic equation

$$\partial_j (C_{ijkl} \partial_k u_l) + \rho \omega^2 u_i = 0$$

In the isotropic case, 2 solutions:

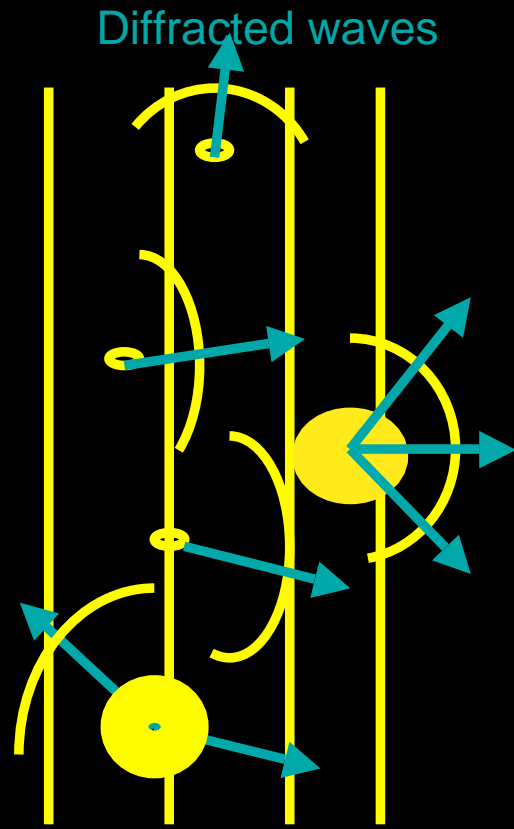
S-wave

P wave

In heterogeneous media, comparison between

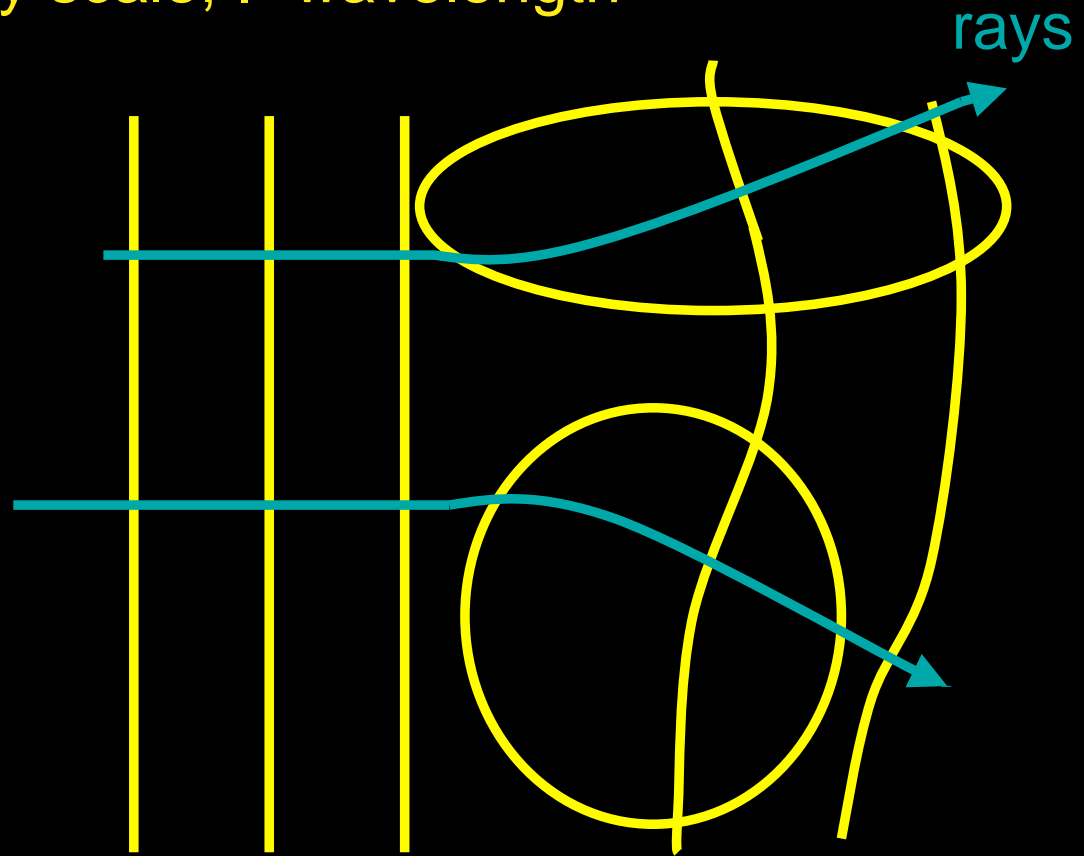
Wavelength λ and scale of heterogeneity Λ

L heterogeneity scale, λ wavelength



wavefronts

$\lambda \sim L$ or $\lambda \gg L$



wavefronts

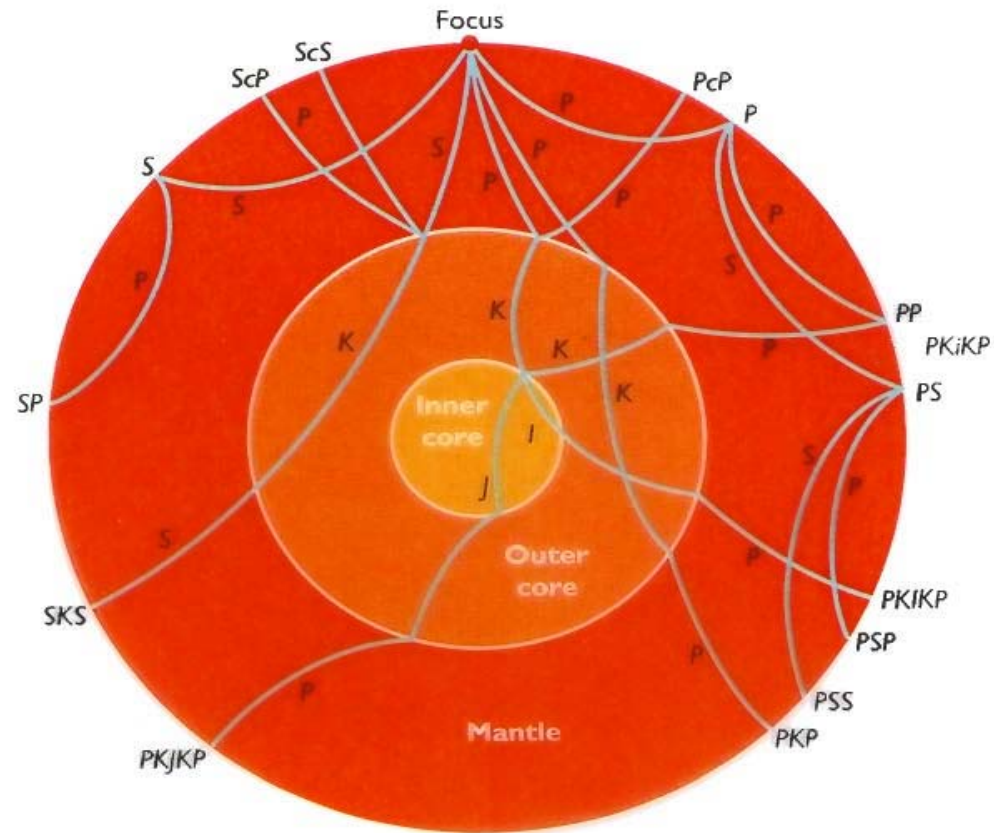
$\lambda \ll L$

Duality wave - particle:

- l seismic wavelength
- L scale heterogeneity
- Particle: Ray theory (XXth century)
 $l \ll L$
- Wave: Normal mode theory (>1970)

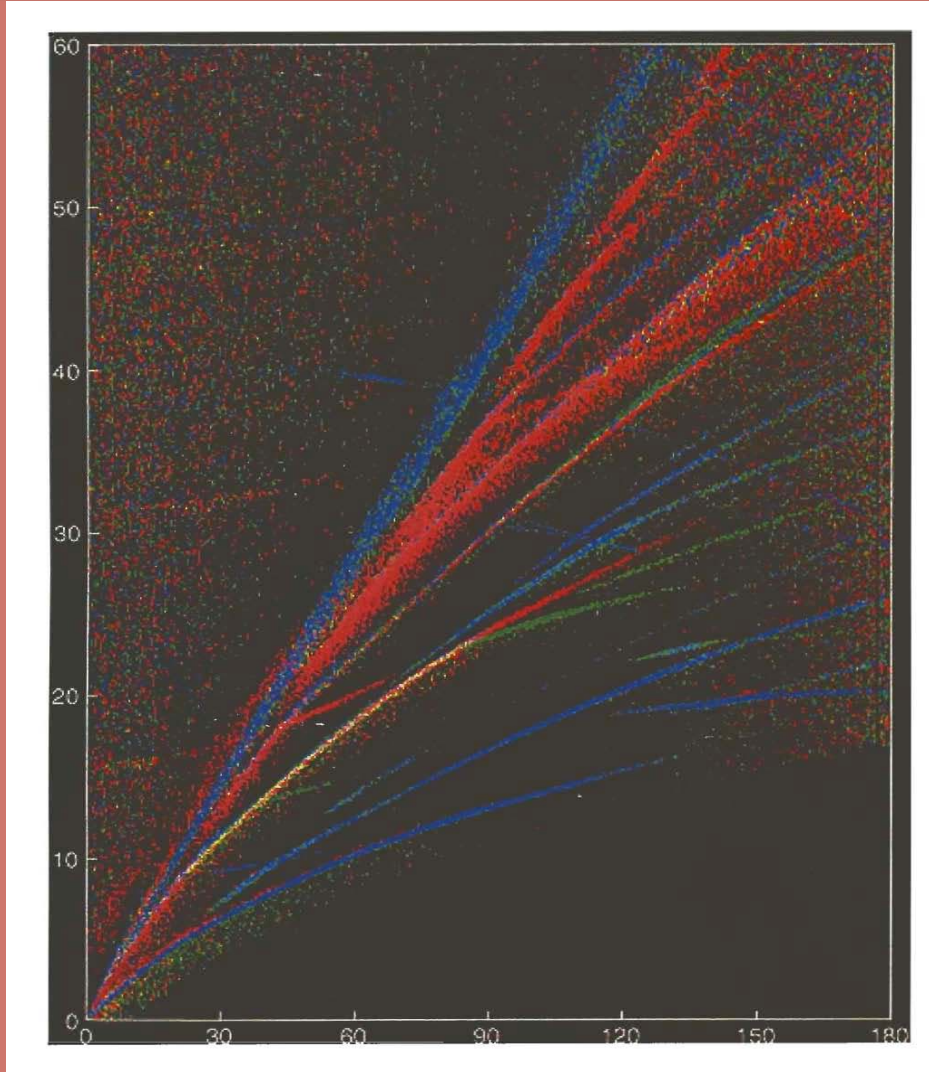


RAY PATHS INSIDE THE EARTH



Bolt, 1993

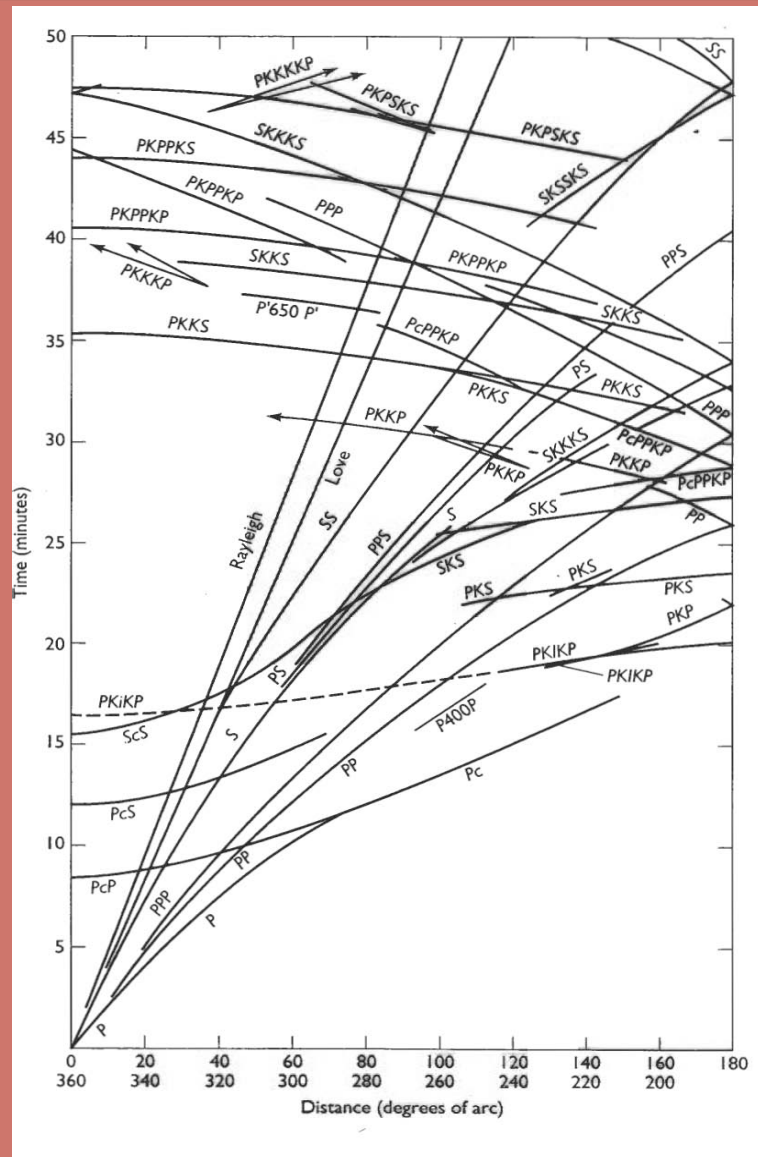
Time



Epicentral distance

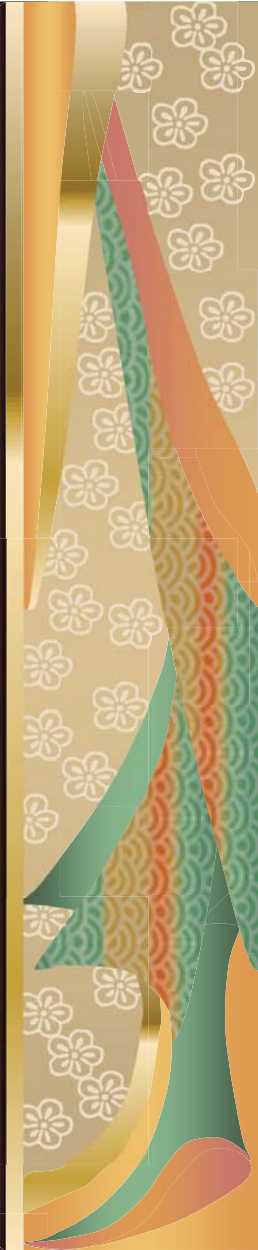
Shearer, 1997



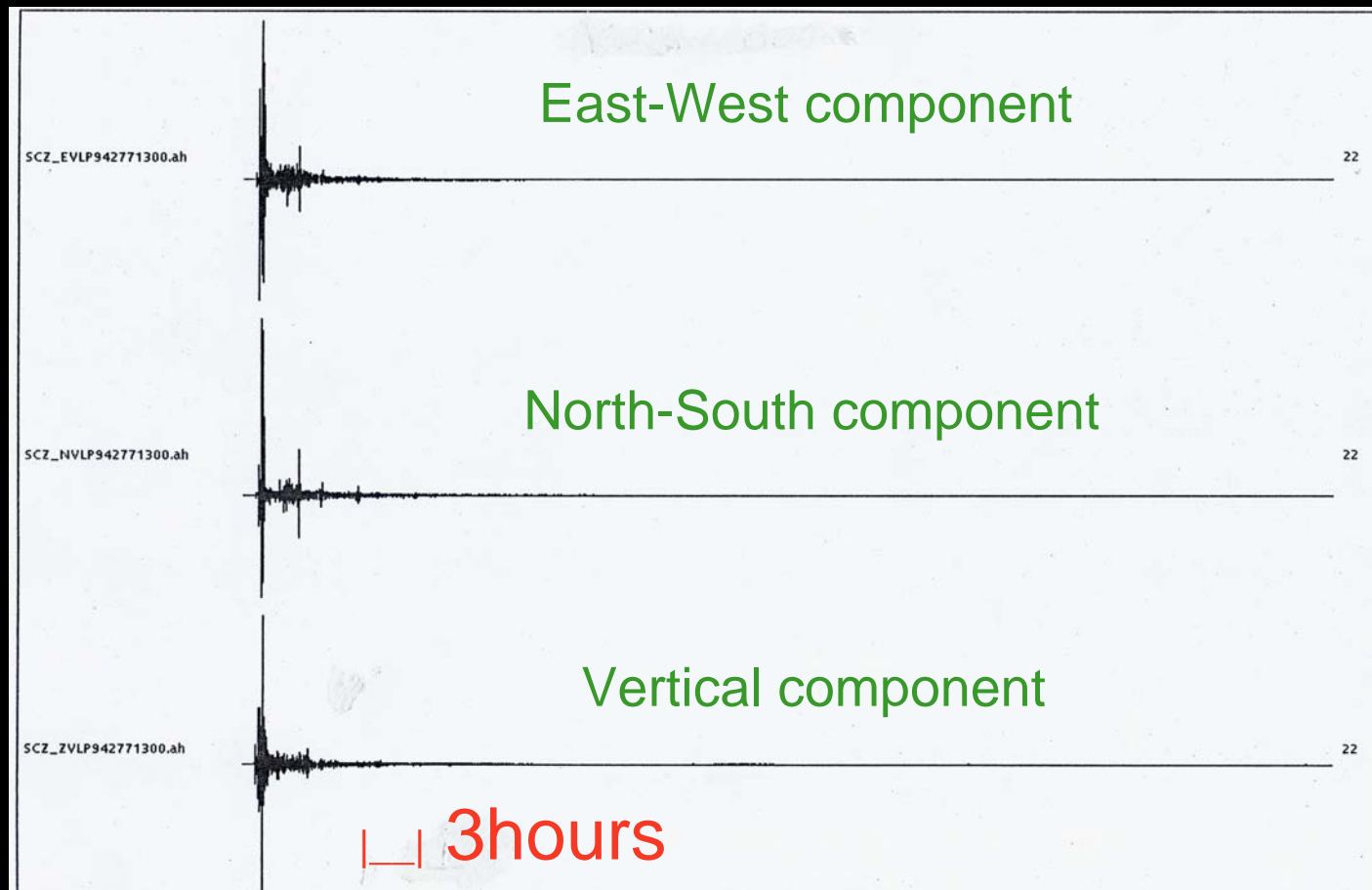


Duality wave - particle:

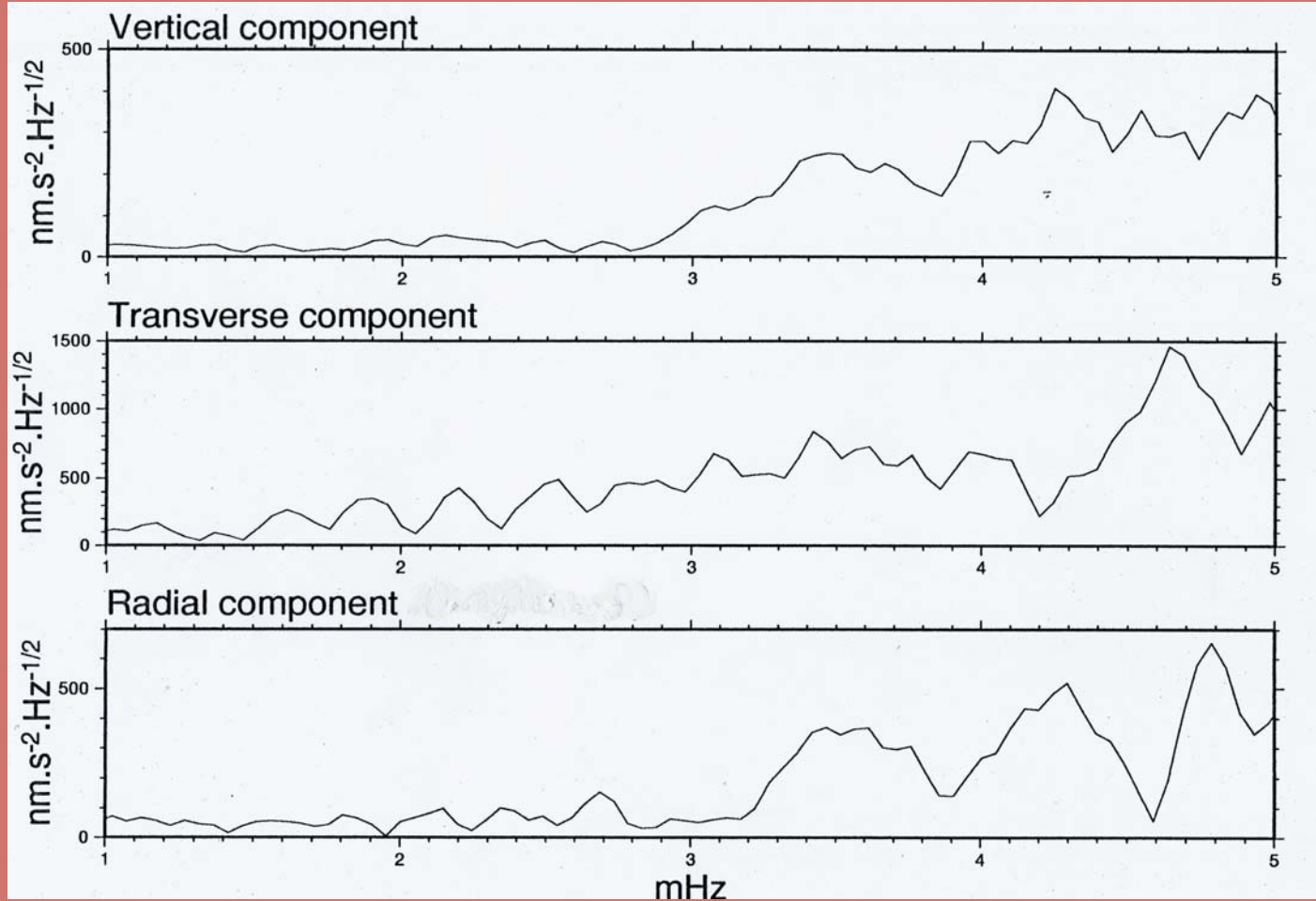
- l seismic wavelength
- L scale heterogeneity
- Particle: Ray theory (XXth century)
 $l \ll L$
- Wave: Normal mode theory (>1970)



Kurils islands 1994-277 Ms=8.3



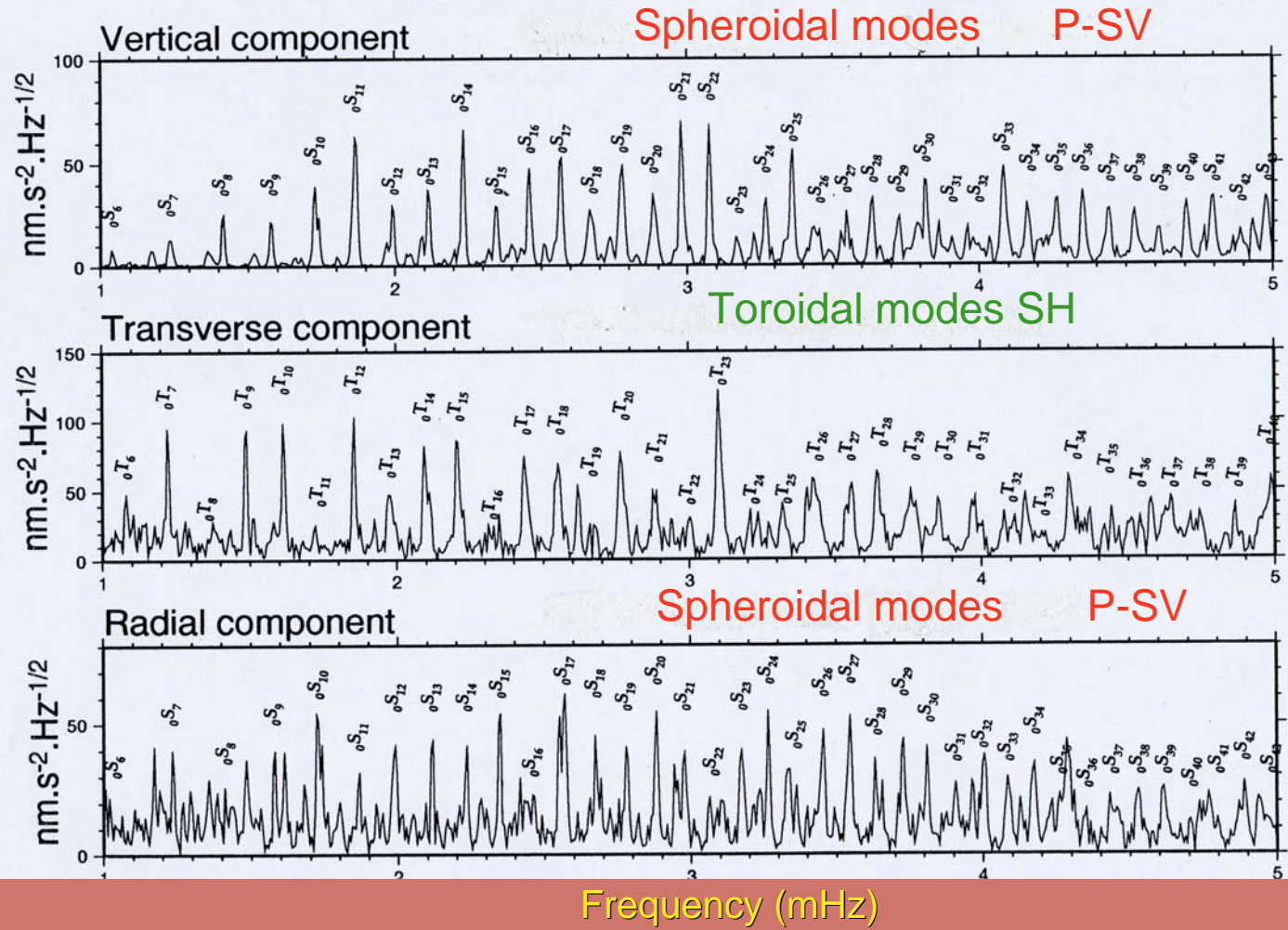
Kurils islands 1994-277 SCZ-VLP Spectra 3 hours



Frequency (mHz)



KURIL 94 277 - SCZ VLP - 36h.



Elasto-dynamic equation

$$\rho \frac{\partial^2 \mathbf{u}_i}{\partial t^2} = \frac{\partial}{\partial x_j} \mathbf{s}_{ij} + \rho \mathbf{g}_i + \mathbf{F}_i (+ \mathbf{F}s_i + \dots)$$

Which can be rewritten:

$$\rho \frac{\partial^2 \mathbf{u}_0}{\partial t^2} = \mathbf{H}_0 \mathbf{u}_0 (+ \mathbf{F}s)$$

\mathbf{H}_0 is an integro-differential operator

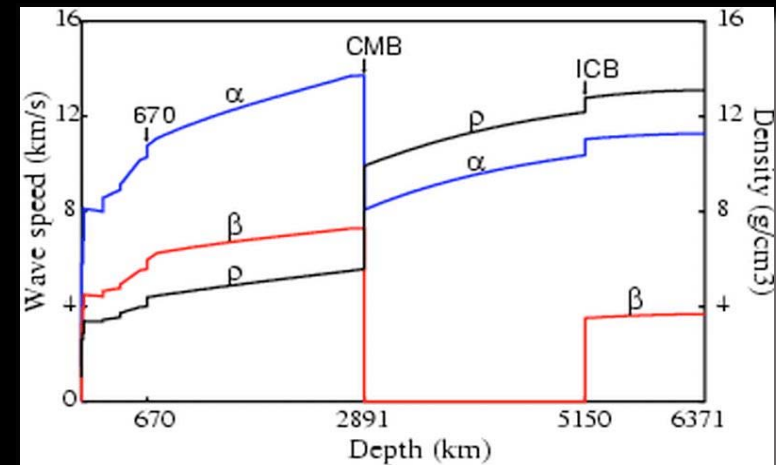
1D-Reference Earth Model:

$$M_0(r), \rho(r), V_P(r), V_S(r)$$

(PREM, Dziewonski and Anderson, 1981
or IASP91, Kennett and Engdahl, 1991)

Eigenfrequencies: ω_n

Eigenfunctions: $u_l^m(r,t) = |n,l,m\rangle$



$$r \leq_{tt} \mathbf{u}_0 = \mathbf{H}_0 \mathbf{u}_0 \quad (+ \mathbf{F}s)$$

Eigenfrequencies: ${}_n \omega_l$

Eigenfunctions: ${}_n \mathbf{u}_l^m (r,t) = |n,l,m\rangle$

3 quantum numbers ($k=\{n,l,m\}$) $\Rightarrow \mathbf{u}_k(r,t)$

$$\int_{\leq r} \mathbf{u}_k^* \cdot \mathbf{u}_k \, d^3x = \delta_{ij}$$

$$\mathbf{H}_0 \mathbf{u}_k = r \, {}_n \omega_l^2 \mathbf{u}_k$$

Displacement:

$$\mathbf{u}(r,t) = \sum_{n,l,m} {}_n \mathbf{a}_l^m |n,l,m\rangle \exp(-i {}_n \omega_l t)$$

$$\begin{aligned} \mathbf{u}_k(r,t) = & \{ U(r) \mathbf{e}_r + V(r) \mathbf{e}_q \leq_q + V(r)/\sin q \mathbf{e}_f \leq_f \} Y_l^m(q,f) \\ & + \{ W(r) \mathbf{e}_q \leq_f - W(r) \mathbf{e}_f \leq_q \} Y_l^m(q,f) \end{aligned}$$

Spheroidal Modes

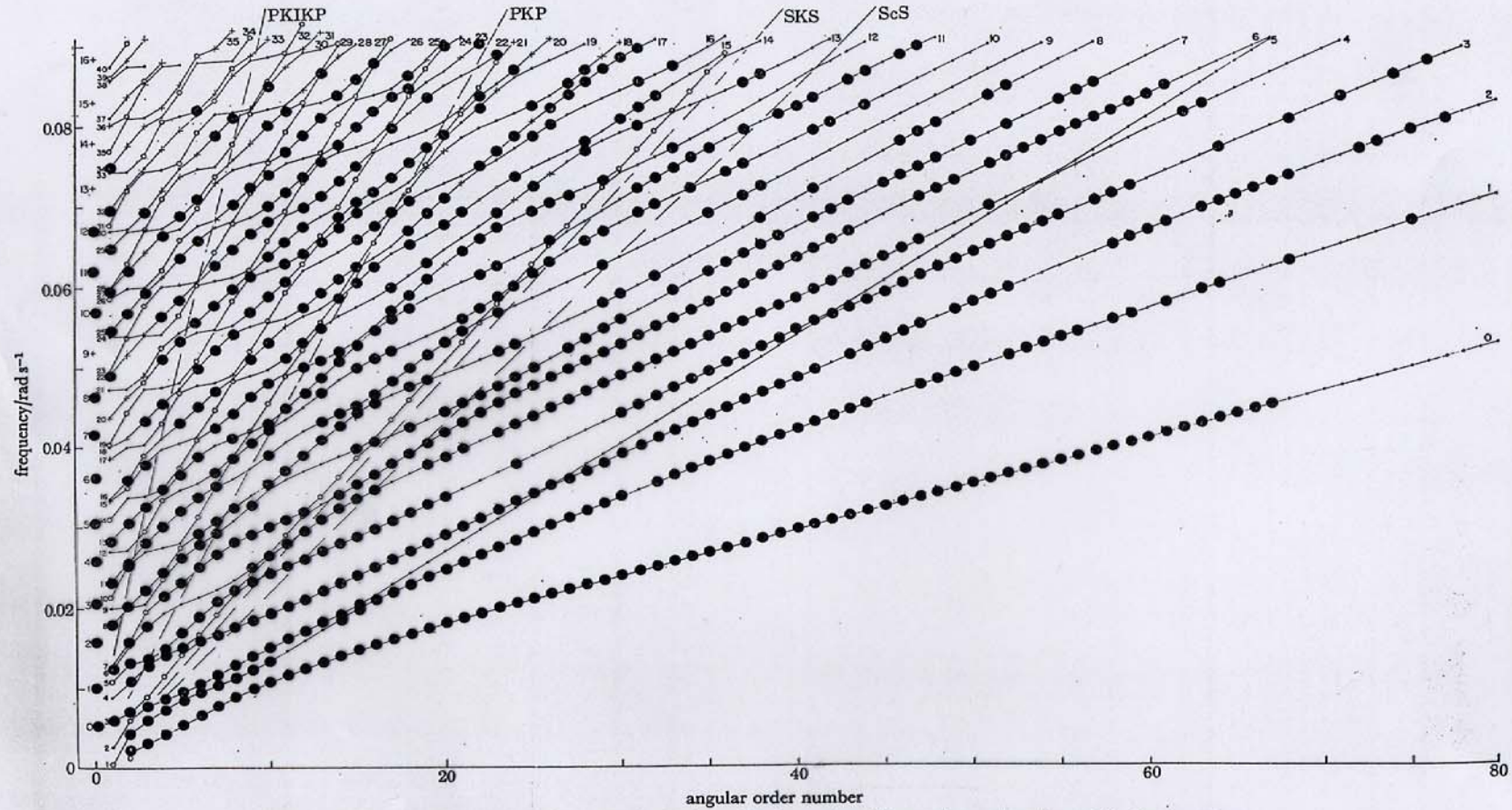


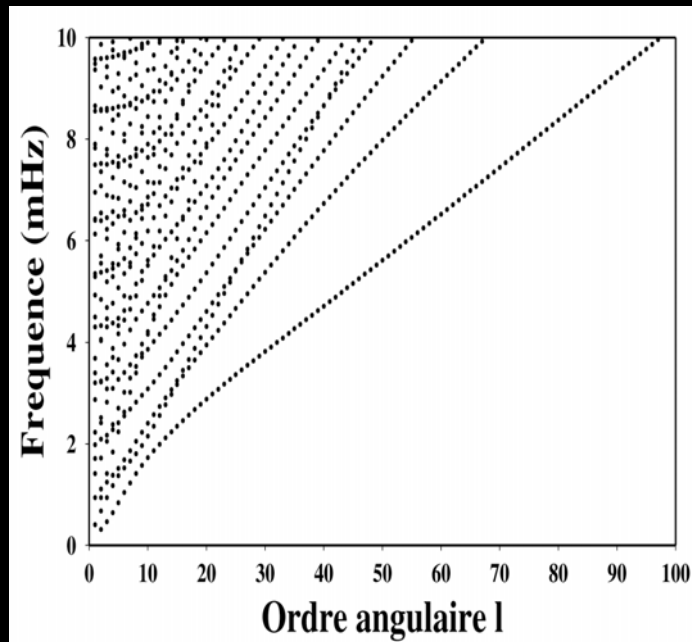
FIGURE 17. Spheroidal normal modes in the (ω, l) plane. The large dots indicate observed modes used in the inversions. For further details we refer the reader to §3 of Alaska II. •, $CE < 0.5$; +, $CE \geq 0.5$; o core modes.

Spherical eigenfrequencies

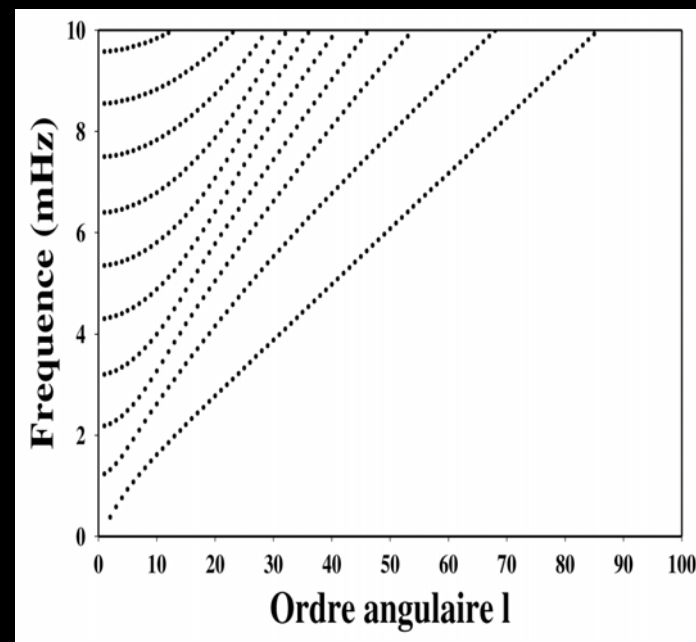
Spheroidal Modes ${}_nS_l$
(P-SV / Rayleigh)

Toroïdal modes ${}_nT_l$
(SH / Love)

Dispersion Branches

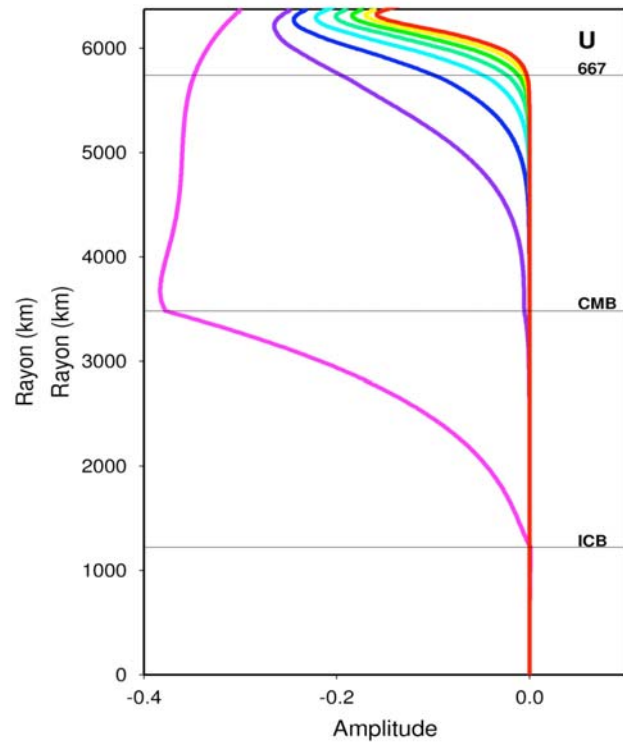


multiplet : $(n,l) = 2l+1$ singlets
singlet : (n,l,m)



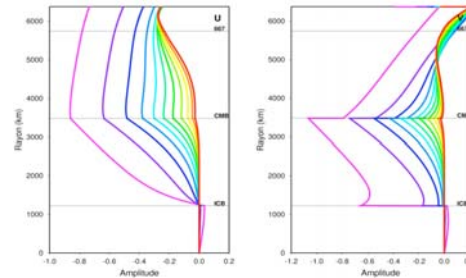
n : radial order
l : angular order
m : azimuthal order

Spherical eigenfunctions

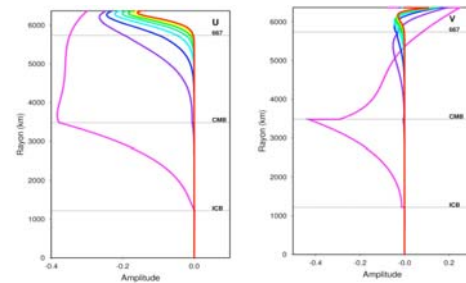


${}_0S$ branch

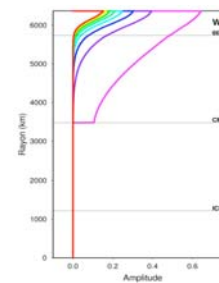
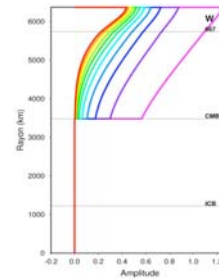
$l = 2, 3, 4, 5, 6, 7, 8, 9, 10, 11, 12$



$l = 5, 15, 25, 35, 45, 55, 65, 75$



${}_0T$ branch



1D- Reference Earth Model

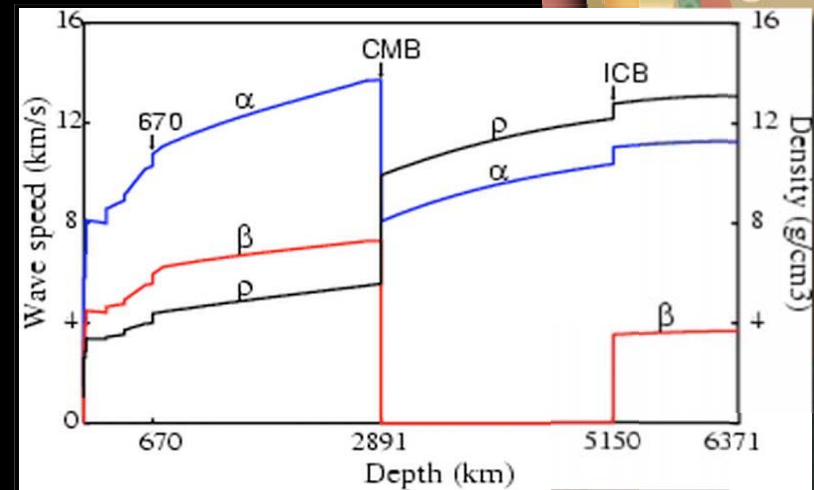
- Normal mode calculation
(eigenfrequencies ${}_n\omega_k$
eigenfunctions ${}_n u_l(r,t)$)
- Synthetic Seismograms by
normal mode summation
($k=\{n,l,m\}$).

$\mathbf{u}(r,t)$ Displacement at point r at time t due
to a force system \mathbf{F} at point source r_s

$$\mathbf{u}(r,t) = \sum_k \mathbf{u}_k(r) \cos \omega_k t / \omega_k^2 \exp(-\omega_k t / 2Q) (\mathbf{u}_k \cdot \mathbf{F})_s$$

Source Term $(\mathbf{u}_k \cdot \mathbf{F})_s = (\mathbf{M} : \mathbf{e})_s$

\mathbf{M} Seismic moment tensor, \mathbf{e} deformation tensor



Data

CAN__VHZ19952110511.a#

Donnée

204304

-164255

169186.703125

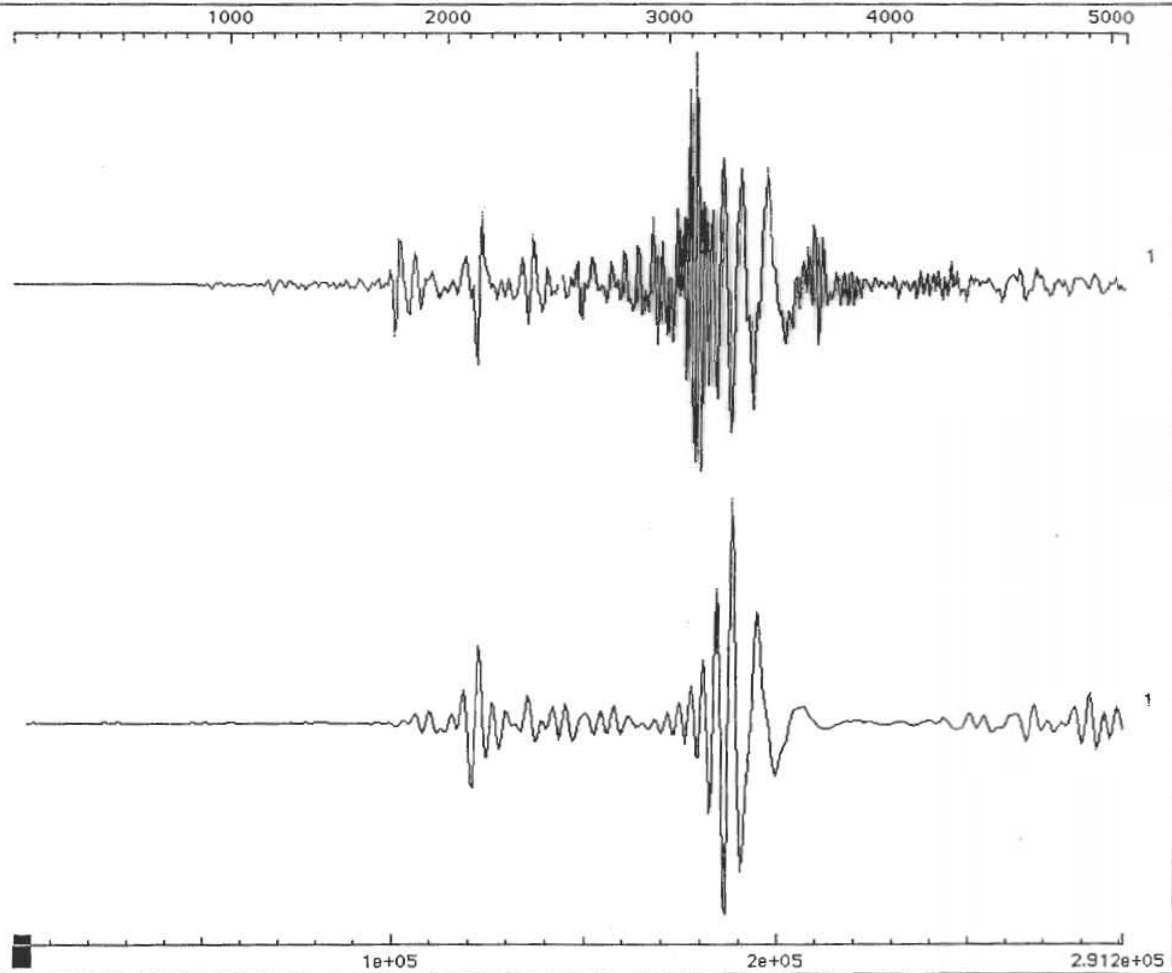
Synthetics

HARMO/ca.syn0-6.a#

Synthétique

-145271.921875

Seconds ->



Data

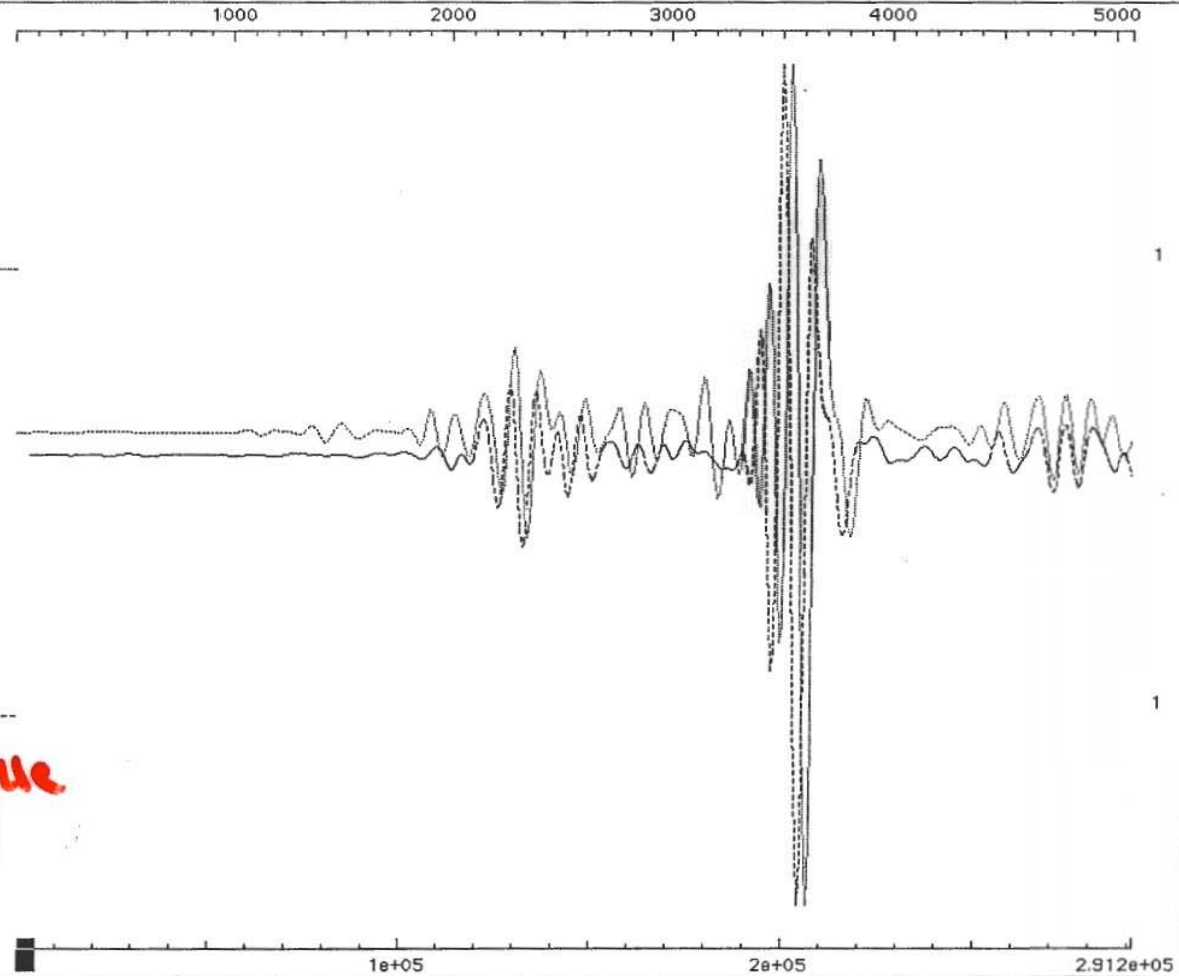
CAN_VHZ19952110511.ah

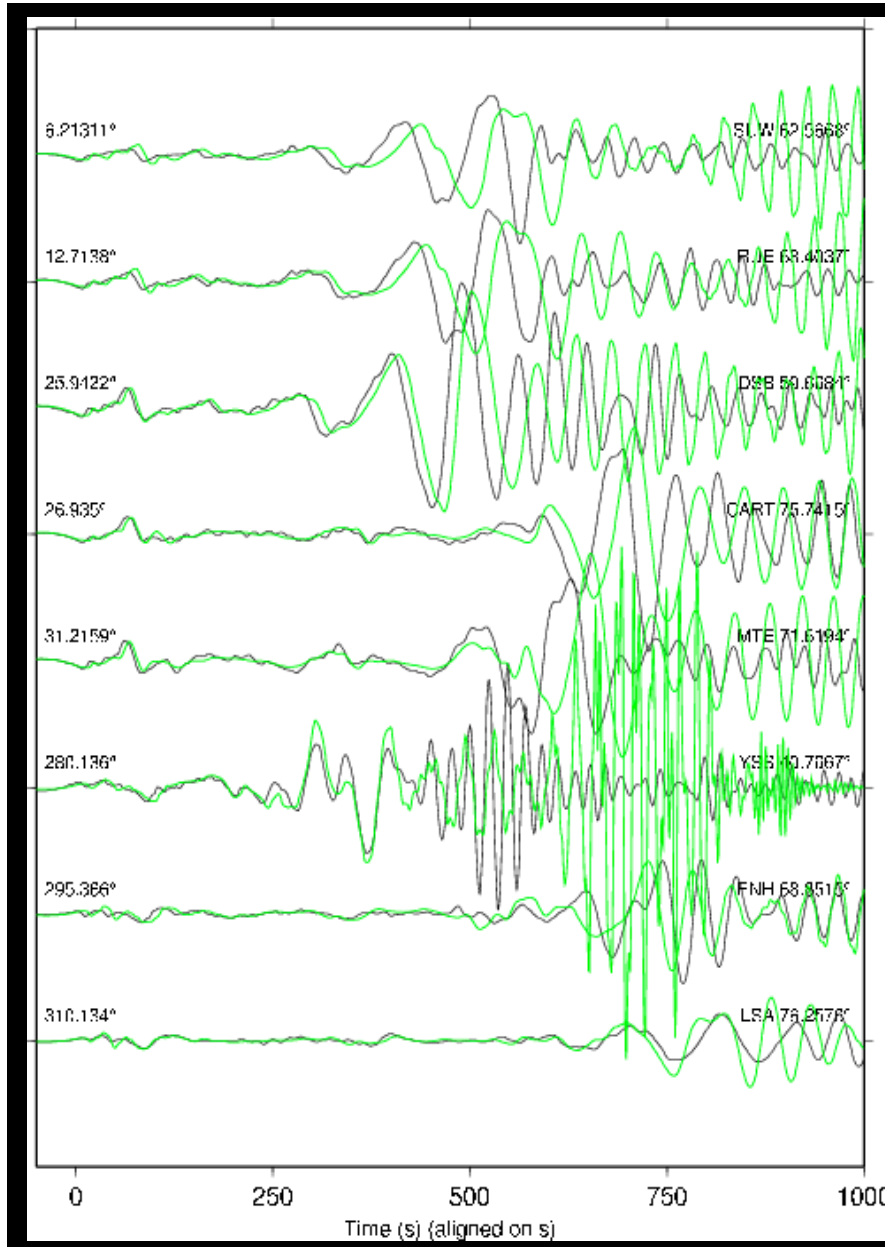
Donnée

Synthetics

HARMO/cansyn0-6.ah

Synthétique





Synthetic seismograms
By normal mode
summation

Denali-Alaska earthquake
(Nov. 2002)

Komatitsch and Tromp, 2003

Eigenfunction basis is a complete basis => any wave can be modelled by normal mode summation including surface waves and body waves.

Asymptotic form of $Y_l^m(q, f)$:

$$Y_l^m(q, f) := p^{-1} (\sin q)^{1/2} \cos[(l+1/2)q + 1/2 mp - 1/4 p] e^{imf}$$

For a source at the pole, q plays the role of epicentral distance.

The horizontal wavenumber k is: $k = (l + 1/2) / a$

And phase velocity is $c(\omega) = \frac{\omega}{k}$

Ray parameter $p = a \sin i / V \Leftrightarrow$ horizontal slowness

$$p = a \frac{k}{\omega} = (l + 1/2) / \omega$$

Duality wave - particle:
l seismic wavelength
L scale heterogeneity

Particle: Ray theory $l \ll L$

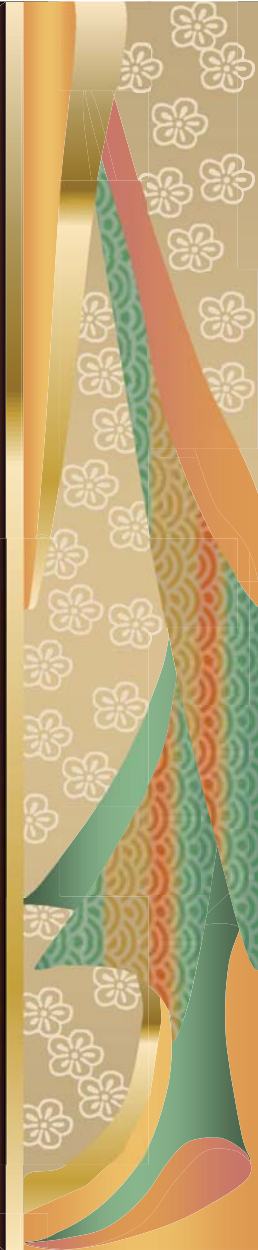
Wave: Normal mode theory (NM) +
Perturbation theories (small amplitude of 3D-
heterogeneities) -> Global tomography

Numerical modelling of wave equation

Strong or weak forms: $l \leq L$

-Spectral Element Method (SEM)

-Coupled SEM-NM method

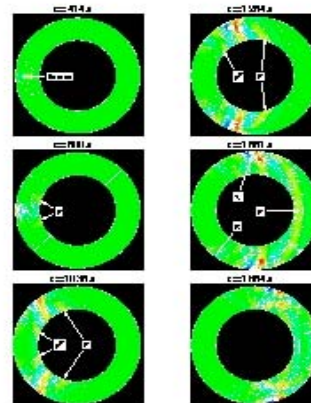
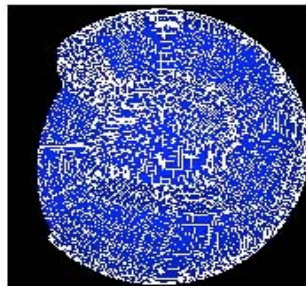
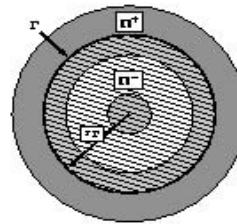


Spectral Element Method: D. Komatitsch (1999)

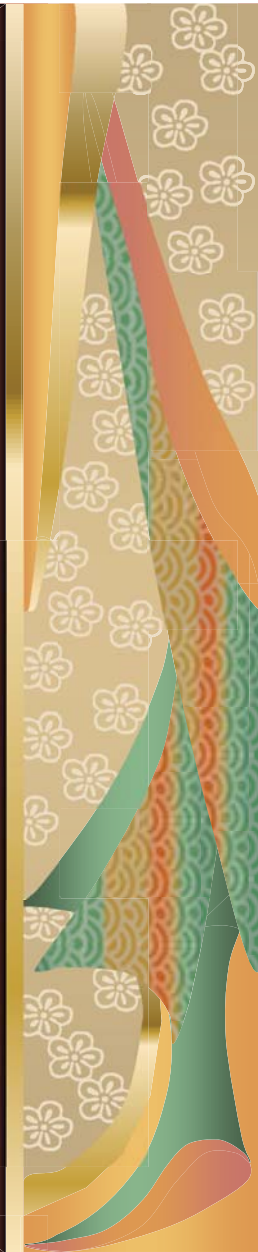
Coupled method of Spectral Elements and Modal Solution

Principle:

- Ω^+ : Spectral Element area:
3D model
- Ω^- : Modal Solution area:
1D model



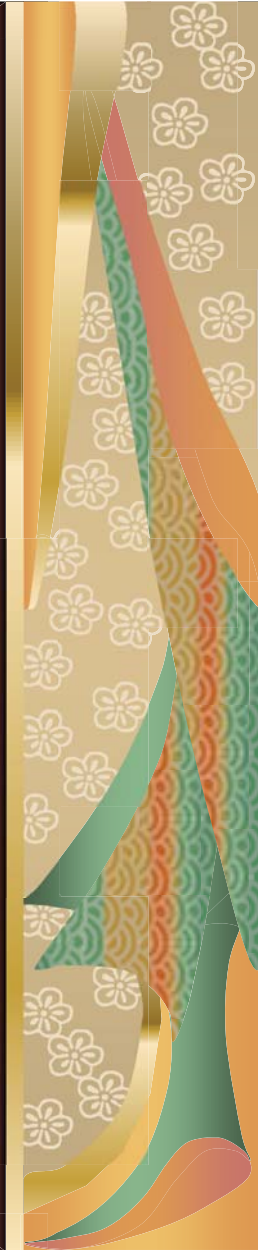
Capdeville et al., 2002



Overview

Large scale Seismology: an observational field

- Data (Seismic source) + Instrument (Seismometer) -> Observations (seismograms)
- Historical evolution: Ray theory, Normal mode theory, Numerical techniques (SEM, NM-SEM)
- Scientific Issues: earthquakes, structure of the Earth and planets
- Seismic Experiment: Plume detection
- NM-SEM and time reversal

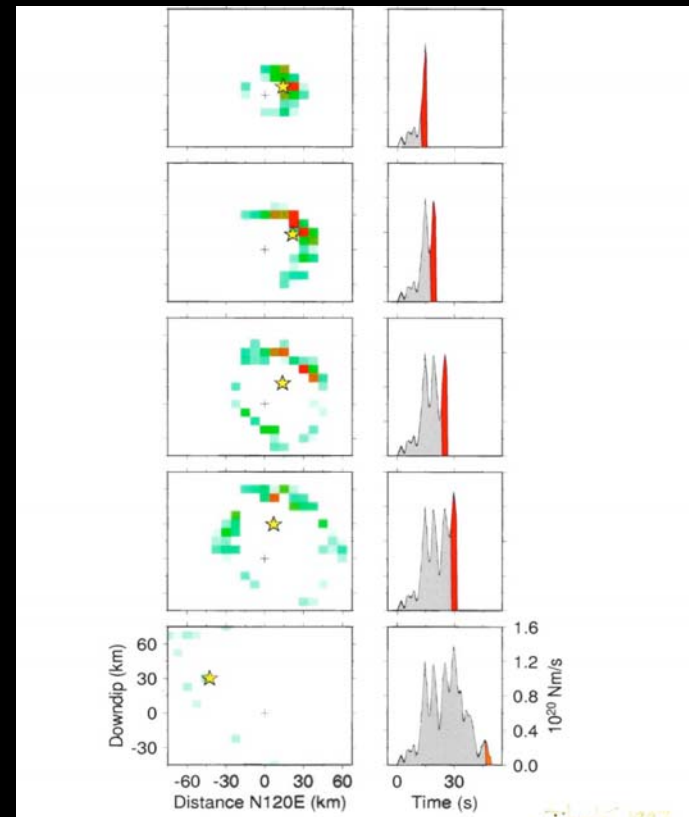
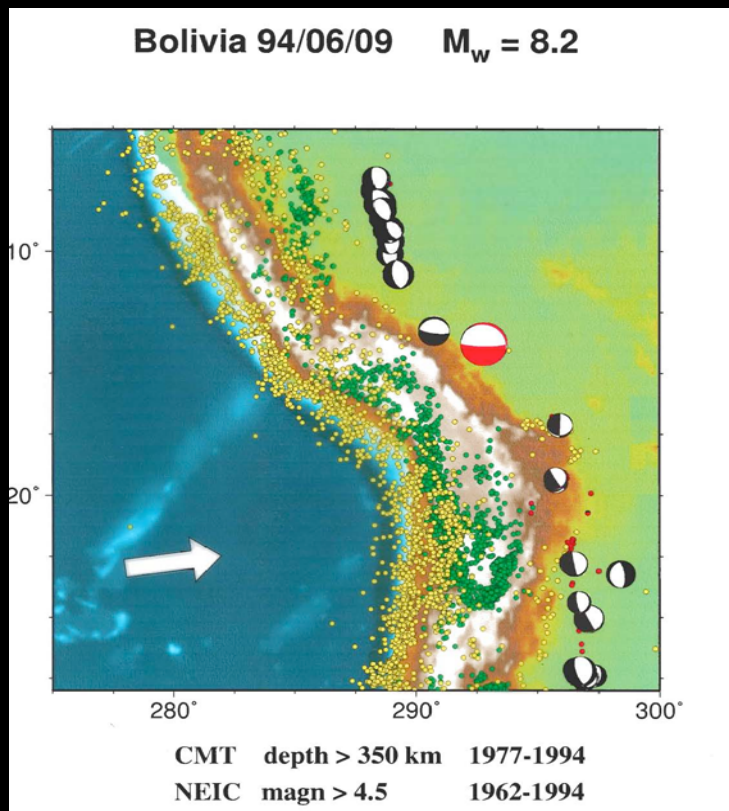


Seismic Source Studies

$$\mathbf{u}(\mathbf{r},t) = \sum_k S_k u_k(\mathbf{r}) \cos \omega_k t / \omega_k^2 \exp(-\omega_k t / 2Q) (\mathbf{u}_k \cdot \mathbf{F})_S$$

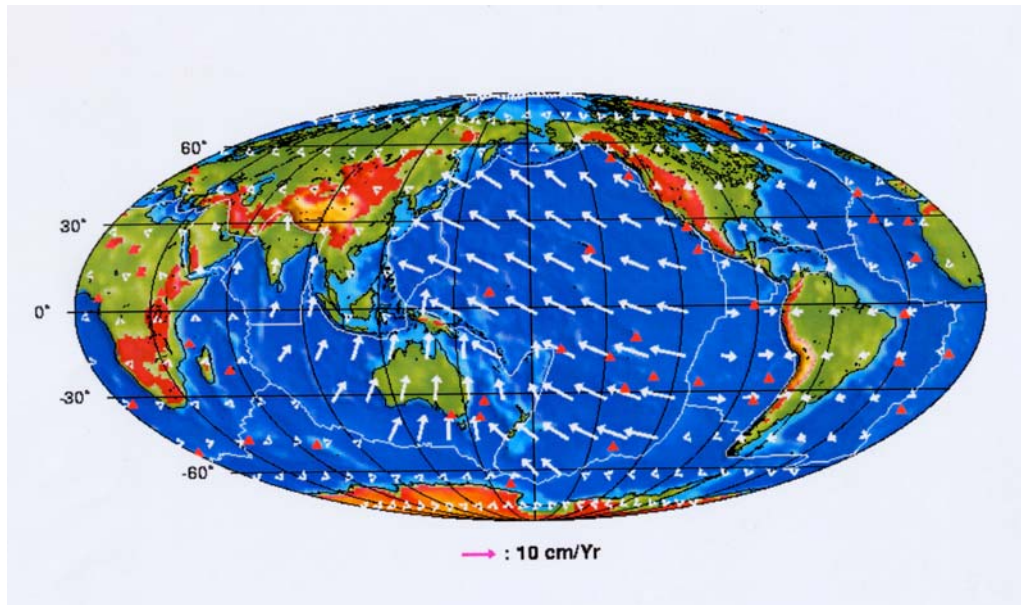
Source Term $(\mathbf{u}_k \cdot \mathbf{F})_S = (\mathbf{M} : \mathbf{e})_S$

\mathbf{M} Seismic moment tensor, \mathbf{e} deformation tensor

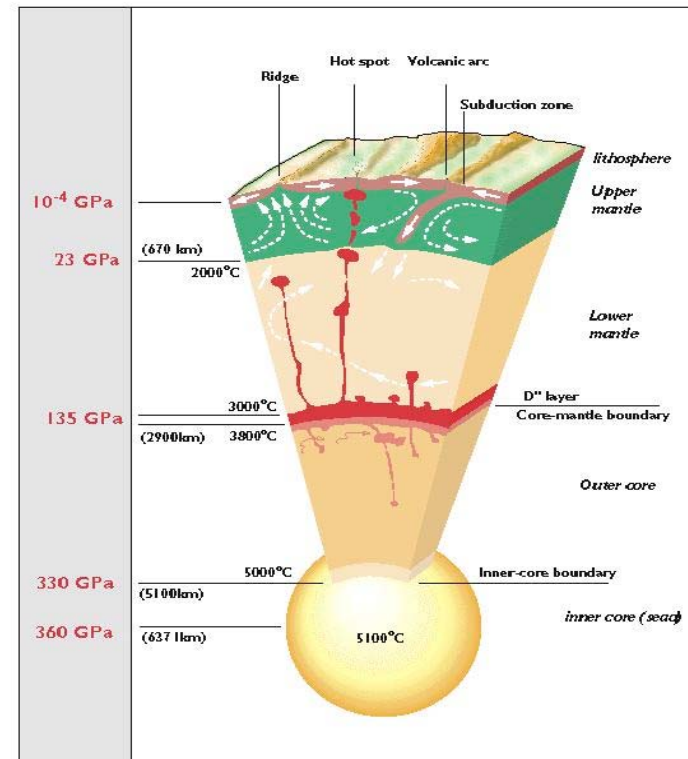


Structure of the Earth

Plate tectonics



Mantle Convection



Tomographic Technique

■ Forward Problem: Theory $\mathbf{d}=\mathbf{g}(\mathbf{p})$

\mathbf{d} data space, \mathbf{p} parameter space

- Reference Earth model \mathbf{p}_0 :

$$\mathbf{d}_0 = \mathbf{g}(\mathbf{p}_0)$$

- Kernels $\leq \mathbf{g} / \leq \mathbf{p}$

- Cd function (or matrix) of covariance of data

■ Inverse Problem: $\mathbf{p}-\mathbf{p}_0 = \mathbf{g}^{-1} (\mathbf{d}-\mathbf{d}_0)$

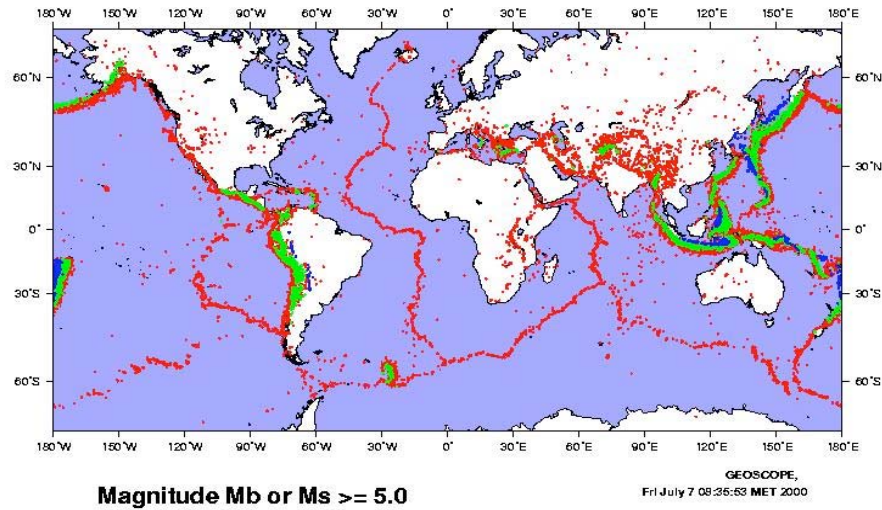
- \mathbf{C}_{p_0} a priori Covariance function of parameters

- \mathbf{C}_{pf} a posteriori Covariance function of parameters

- R Resolution



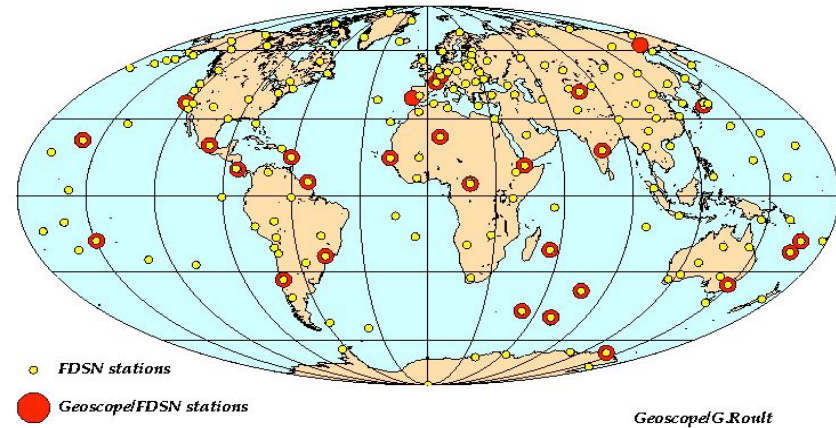
Global seismicity 1928-1999



Receivers

Seismic sources

GEOSCOPE stations and FDSN stations

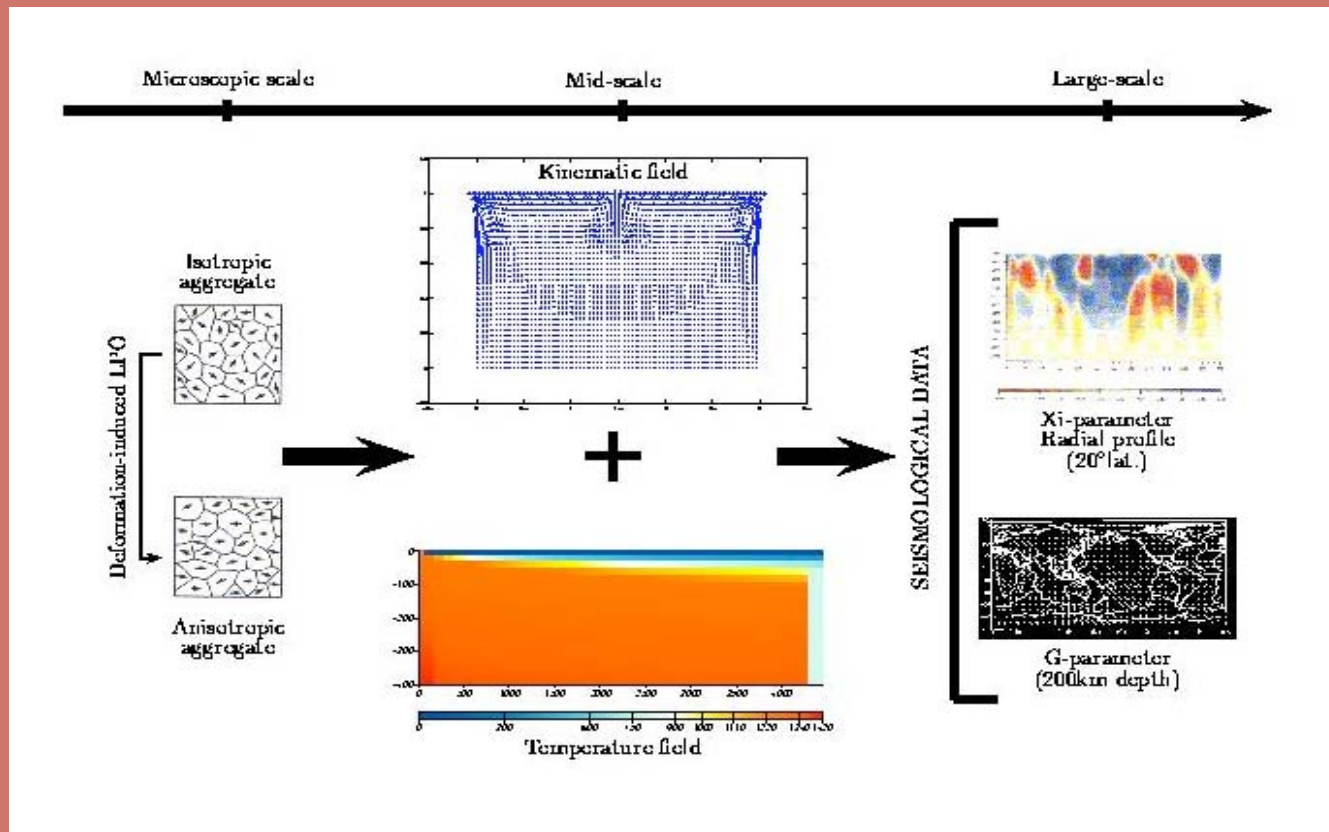




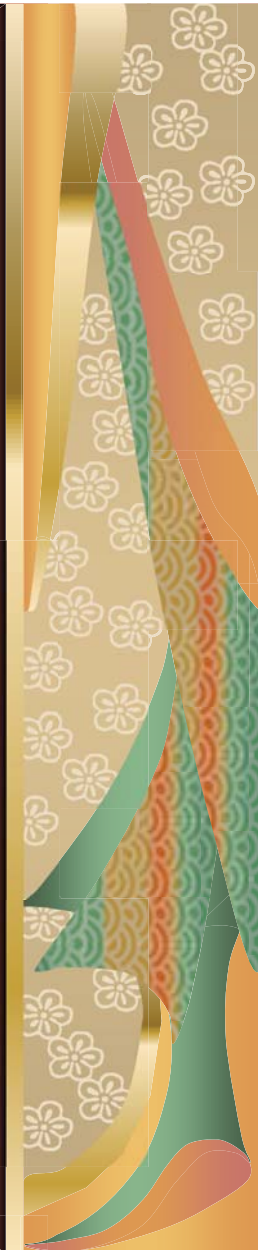
Importance of seismic anisotropy

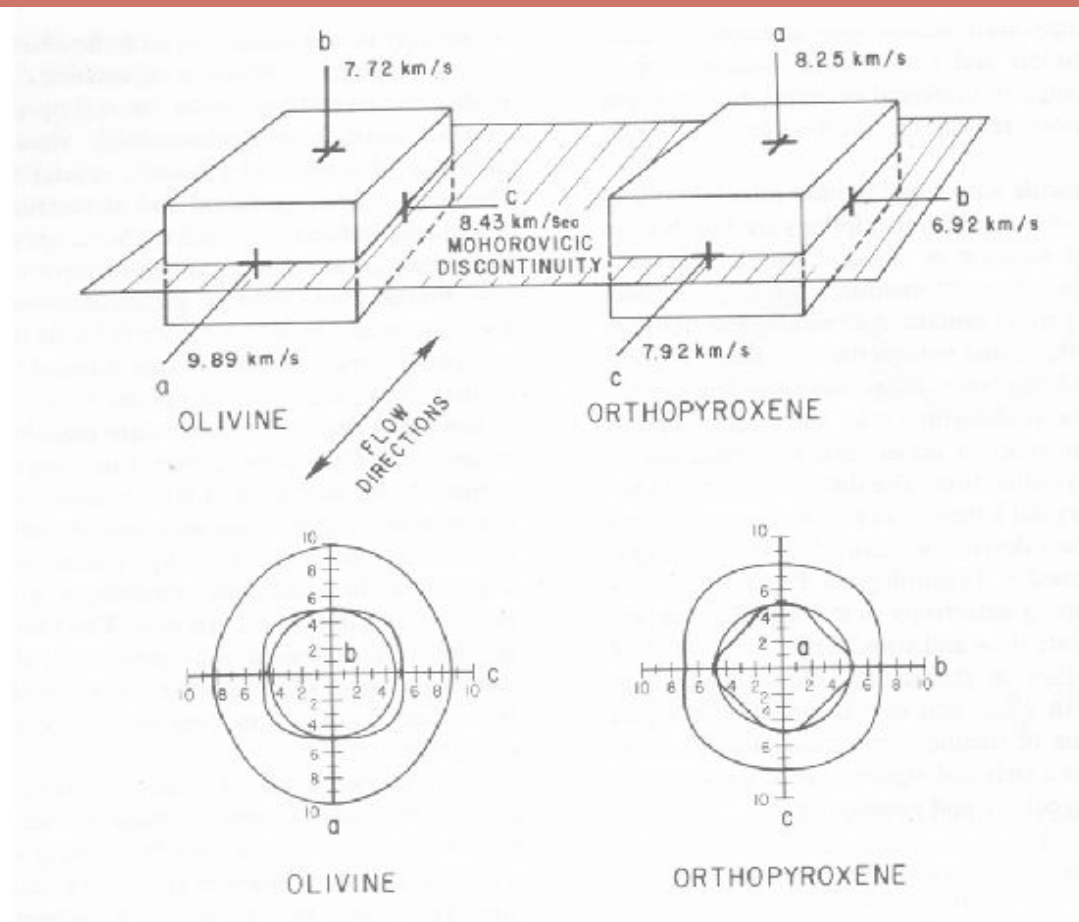
ANISOTROPY is the Rule not the Exception

Seismic Anisotropy is present at all scales



(Montagner and Guillot, 2001)



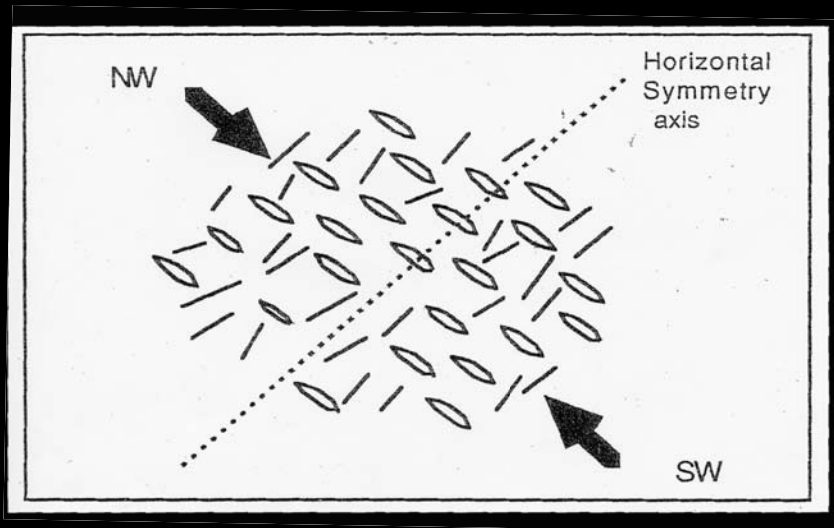


From Christensen and Lundquist, 1982



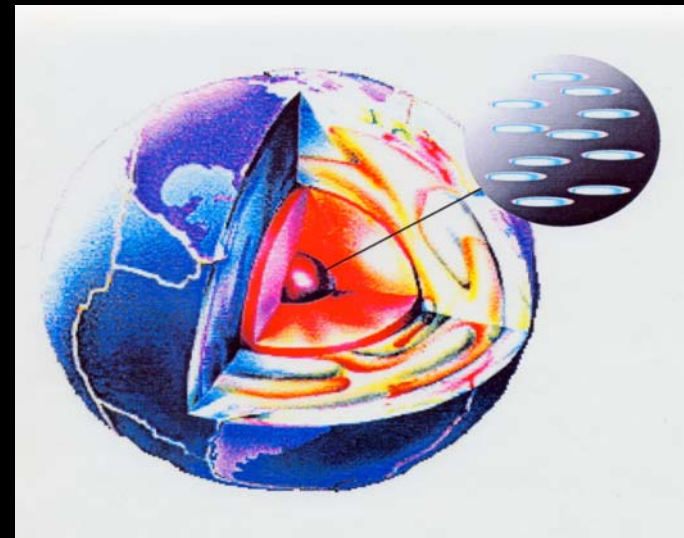
Cracks, fluid inclusions

Crust



(Babuska and Cara, 1991)

Inner core



(Singh et al., 2001)

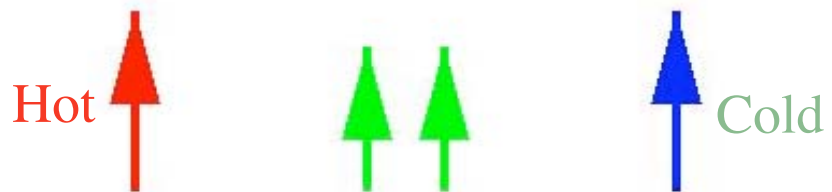
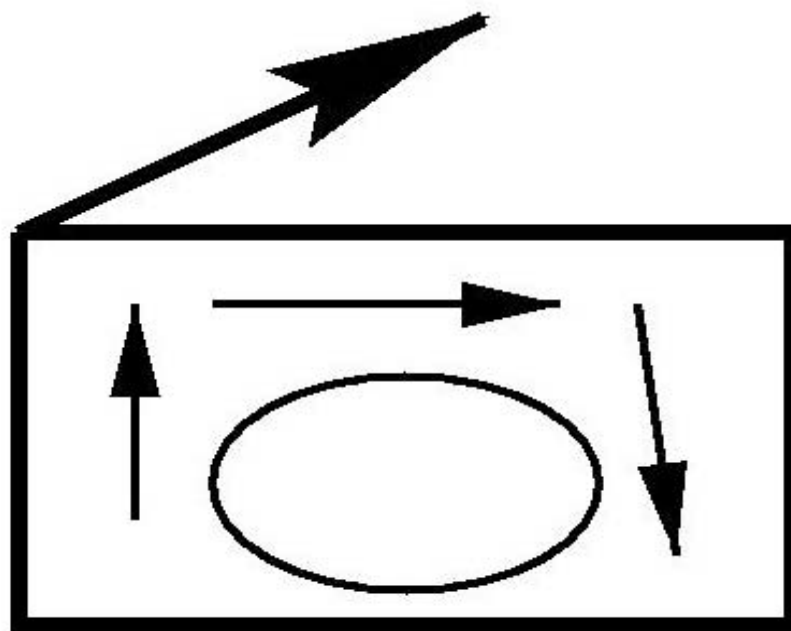


Importance of seismic anisotropy **ANISOTROPY is the Rule not the Exception**

Anisotropy is present at all scales

- From microscopic scale up to macroscopic scale**
- Efficient mechanisms of alignment
(L.P.O.: lattice preferred orientation
S.P.O.: shape preferred orientation; fine layering)**

Montagner & Guillot, 2001



$\Delta\alpha$ Effect of Mineral Orientation

ΔT Effect of Temperature Heterogeneities

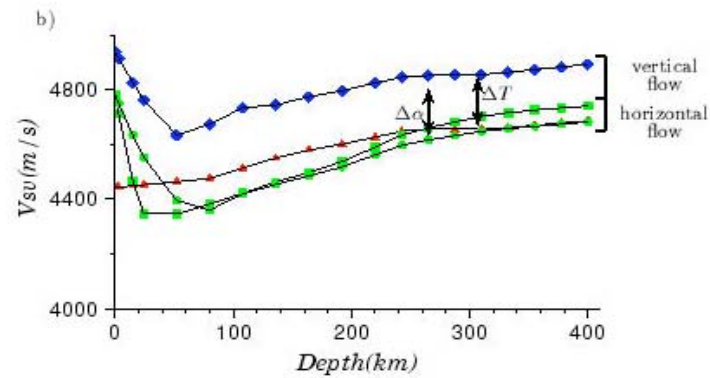
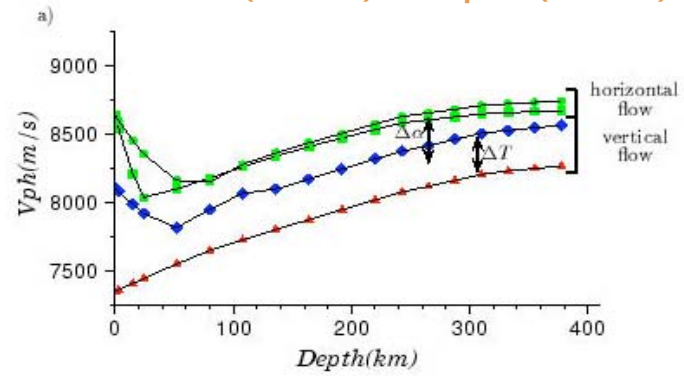


Da: Anisotropy
Effect

DT: Temperature
Effect

$$Da \approx DT$$

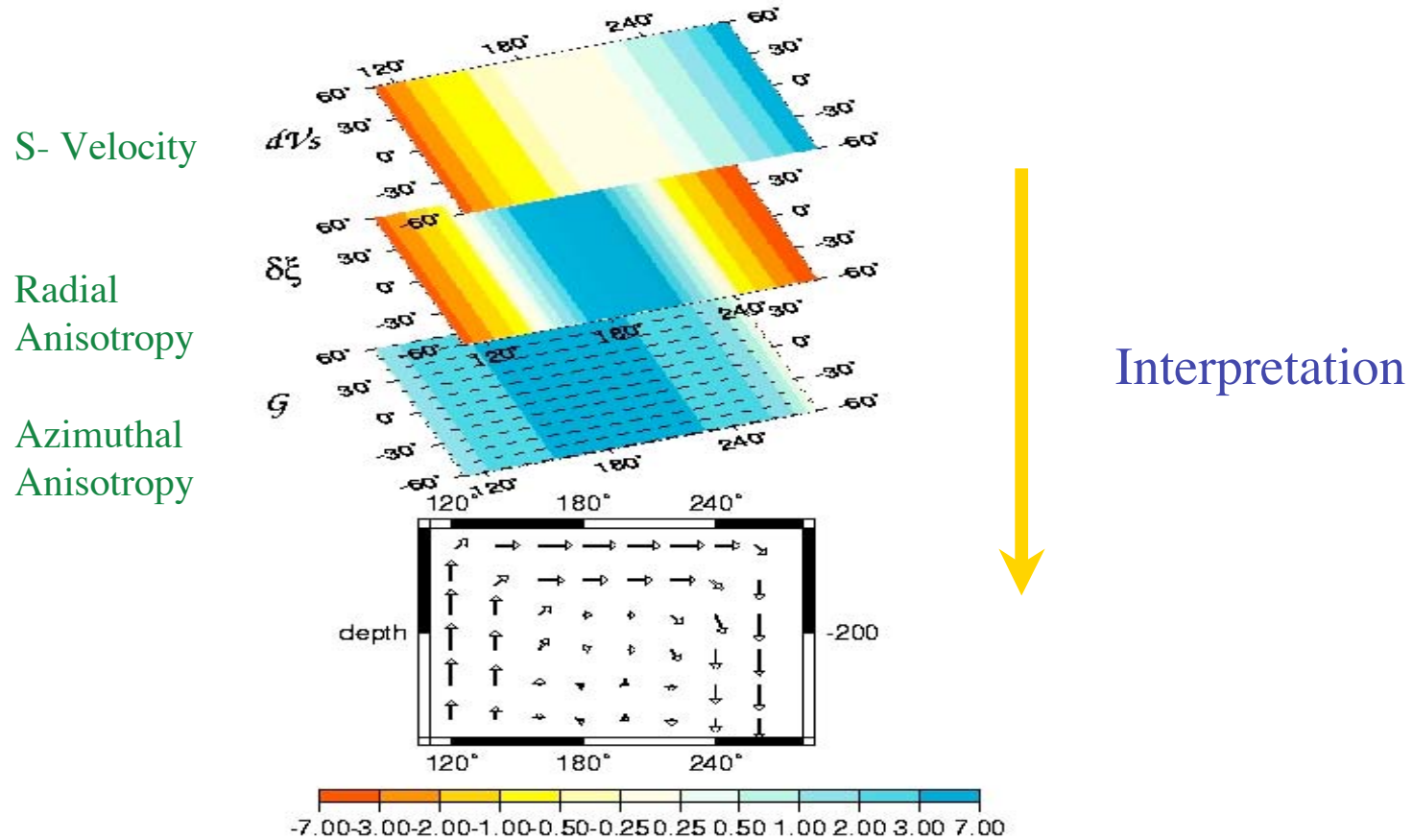
OI (60%) + Opx (40%)



Montagner & Guillot, 2001



Convective cell: anisotropic parameters



Anisotropy is observed on different kinds of seismic waves

- Body waves (Pn, Shear wave splitting)
- Surface waves (Rayleigh-Love discrepancy; Azimuthal anisotropy)



Importance of seismic anisotropy **ANISOTROPY is the Rule not the Exception**



Anisotropy is present at all scales

- from microscopic scale to macroscopic scale
- Efficient mechanisms of alignment
(L.P.O.: lattice preferred orientation
S.P.O.: shape preferred orientation; fine layering)

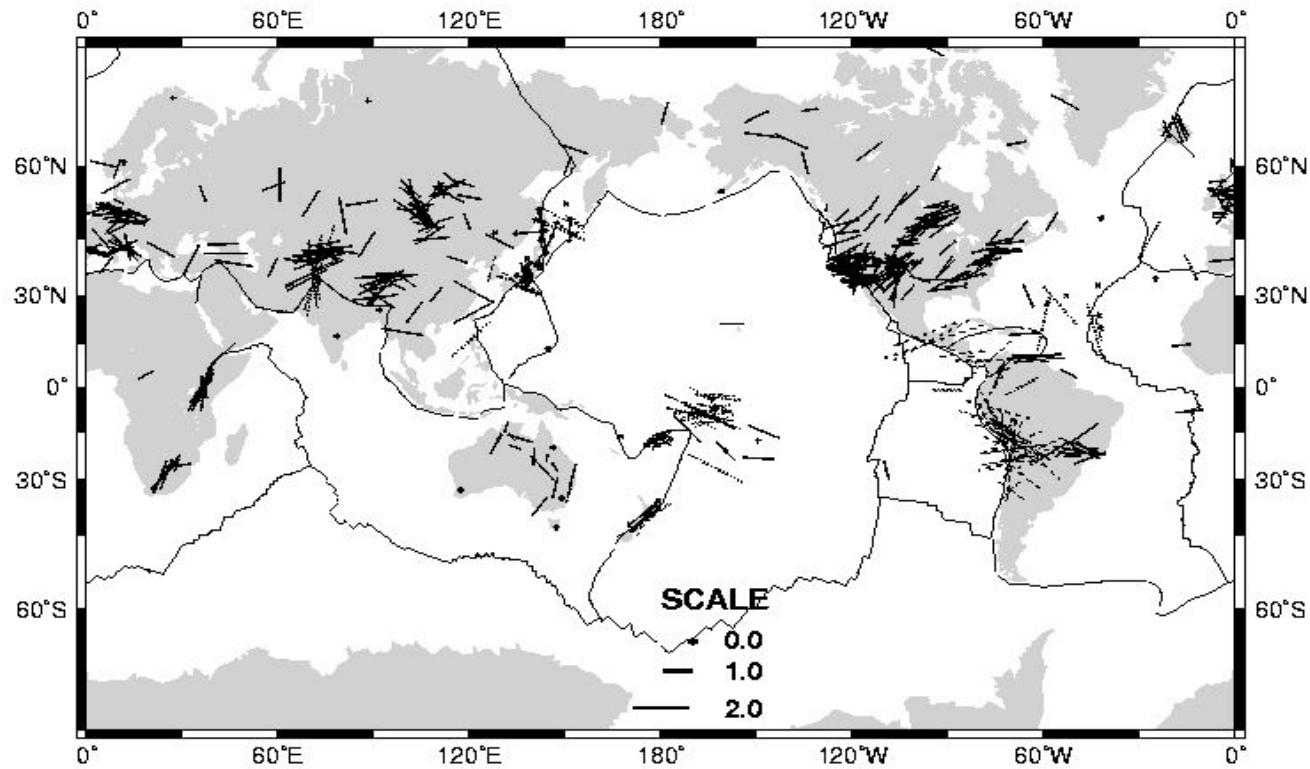
Anisotropy is observed on different kinds of seismic waves

- Body waves (Pn; S-wave splitting)
- Surface waves (Rayleigh-Love discrepancy, azimuthal anisotropy)

ANISOTROPY REFLECTS AN INNER ORGANIZATION

ANISOTROPY IS NOT A SECOND ORDER EFFECT

Compilation of S-wave splitting measurements



Savage, Rev. Geophys., 1999

Effect of anisotropy on surface waves

$$\frac{\delta\omega_k}{\omega_k} = \frac{\int_V \epsilon_{ij}^* \delta C_{ijpq} \epsilon_{pq} dV}{\int_V \rho_0 u_r^* u_r dV}$$

ω_k eigenfrequency corresponding to multiplet $k = \{n, l, m\}$

ϵ strain tensor, u displacement, δC elastic tensor perturbation.

- Phase velocity $v(\omega, \theta, \phi, \Psi)$ at $\mathbf{r}(\theta, \phi, r)$ (Smith & Dahlen, 1973)

$$v(\omega, \theta, \phi, \Psi) = A_0(\omega, \theta, \phi) + A_1(\omega, \theta, \phi) \cos 2\Psi + A_2(\omega, \theta, \phi) \sin 2\Psi + A_3(\omega, \theta, \phi) \cos 4\Psi + A_4(\omega, \theta, \phi) \sin 4\Psi$$

Ψ azimuth (angle between North and wave vector).

The first order perturbation in Love wave phase velocity $\delta C_L(k, \Psi)$ can be expressed as:

$$\delta C_L(k, \Psi) = \frac{1}{2C_{0L}(k)} [L_1(k) + L_2(k)\cos 2\Psi + L_3(k)\sin 2\Psi + L_4(k)\cos 4\Psi + L_5(k)\sin 4\Psi]$$

where

$$\begin{aligned}
 & L_0(k) = \int_0^\infty \rho W^2 dz \\
 0\Psi \leftarrow & L_1(k) = \frac{1}{L_0} \int_0^\infty (W^2 dN + \frac{W'^2}{k^2} dL) dz \\
 2\Psi \leftarrow & \begin{cases} L_2(k) = \frac{1}{L_0} \int_0^\infty -G_c(\frac{W'^2}{k^2}) dz \\ L_3(k) = \frac{1}{L_0} \int_0^\infty -G_s(\frac{W'^2}{k^2}) dz \end{cases} \\
 4\Psi \leftarrow & \begin{cases} L_4(k) = \frac{1}{L_0} \int_0^\infty -E_c \cdot W^2 dz \\ L_5(k) = \frac{1}{L_0} \int_0^\infty -E_s \cdot W^2 dz \end{cases}
 \end{aligned}$$

The same procedure holds for Rayleigh waves, starting from the displacement given previously.

$$\delta C_R(k, \Psi) = \frac{1}{2C_{0R}(k)} [R_1(k) + R_2(k)\cos 2\Psi + R_3(k)\sin 2\Psi + R_4(k)\cos 4\Psi + R_5(k)\sin 4\Psi]$$

where

$$\begin{aligned} R_0(k) &= \int_0^\infty \rho(U^2 + V^2)dz \\ R_1(k) &= \frac{1}{R_0} \int_0^\infty [V^2 dA + \frac{U^2}{k^2} .dC + \frac{2U'V}{k} .dF + (\frac{V'}{k} - U)^2 dL] dz \\ R_2(k) &= \frac{1}{R_0} \int_0^\infty [V^2 .B_c + \frac{2U'V}{k} .H_c + (\frac{V'}{k} - U)^2 G_c] dz \\ R_3(k) &= \frac{1}{R_0} \int_0^\infty [V^2 .B_s + \frac{2U'V}{k} .H_s + (\frac{V'}{k} - U)^2 G_s] dz \\ R_4(k) &= \frac{1}{R_0} \int_0^\infty E_c .V^2 dz \\ R_5(k) &= \frac{1}{R_0} \int_0^\infty E_s .V^2 dz \end{aligned}$$

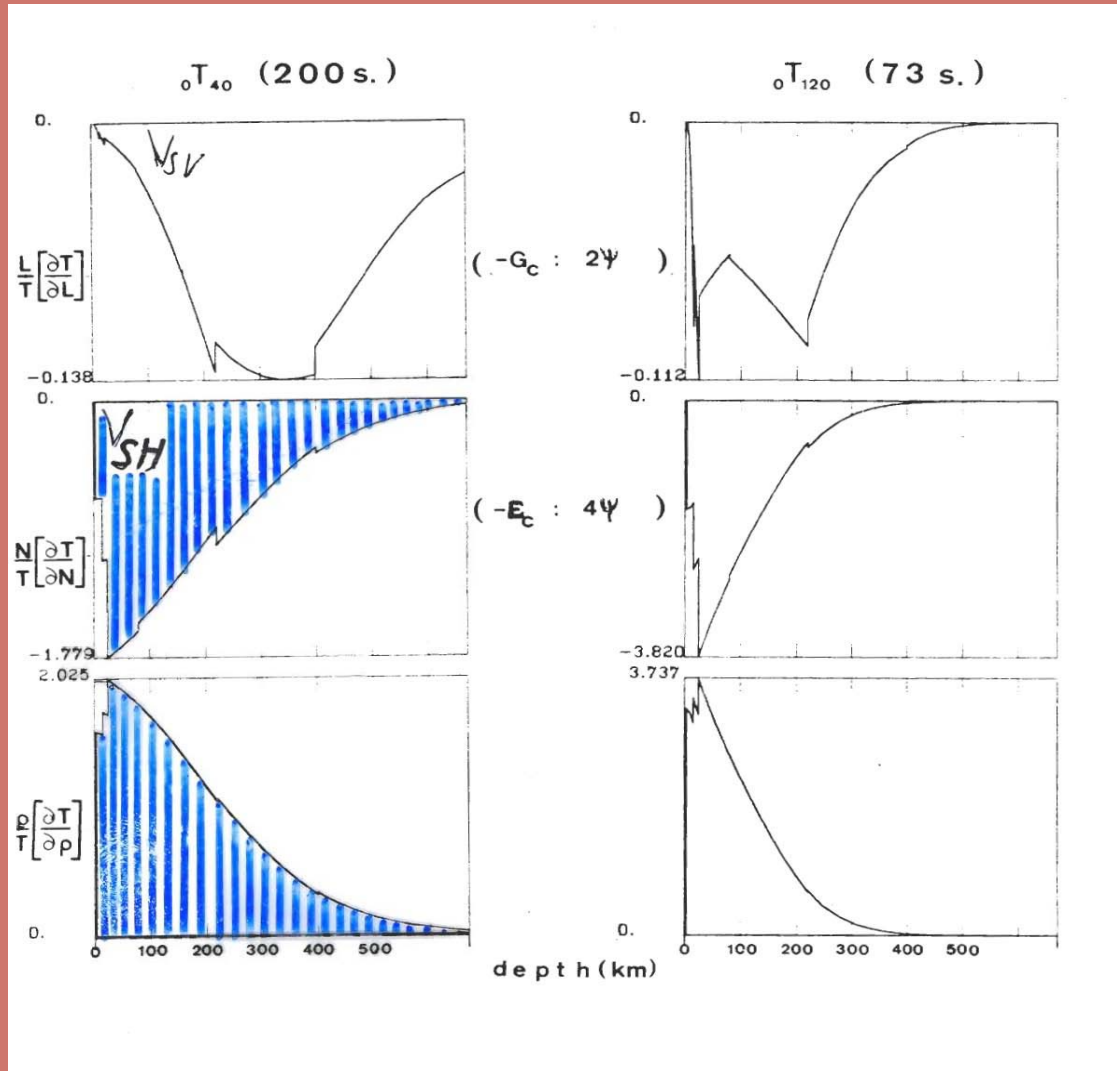
The 13 depth-functions $A, C, F, L, N, B_c, B_s, H_c, H_s, G_c, G_s, E_c, E_s$ are linear combinations of the elastic coefficients C_{ij} and are explicitly given as follows:

Table 1: Calculation of the various $c_{ij}\epsilon_i\epsilon_j$ for Love waves
 $\alpha = \cos\Psi$; $\beta = \sin\Psi$

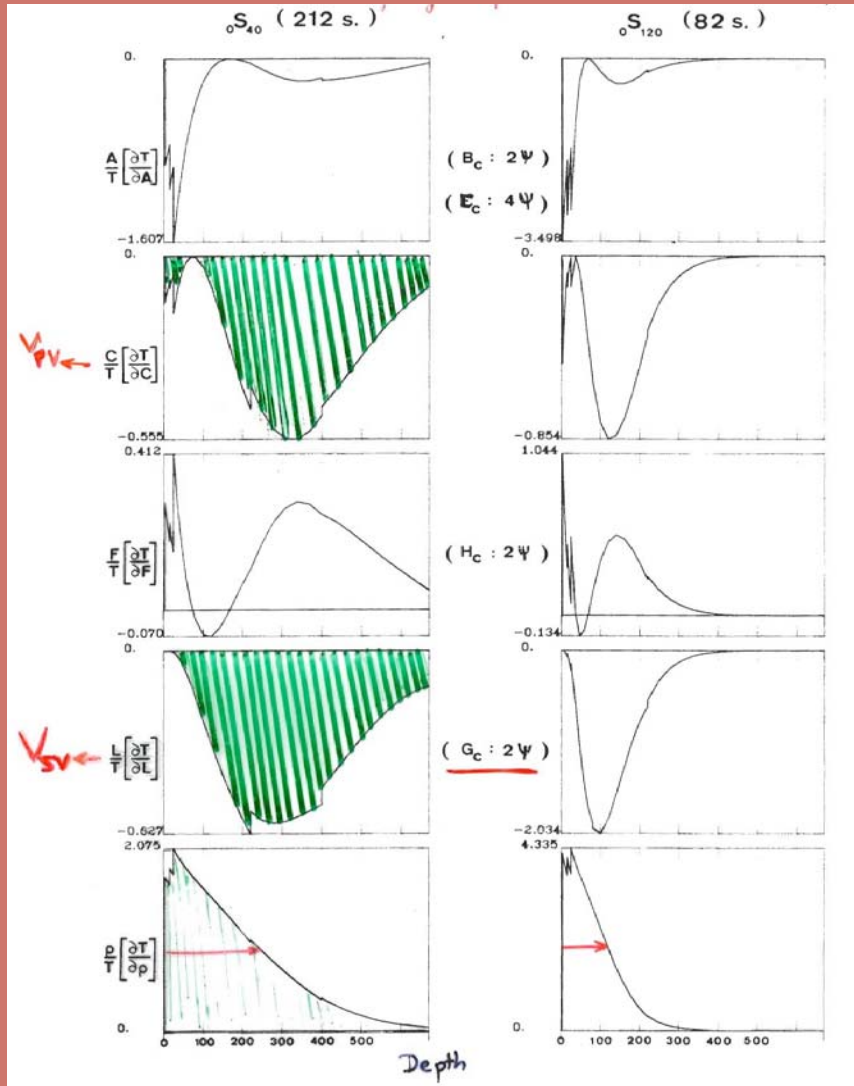
n	ij	$c_{ij}\epsilon_i\epsilon_j$
1	11	$c_{11}\alpha^2\beta^2.k^2W^2$
1	22	$c_{22}\alpha^2\beta^2.k^2W^2$
1	33	0
2	12	$-c_{12}\alpha^2\beta^2.k^2W^2$
2	13	0
2	23	0
2	24	
4	14	$c_{14}(-i\alpha^2\beta).\frac{kWW'}{2}$
4	15	$c_{15}(i\alpha^2\beta).\frac{kWW'}{2}$
4	16	$c_{16}(-\alpha\beta)(\alpha^2 - \beta^2).\frac{k^2W^2}{2}$
4	24	$c_{24}(-i\alpha^2\beta).\frac{kWW'}{2}$
4	25	$c_{25}(-i\alpha\beta^2).\frac{kWW'}{2}$
4	26	$c_{26}(\alpha\beta)(\alpha^2 - \beta^2).\frac{k^2W^2}{2}$
4	34	0
4	35	0
4	36	0
4	44	$c_{44}\alpha^2.\frac{W'^2}{4}$
8	45	$c_{45}(-\alpha\beta).\frac{W'^2}{4}$
8	46	$c_{46}(-i\alpha)(\alpha^2 - \beta^2).\frac{kWW'}{2}$
4	55	$c_{55}\beta^2.\frac{W'^2}{4}$
8	56	$c_{56}(i\beta)(\alpha^2 - \beta^2).\frac{kWW'}{2}$
4	66	$c_{66}(\alpha^2 - \beta^2).\frac{k^2W^2}{4}$



Love wave partial derivatives



Rayleigh wave partial derivatives



0Ψ term	$A = \frac{3}{8}(C_{11} + C_{22}) + \frac{1}{4}C_{12} + \frac{1}{2}C_{66}$	V_{PH}
	$C = C_{33}$	
	$F = \frac{1}{2}(C_{13} + C_{23})$	
	$L = \frac{1}{2}(C_{44} + C_{55})$	V_{SV}
	$N = \frac{1}{8}(C_{11} + C_{22}) - \frac{1}{4}C_{12} + \frac{1}{2}C_{66}$	V_{SH}
	cos	sin
2Ψ term	$B_c = \frac{1}{2}(C_{11} - C_{22})$	$B_s = C_{16} + C_{26} \rightarrow B$
	$G_c = \frac{1}{2}(C_{55} - C_{44})$	$G_s = C_{54} \rightarrow G$
	$H_c = \frac{1}{2}(C_{13} - C_{23})$	$H_s = C_{36} \rightarrow H$
4Ψ term	$E_c = \frac{1}{8}(C_{11} + C_{22}) - \frac{1}{4}C_{12} - \frac{1}{2}C_{66}$	$E_s = \frac{1}{2}(C_{16} - C_{26}) \rightarrow E$

- 1: horizontal direction **North**
- 2: horizontal direction perpendicular to 1-axis
- 3: vertical direction

$$B = \sqrt{B_c^2 + B_s^2}$$

$$G = \sqrt{G_c^2 + G_s^2}$$

$$H = \sqrt{H_c^2 + H_s^2}$$

$$E = \sqrt{E_c^2 + E_s^2}$$

Montagner and Nataf, 1986



- Best Resolved parameters for Surface Waves

$L = \rho V_{SV}^2$ Isotropic part of V_{SV} .

$\xi = \frac{N}{L} = \frac{V_{SH}^2}{V_{SV}^2}$ Radial Anisotropy.

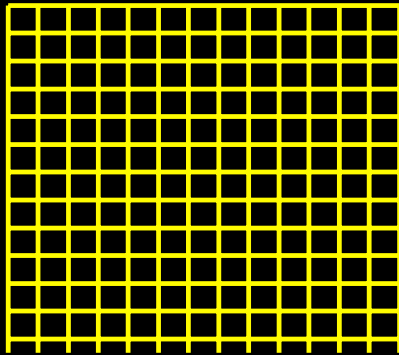
G, Ψ_G Azimuthal Anisotropy of V_{SV} , also related to SKS splitting (when horizontal symmetry axis).

- Body Waves (*Crampin, 1984*)

$$\rho V_{qSV}^2 = L + G_c \cos 2\Psi + G_s \sin 2\Psi$$

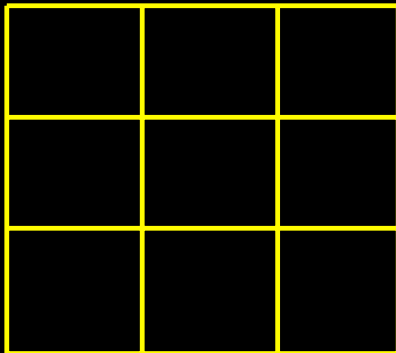
$$\rho V_{qSH}^2 = N - E_c \cos 4\Psi - E_s \sin 4\Psi$$

Isotropic Inversion



N independent parameters
0-Y term
VR1
Variance reduction

Anisotropic inversion



$3N' = N$
0+2 Y term
VR2

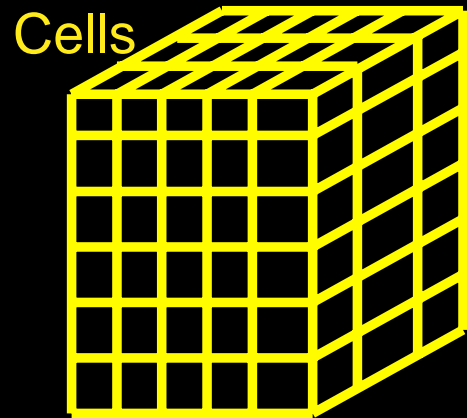
$VR2 > VR1 \Rightarrow$ the anisotropic model can be simpler than the isotropic model



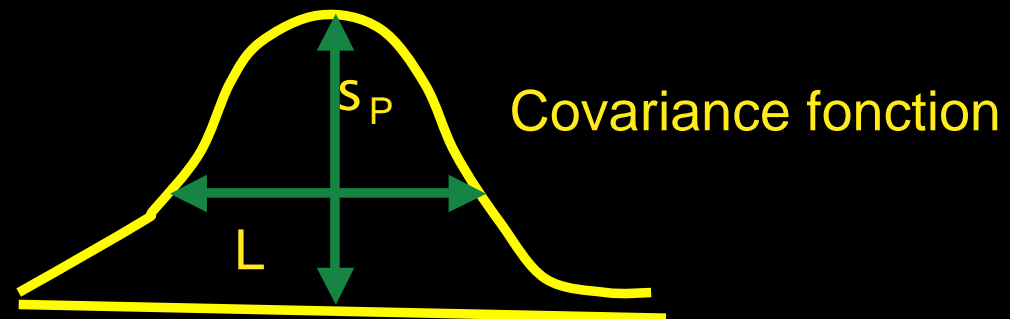
Parameter Space

Physical parameters: $r + 13$ physical parameters

Geographical parameterization: $\mathbf{p}(r, q, f)$



Continuous parameterization

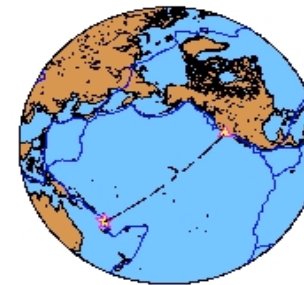
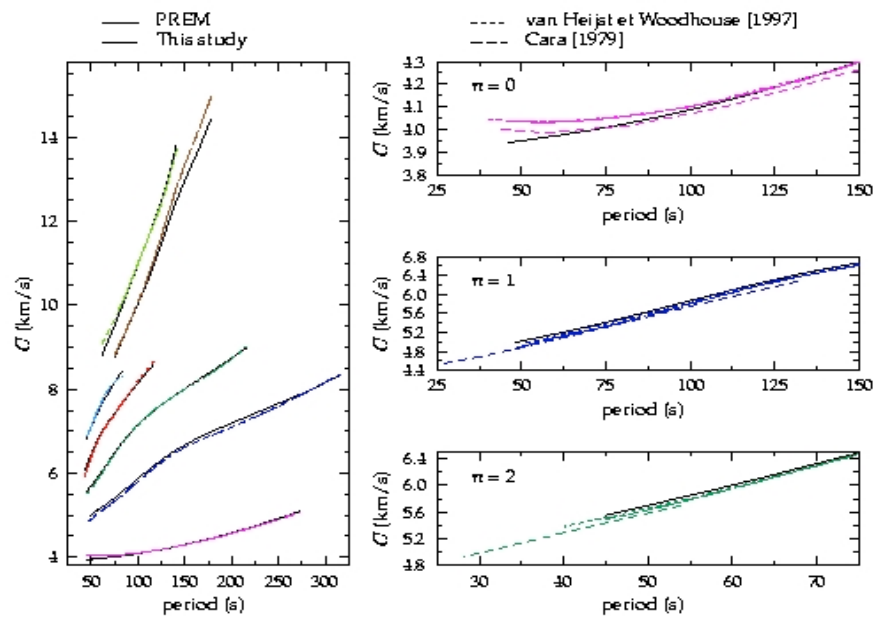


- Spherical harmonic expansion

- Lateral resolution:

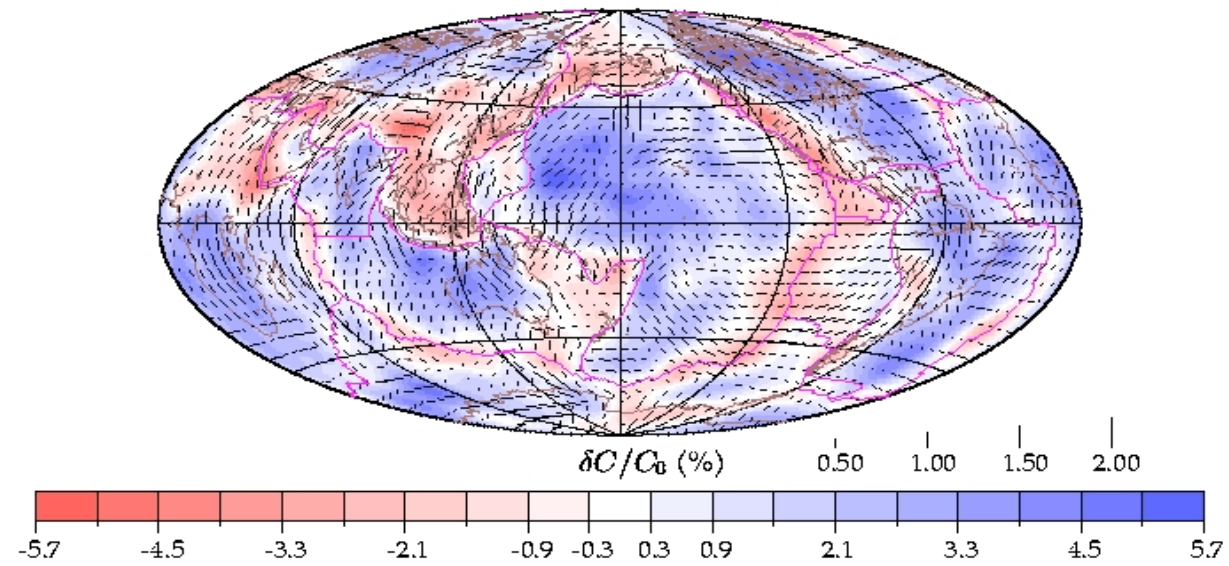
Hor 1000km, Rad 50km $\Rightarrow 500 \cdot 60 \cdot 14 \leq 420,000$ parameters

Calculation of dispersion curves: Fundamental modes and higher modes



Comparison with previous results along the Vanuatu-California path.

Beucler et al., 2002



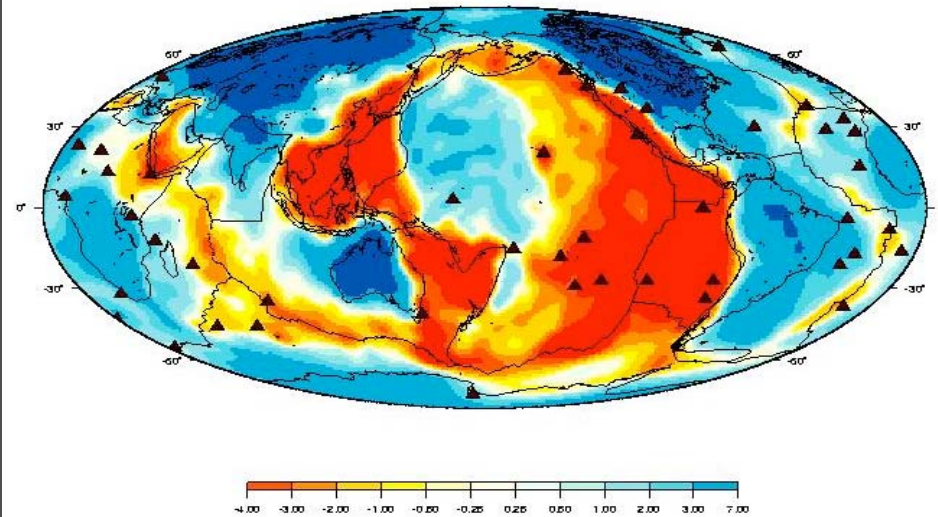
Anisotropic model resulting from phase velocities inversion (C.L.A.S.H., including 2Ψ and 4Ψ terms),
 $\alpha = 0$, $T = 50$ s.

Global Tomography

Scale $L \leq 2000\text{km}$ (degree 20)
Seismic wavelength $\lambda \leq 500\text{km}$

⇒ Ray theory applies

Shear wave velocities - depth =
100km

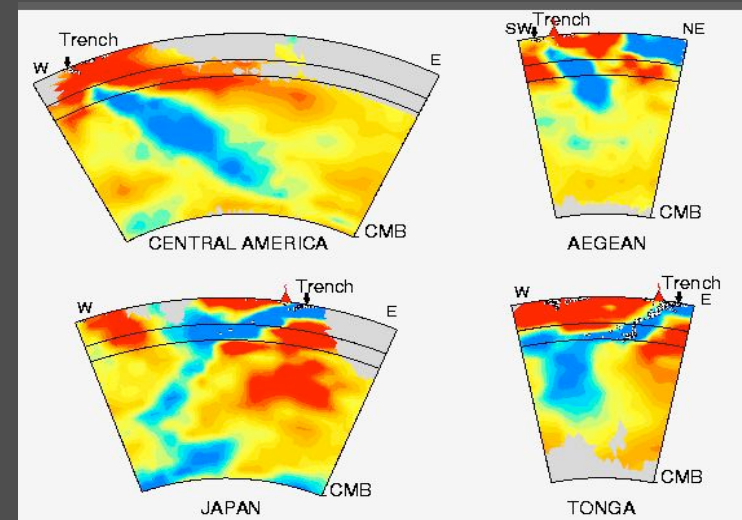
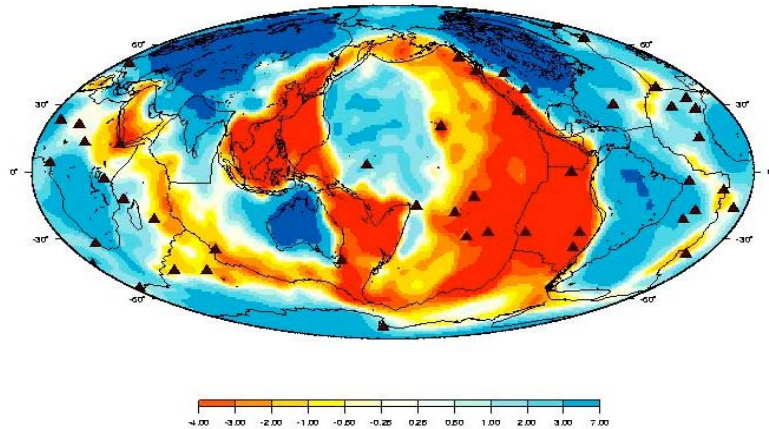


From Global Scale to Regional scale

Scale $L \leq 200\text{-}500\text{km}$

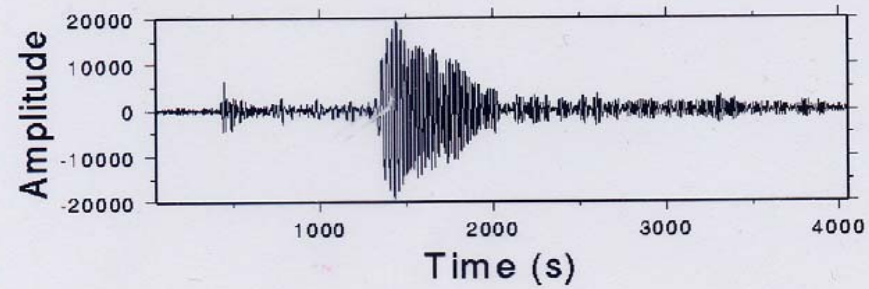
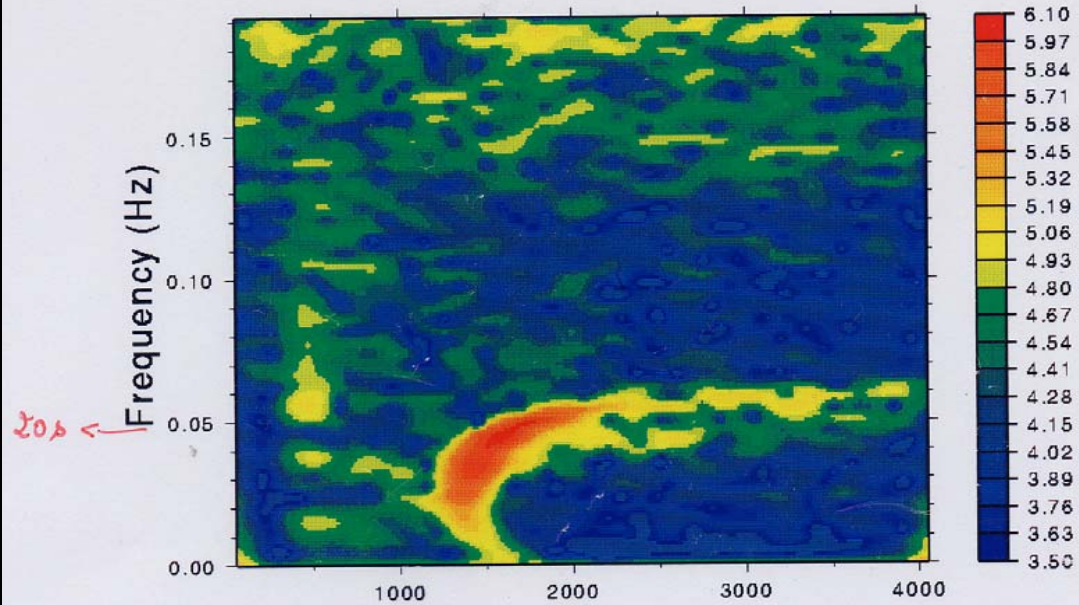
Seismic wavelength $20\text{km} \leq \lambda \leq 500\text{km}$

S-wave velocity -
depth = 100km



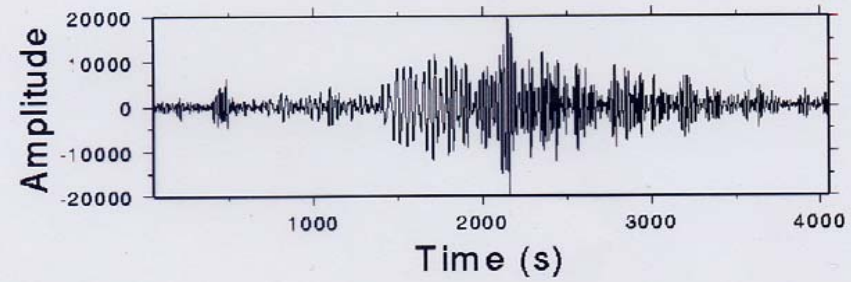
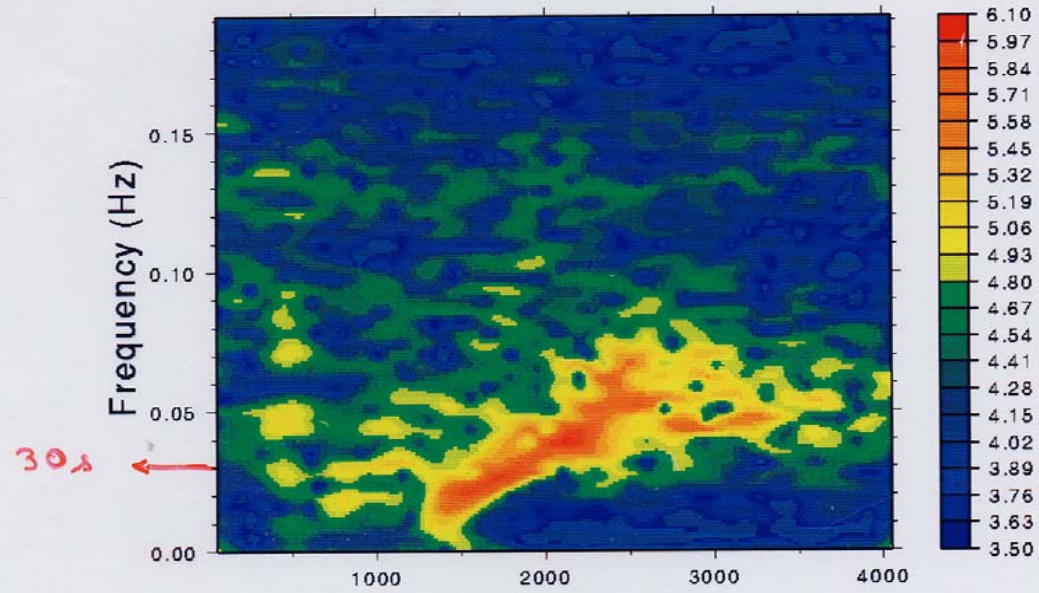
Spectrogram at station PPT (Z component, distance=82 degrees)

Aleutians 1992/03/02 depth=39km ms=6.8



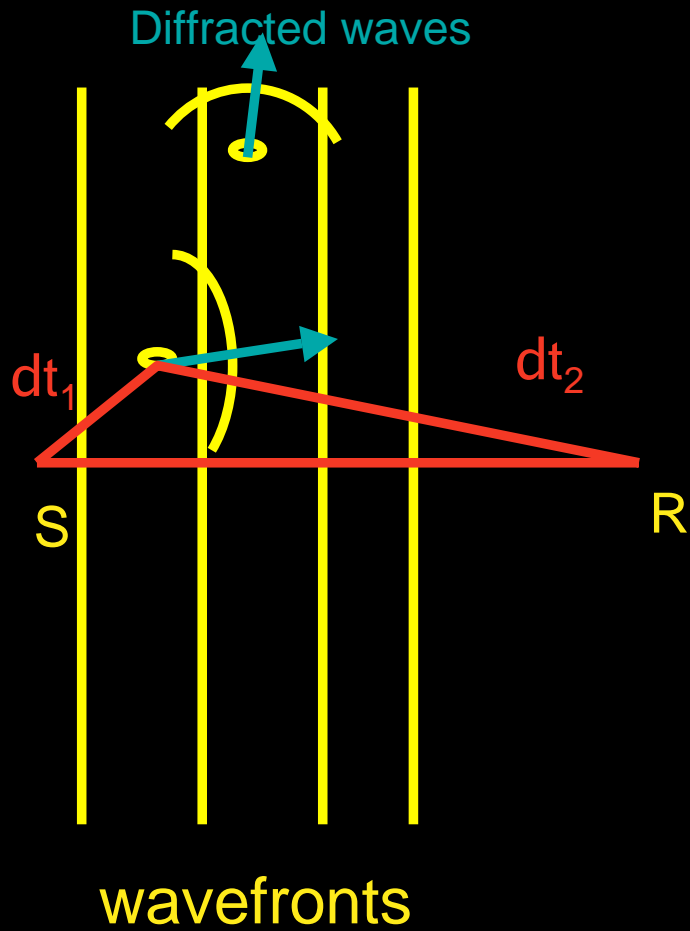
Spectrogram at station SSB (Z component, distance=80 degrees)

Aleutians 1992/03/02 depth=39km ms=6.8

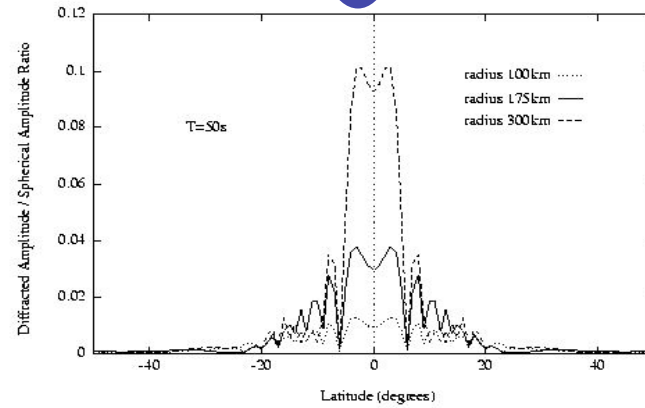
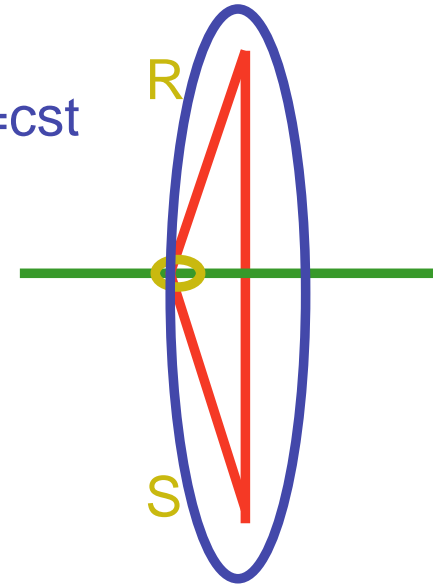


L heterogeneity scale, λ wavelength

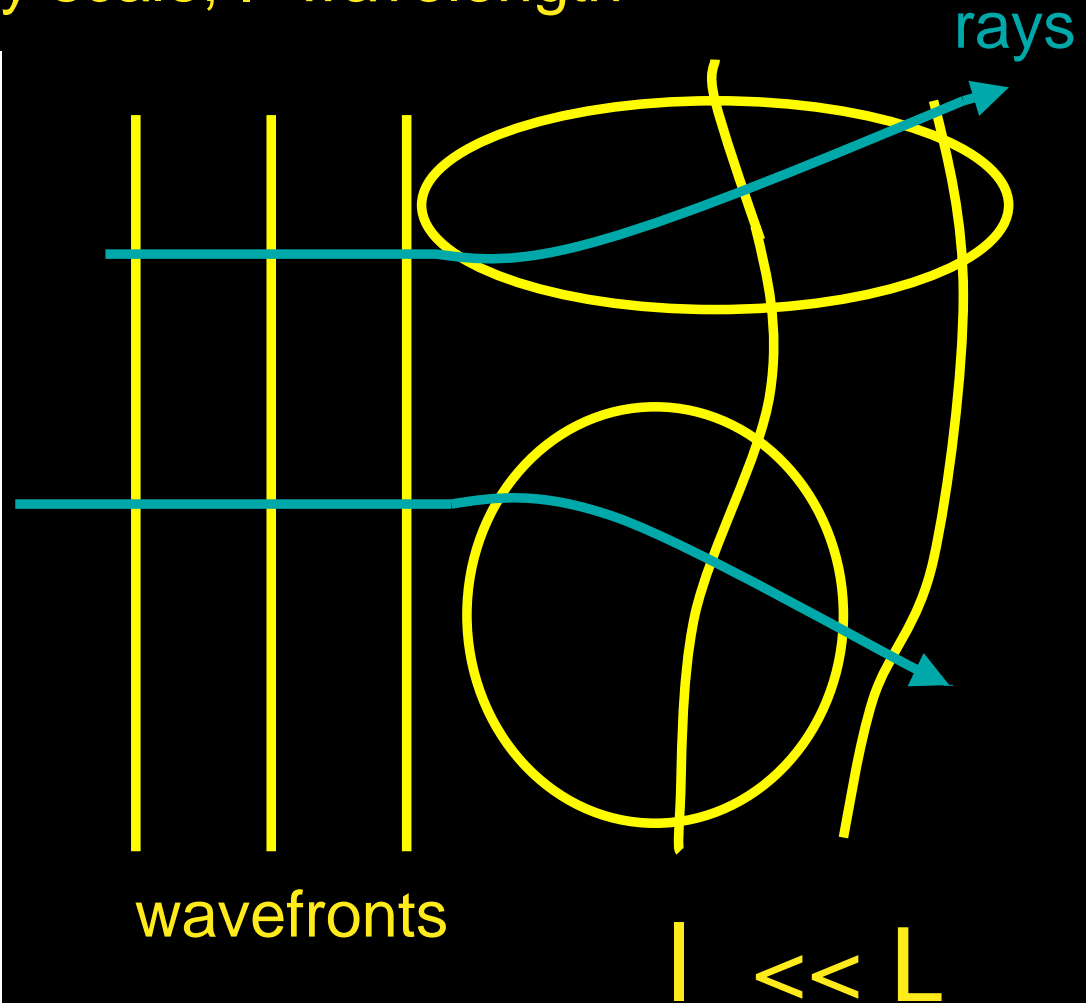
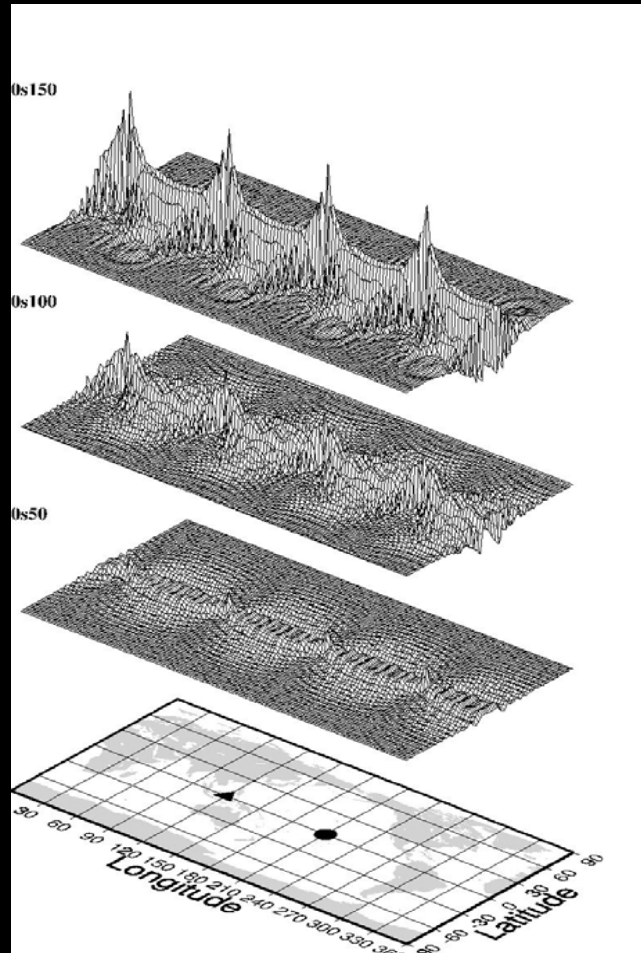
$$\lambda \sim L \text{ or } \lambda \gg L$$



$$dt_1 + dt_2 = cst$$



L heterogeneity scale, l wavelength



Typical scales $L \leq 2,000\text{km}$, $l \leq 500\text{km}$

Overview

Large scale Seismology: an observational field

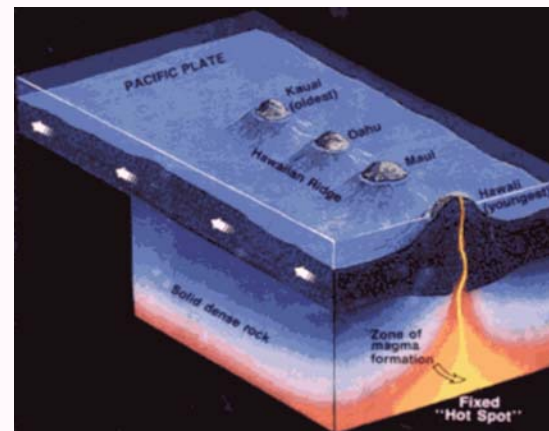
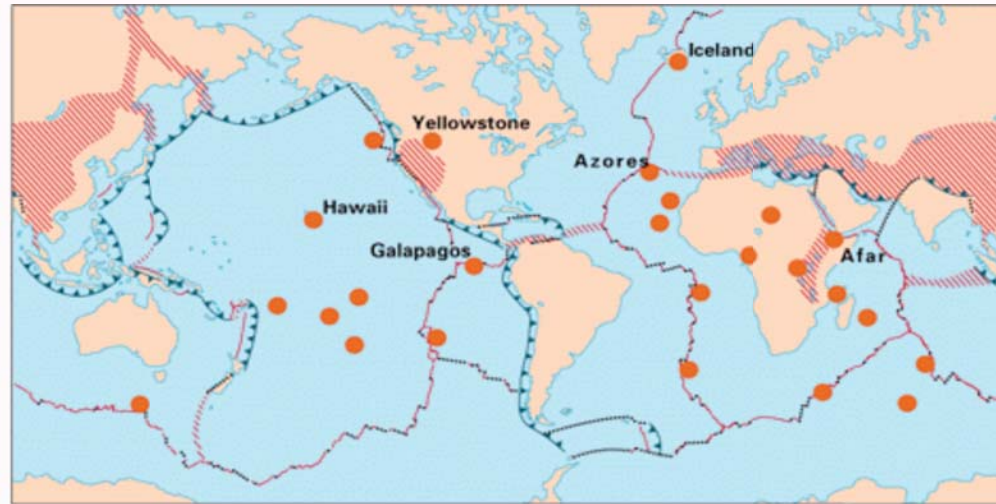
- Data (Seismic source) + Instrument (Seismometer) -> Observations (seismograms)
- Historical evolution: Ray theory, Normal mode theory, Numerical techniques (SEM, NM-SEM)
- Scientific Issues: earthquakes, structure of the Earth and planets
- **Seismic Experiment: Plume detection**
- NM-SEM and time reversal



Hotspots - Plumes

EXPLANATION

- Divergent plate boundaries— Where new crust is generated as the plates pull away from each other.
- Convergent plate boundaries— Where crust is consumed in the Earth's interior as one plate dives under another.
- Transform plate boundaries— Where crust is neither produced nor destroyed as plates slide horizontally past each other.
- ▨ Plate boundary zones— Broad belts in which deformation is diffuse and boundaries are not well defined.
- Selected prominent hotspots



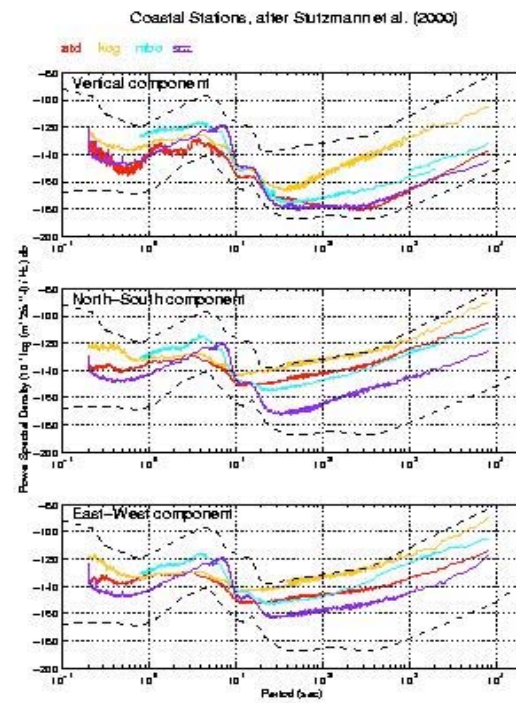


Figure 5c. Power spectral density estimated over noise data from the year 1995 for the three components (vertical: top, North-South: middle and East-West: bottom) of all coastal GEOSCOPE stations.

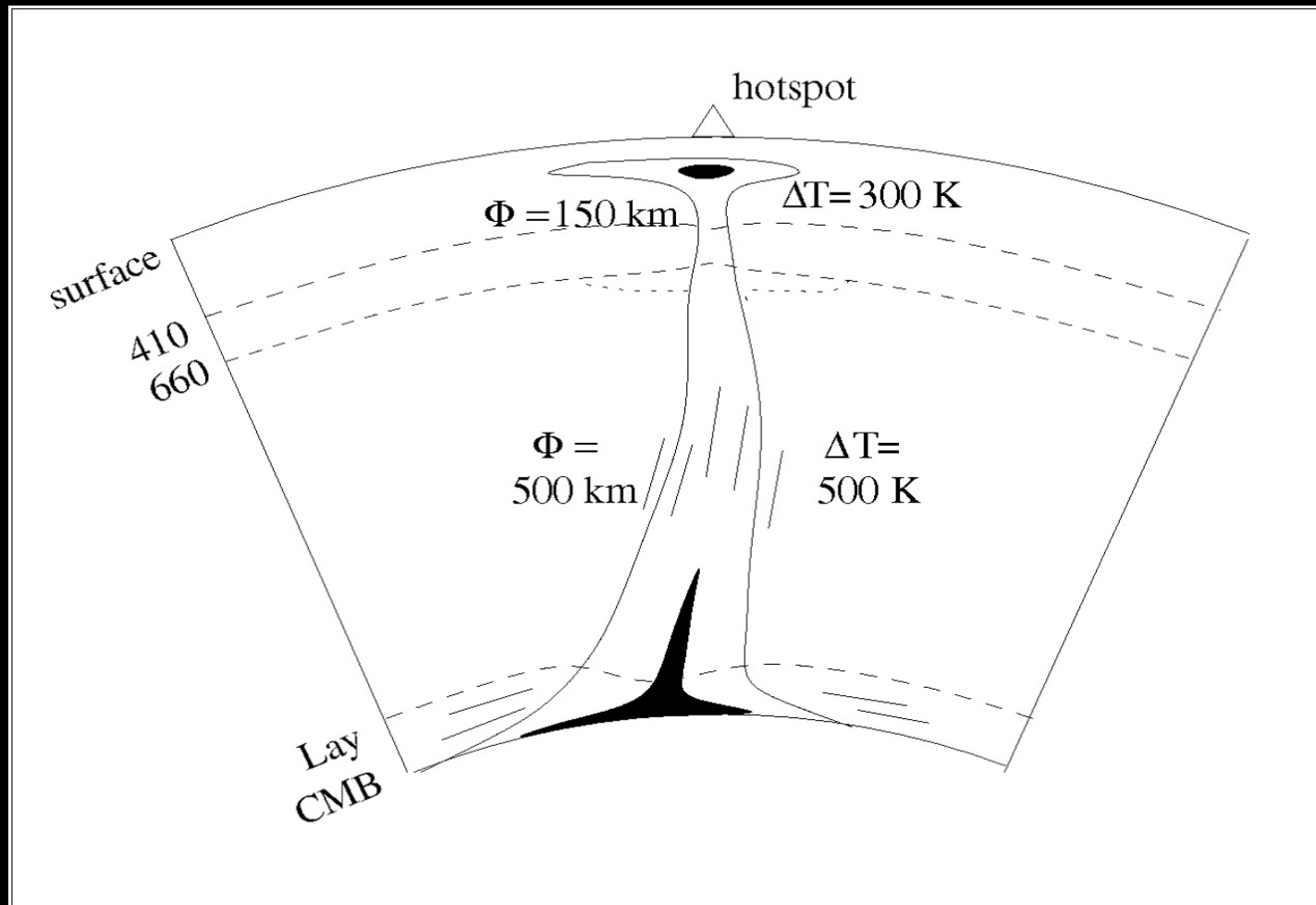




10 5:42

Th. Staudacher
OVPE / IPGP

Classical Plume Model (Nataf, 1999)

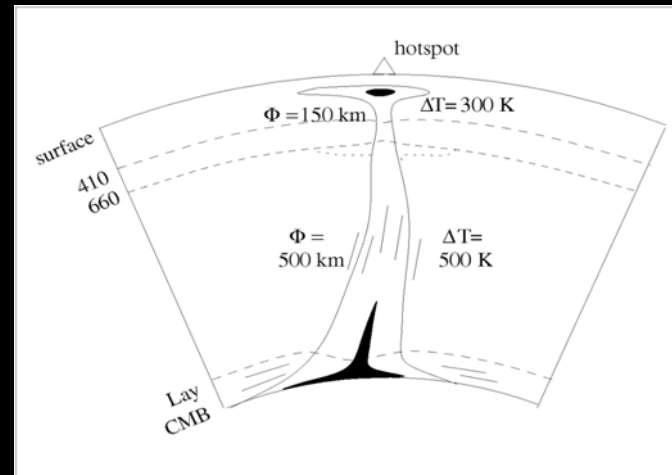


Definition of plume: thermal instability in a boundary layer:

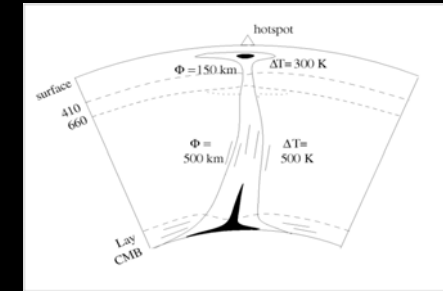
- Core-mantle boundary
- Transition Zone (400-660- 1000km)?
- Asthenosphere- lithosphere?

But

- Is the plume model correct?
- What is their geodynamical role?
- What is their biological role?
- What is their structure, their origin at depth?
- Are there really several types of plumes?



Detection of a Plume



Expected Effects of plume on seismic data

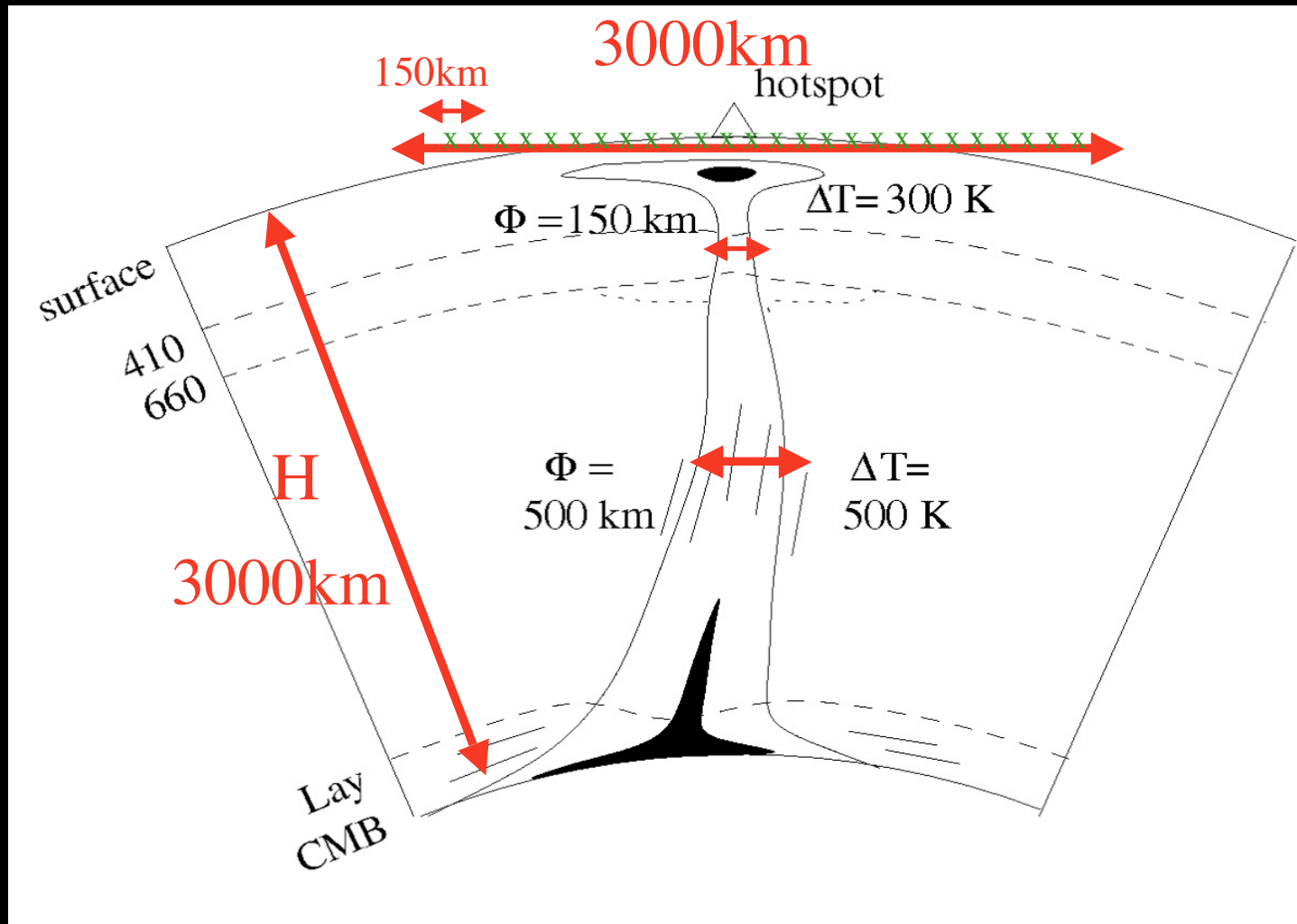
- Thermal effect: $\Delta T > 0 \Rightarrow dV_S < 0, dV_P < 0$

- Upwelling flow \Rightarrow crystal alignment by LPO
Weak azimuthal seismic anisotropy,
 $V_{SV} > V_{SH}$ ($\alpha < 1$: radial seismic anisotropy)

- Large attenuation \Rightarrow low quality factor Q

- Thinning of the Transition zone thickness
(410km deflected downward, 660km upward)

$H/F \gg 20 \Rightarrow$ at least 40 stations (2 per l)





Plume affects not only S-wave velocity distribution but also seismic anisotropy





Plume affects not only S-wave distribution but also seismic anisotropy

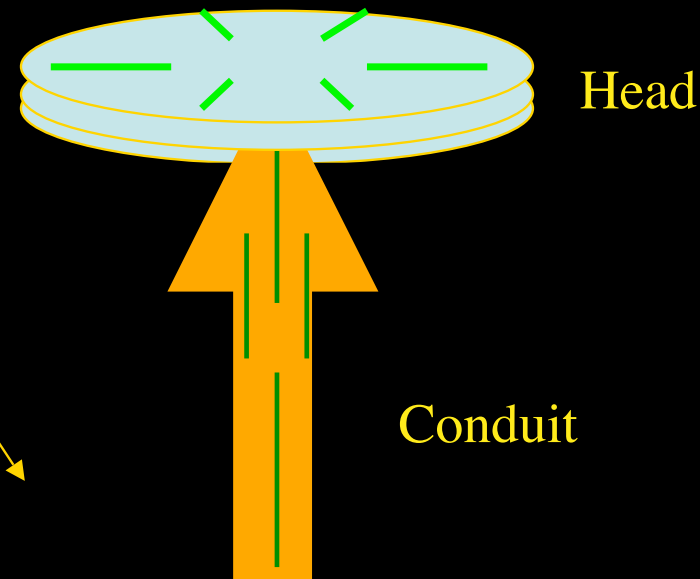
- Head: Not a problem

- Conduit: difficult to detect

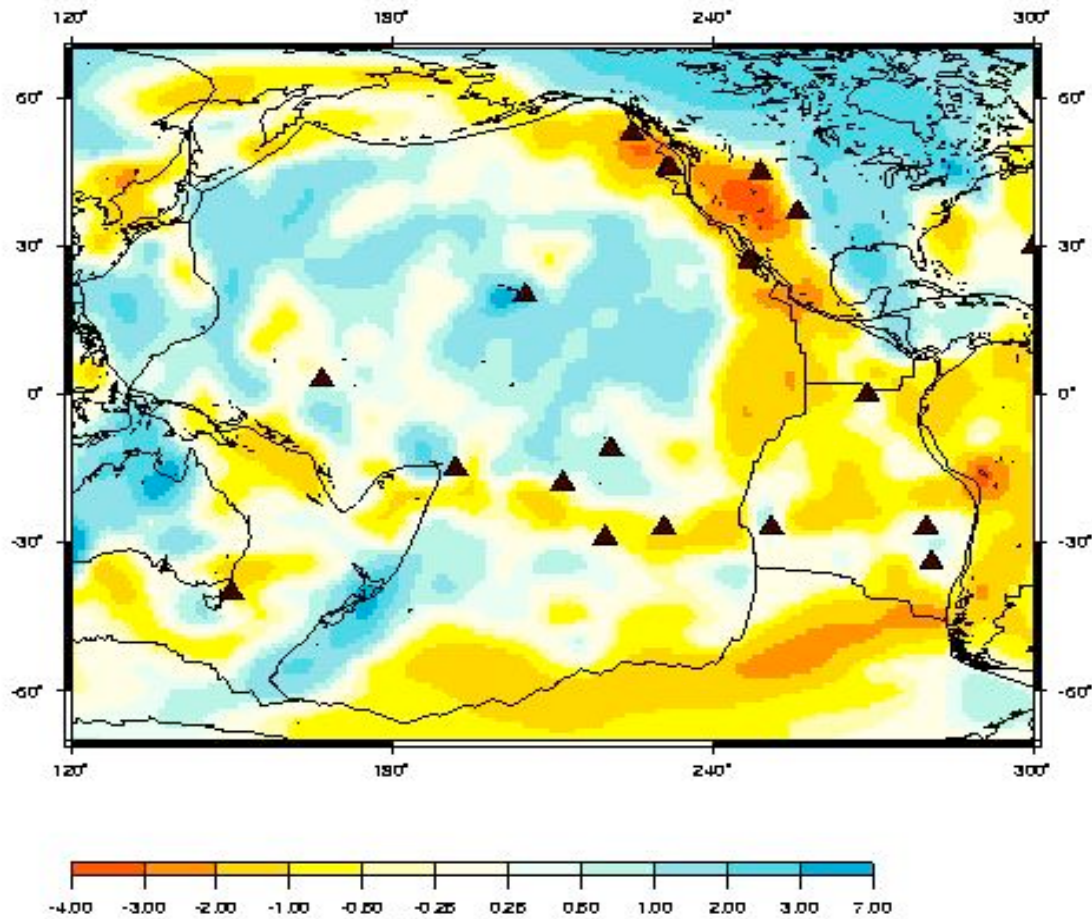
Da: Anisotropy Effect $\Rightarrow V_{SV}$ 

DT: Temperature Effect $\Rightarrow V_{SV}$ 

Opposite effects



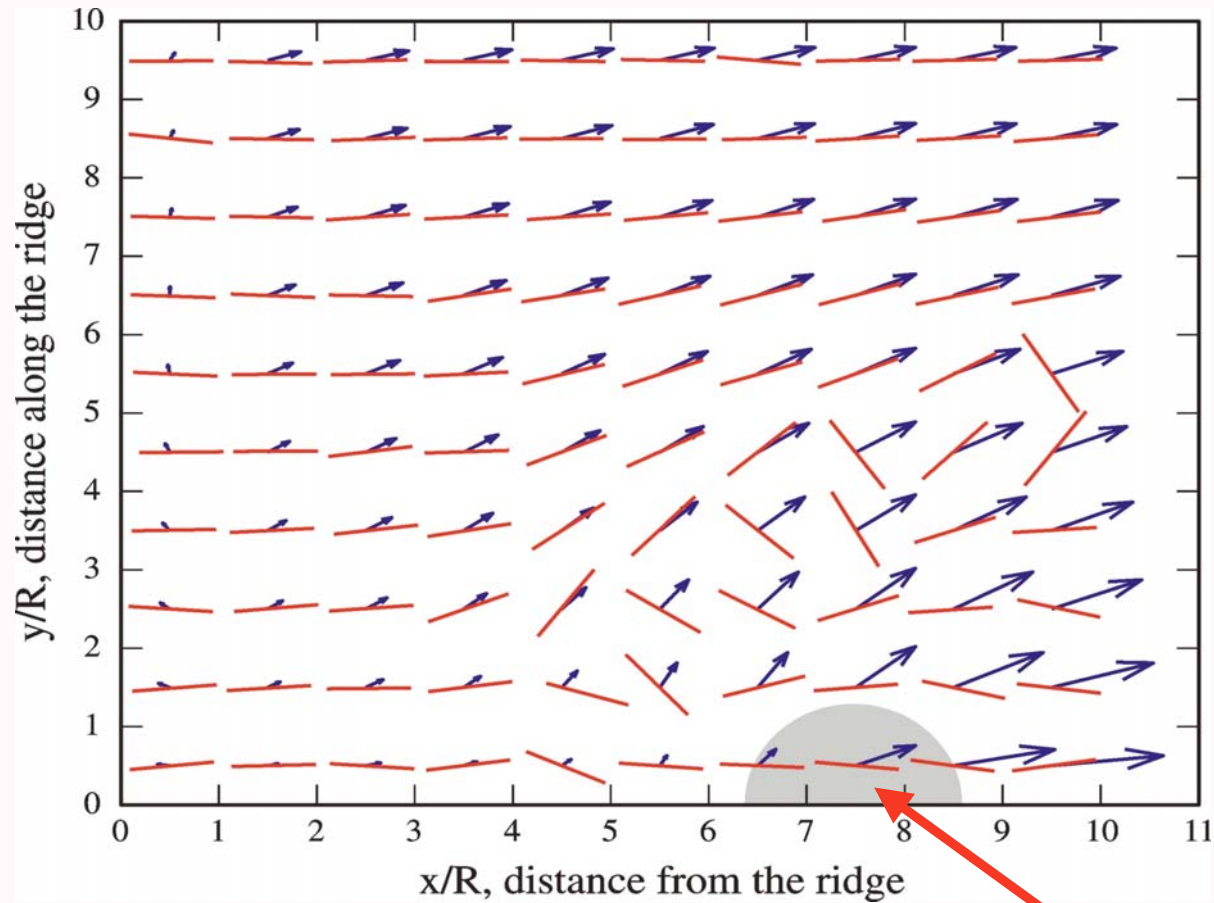
Xi: Radial Anisotropy - Depth=100km



(Montagner, 2002)



Azimuthal anisotropy



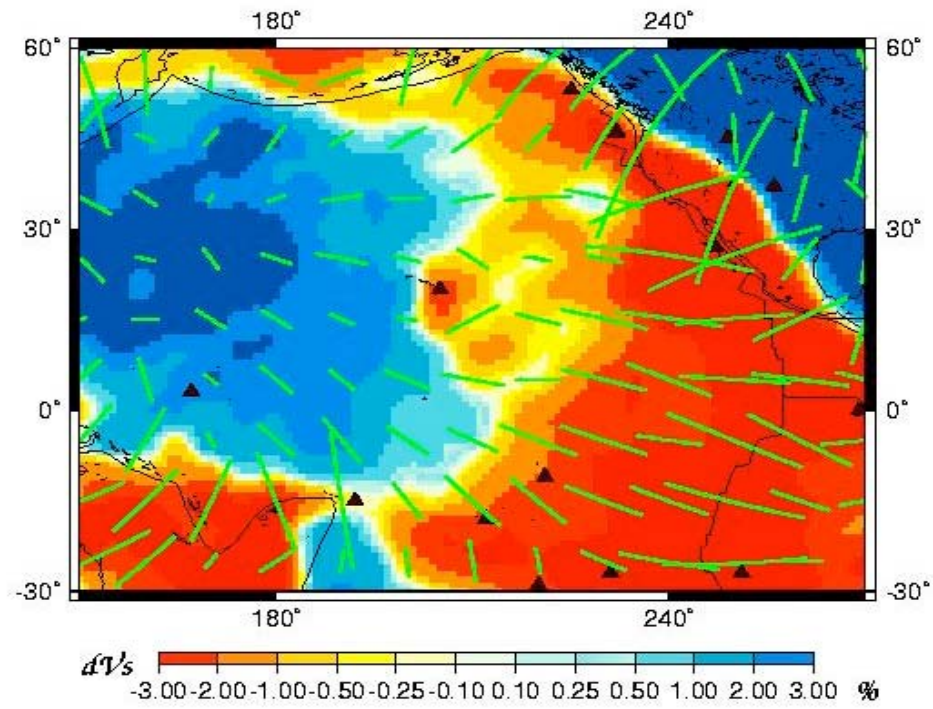
(Kaminski and Ribe, 2001)

Plume



S-wave velocity + Azimuthal Anisotropy

Depth=120 km



A plume is very difficult to detect below asthenosphere
(narrow conduit $\partial 150\text{km}$, small velocity contrast $\partial 1-2\%$)

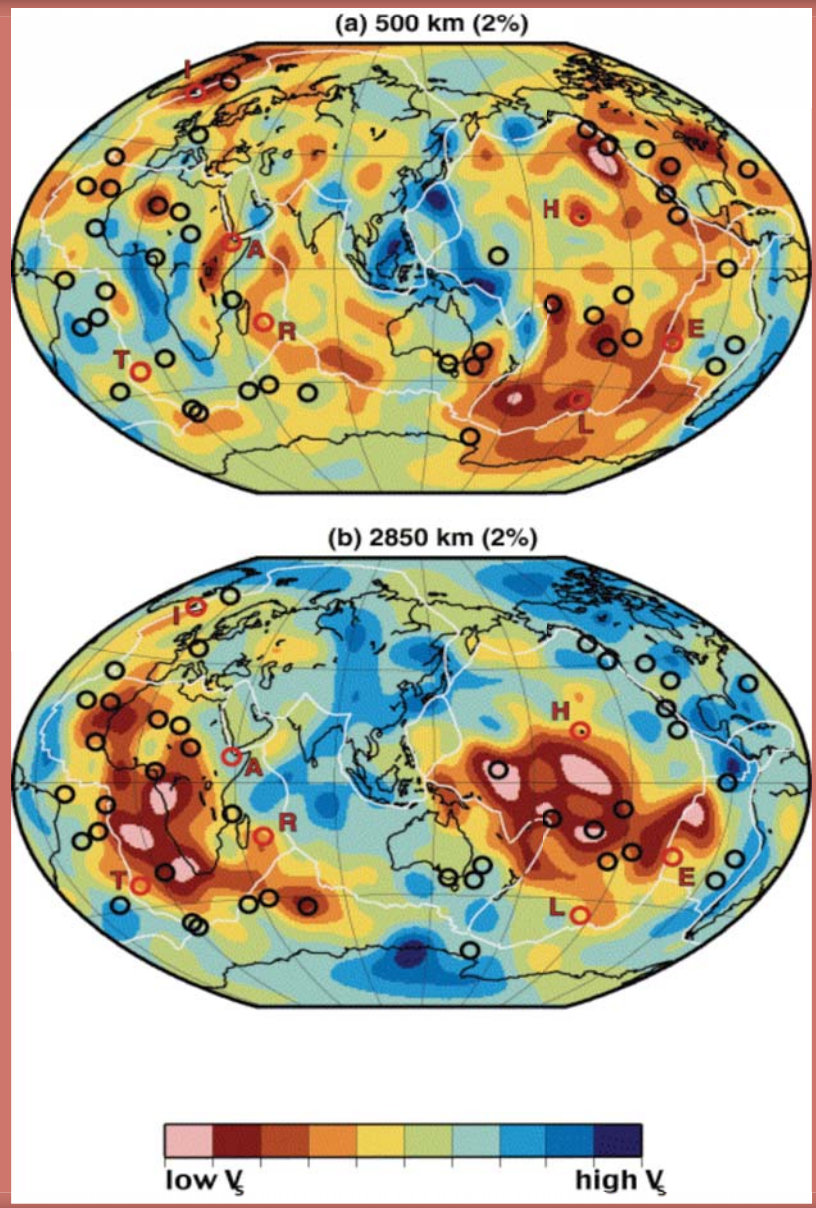
Head is easier to detect: large lateral extent, interaction with lithosphere, asthenosphere, or continent

Indirect detection through the perturbation of flow pattern around plume

Several regional investigations: Resolution 500km

Horn of Africa (Debayle et al., 2000; Sicilia et al., 2003)

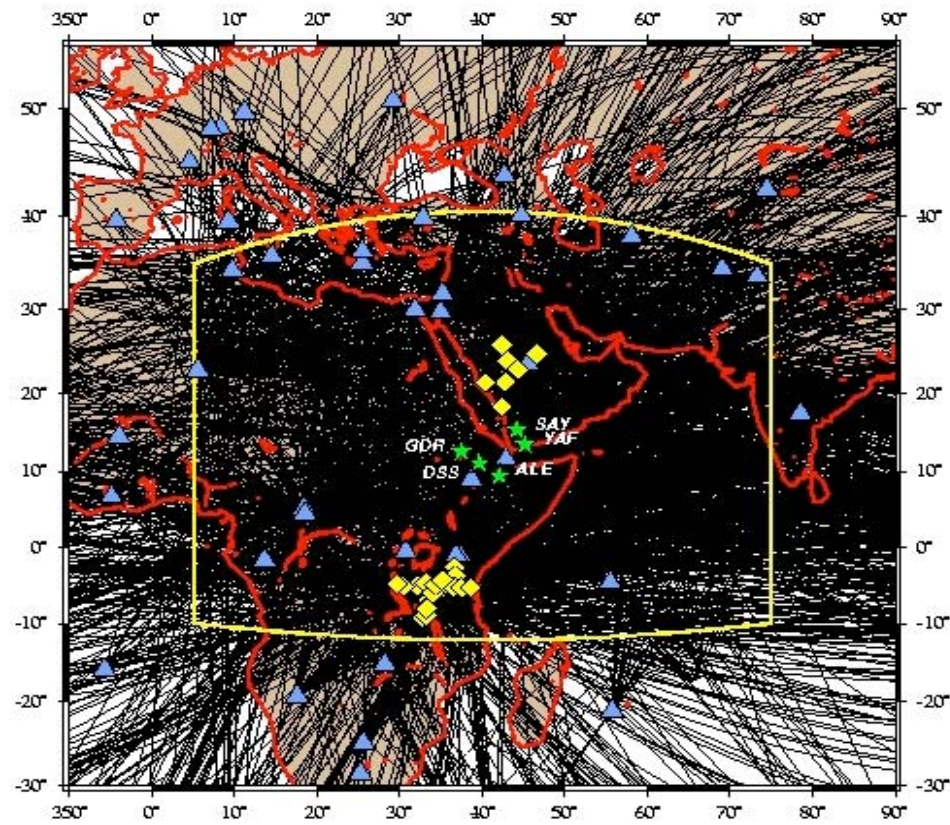
Global Scale



Ritsema et al., 2000



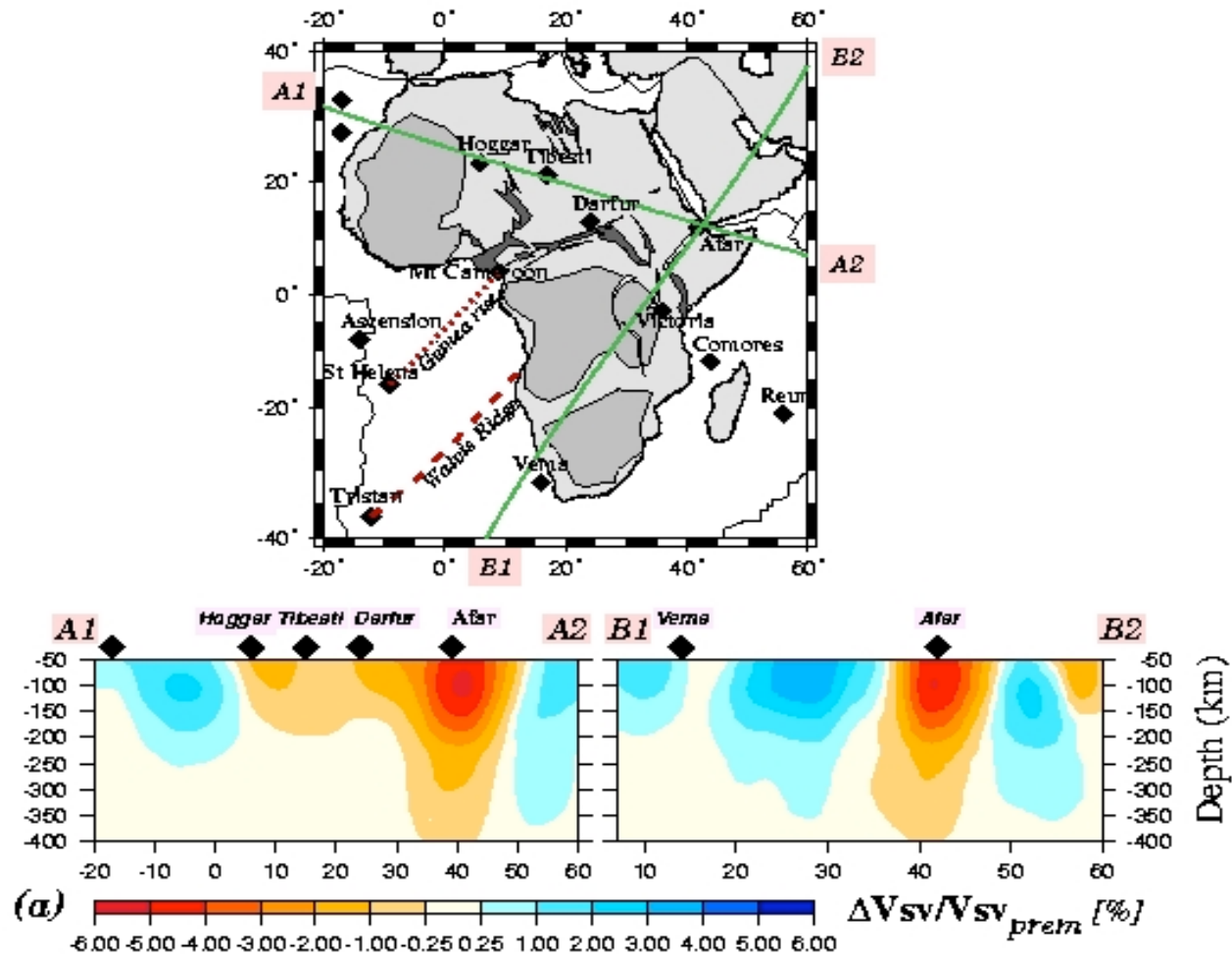
Horn of Africa

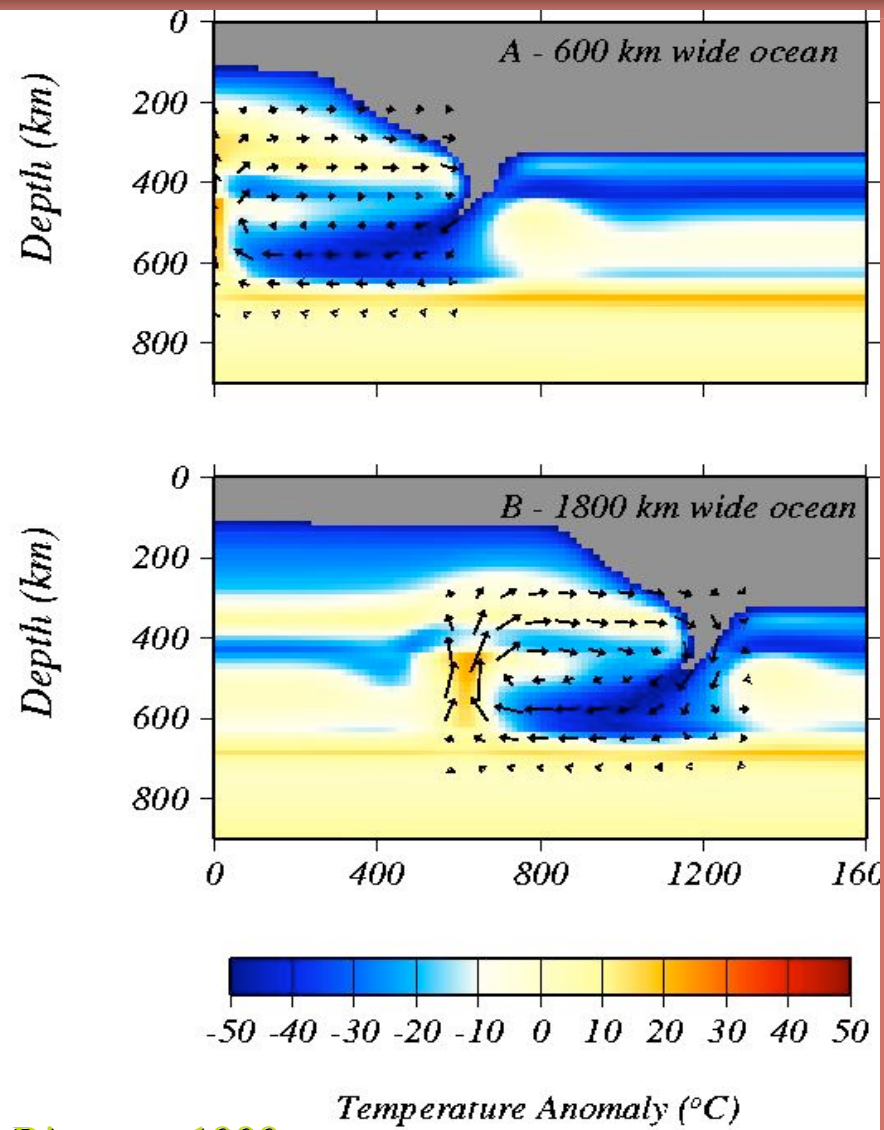


(Sicilia et al., 2003)



(Sebai et al., 2003)

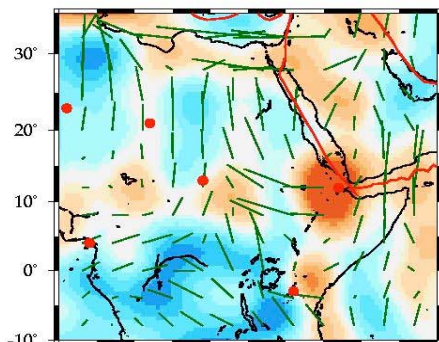




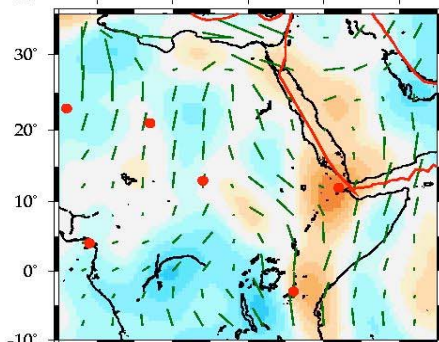
King & Ritsema, 1999



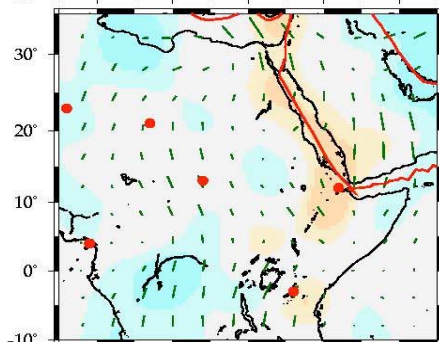
Depth= 100km



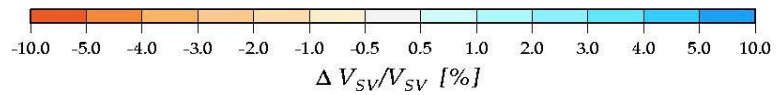
Depth= 200km



Depth= 310km



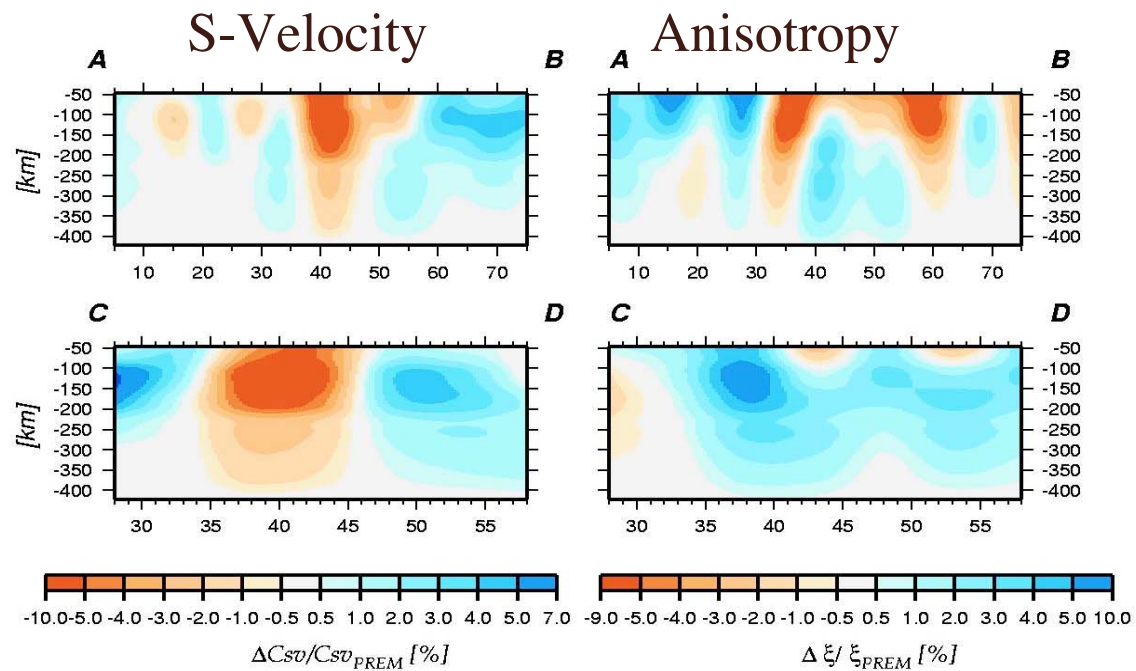
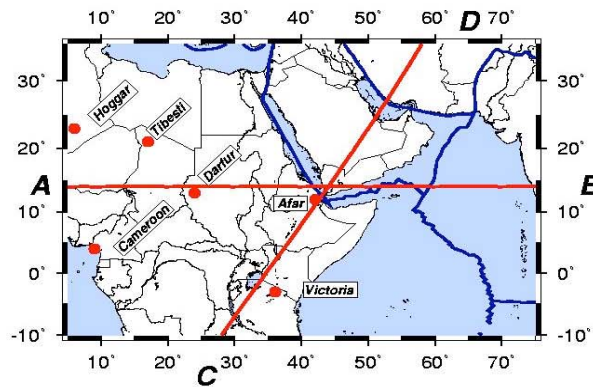
anisotropy



S-velocity

E-W

N-S

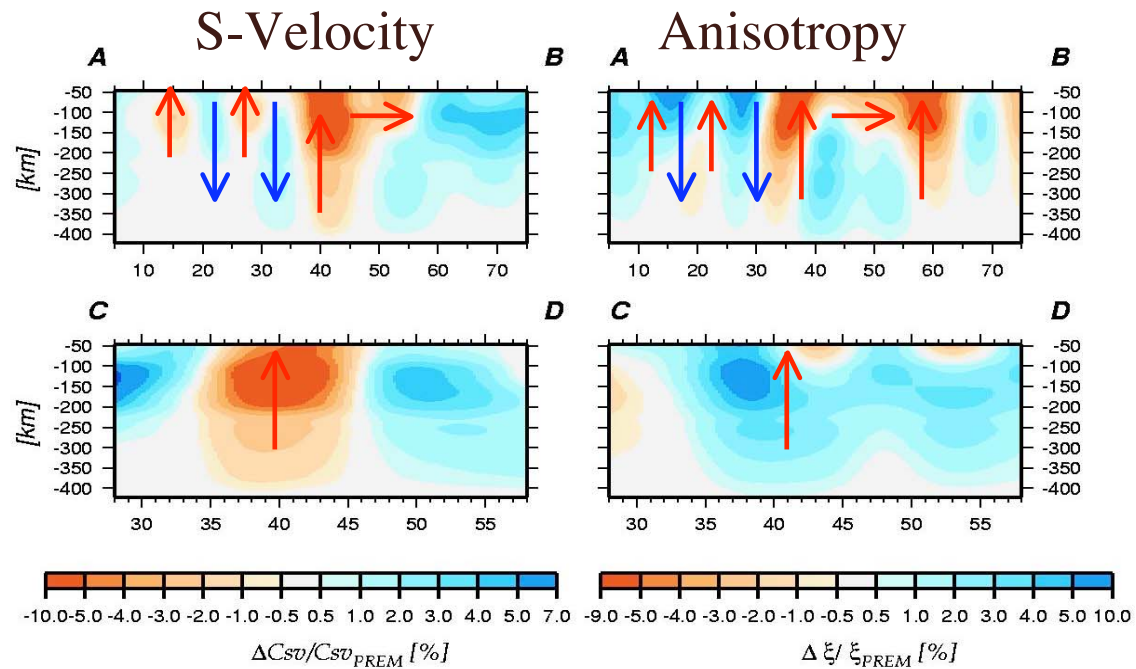
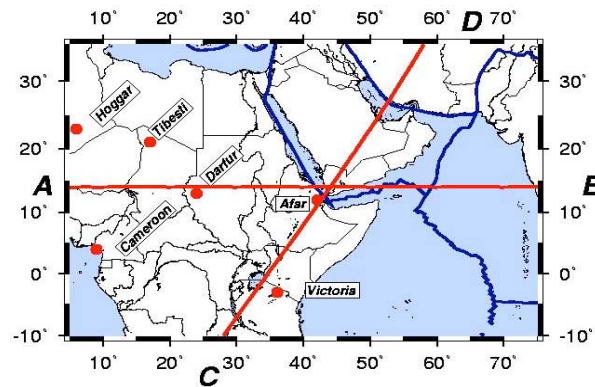


D. Sicilia, 2002 (IPGP)



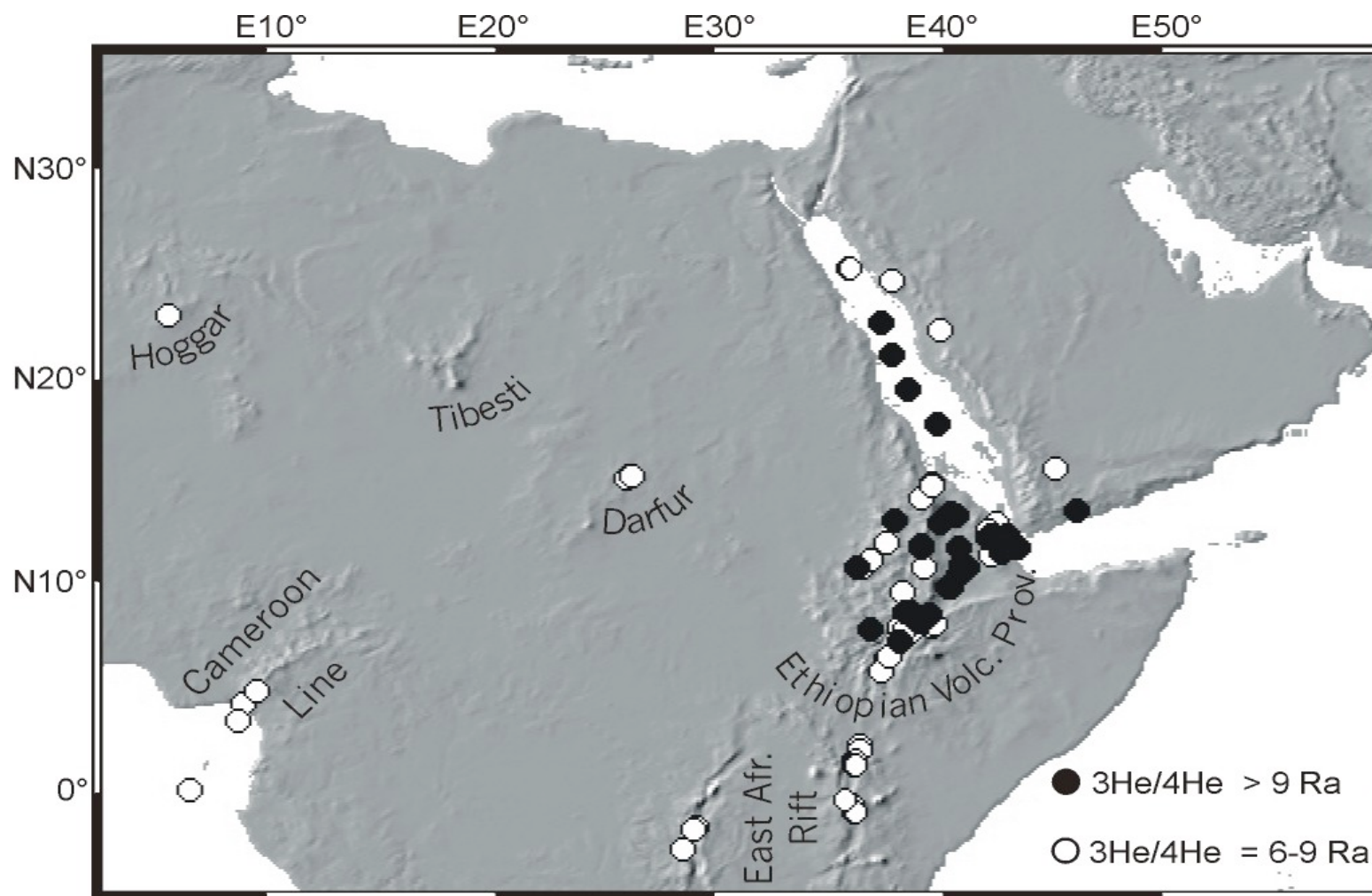
E-W

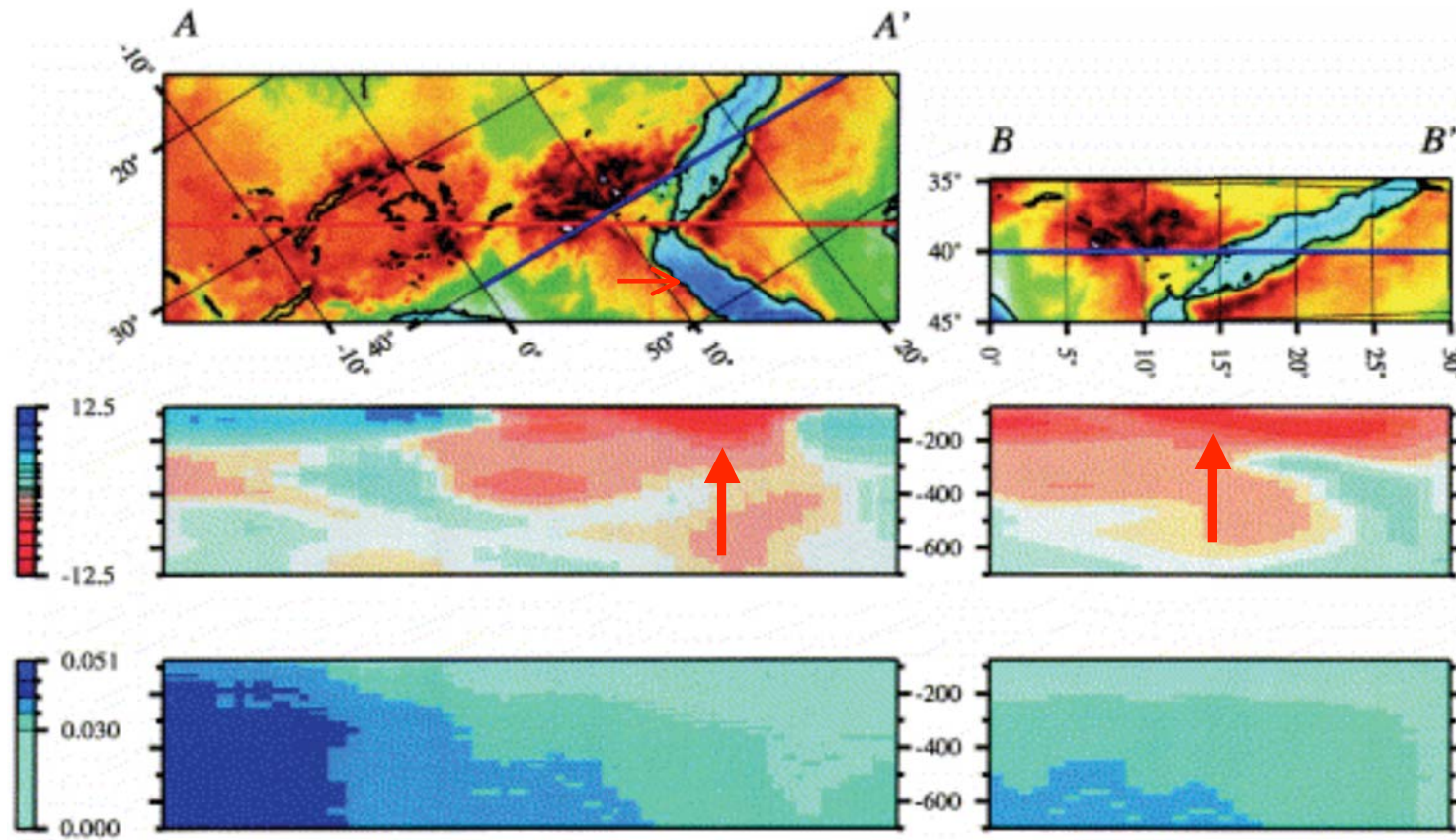
N-S



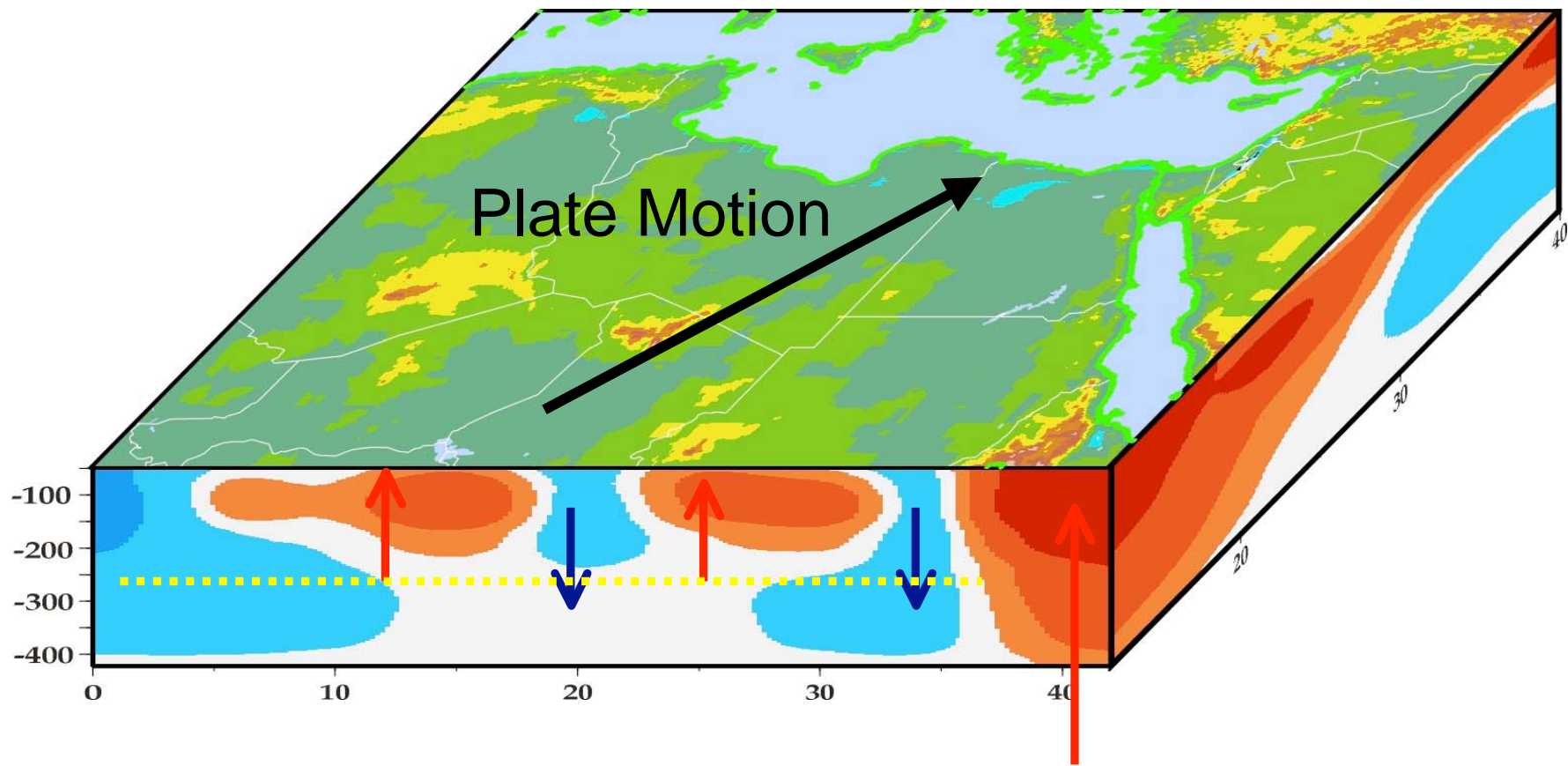
D.Sicilia, 2002 (IPGP)

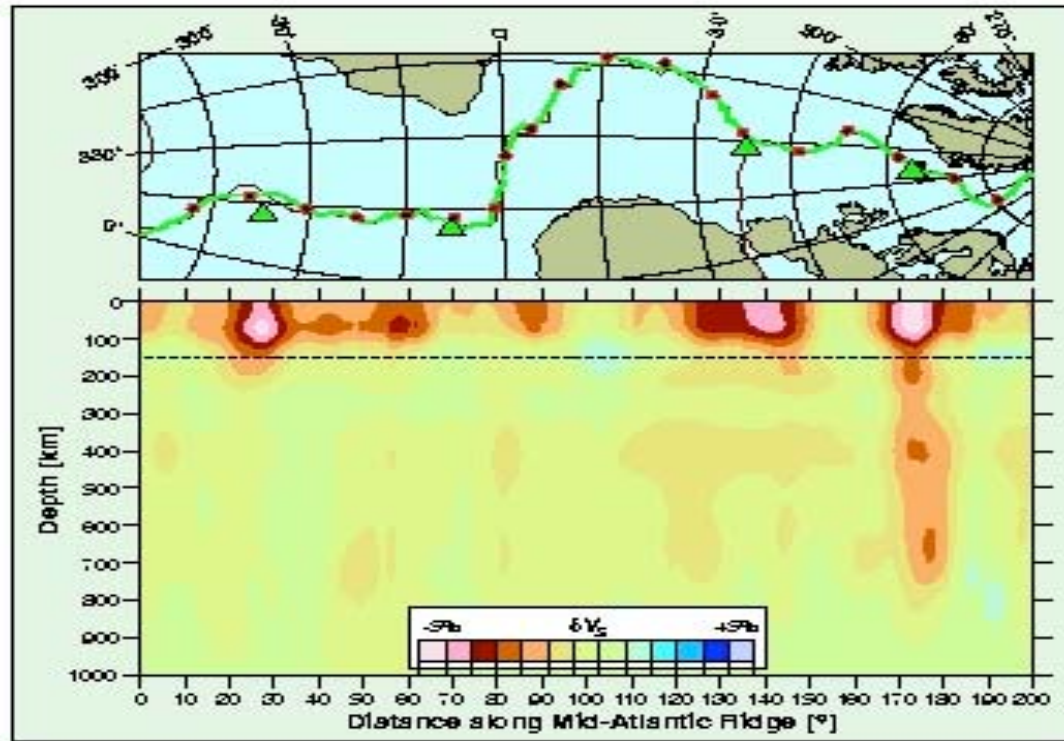






(Debayle et al., 2001)

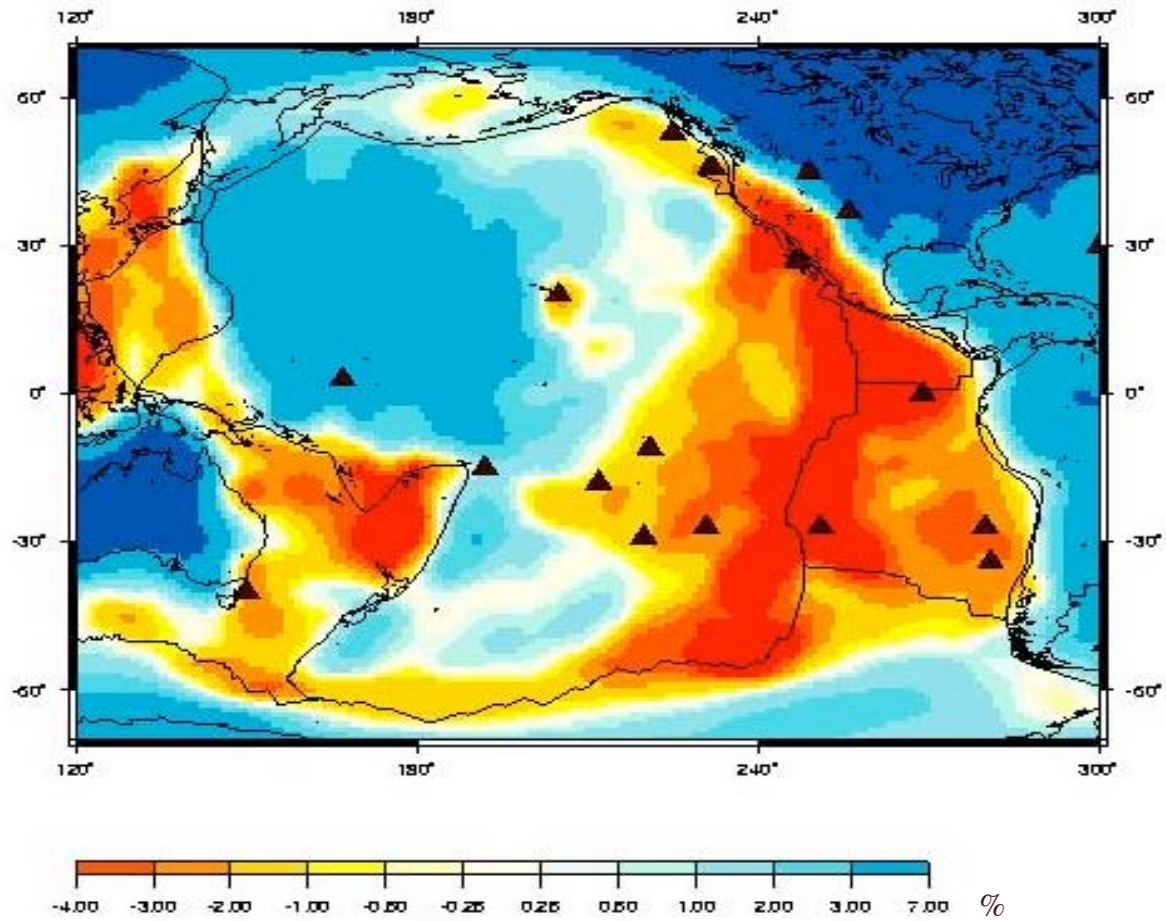




(Montagner and Ritsema, 2001)



Vs Velocity Depth=100km

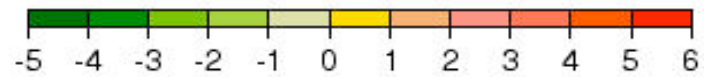
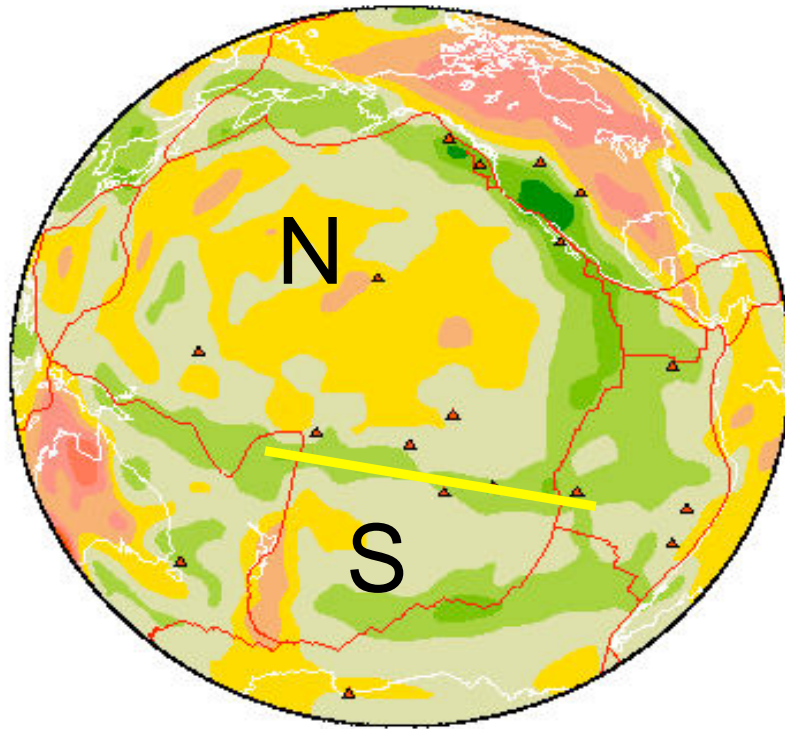


(Montagner, 2002)

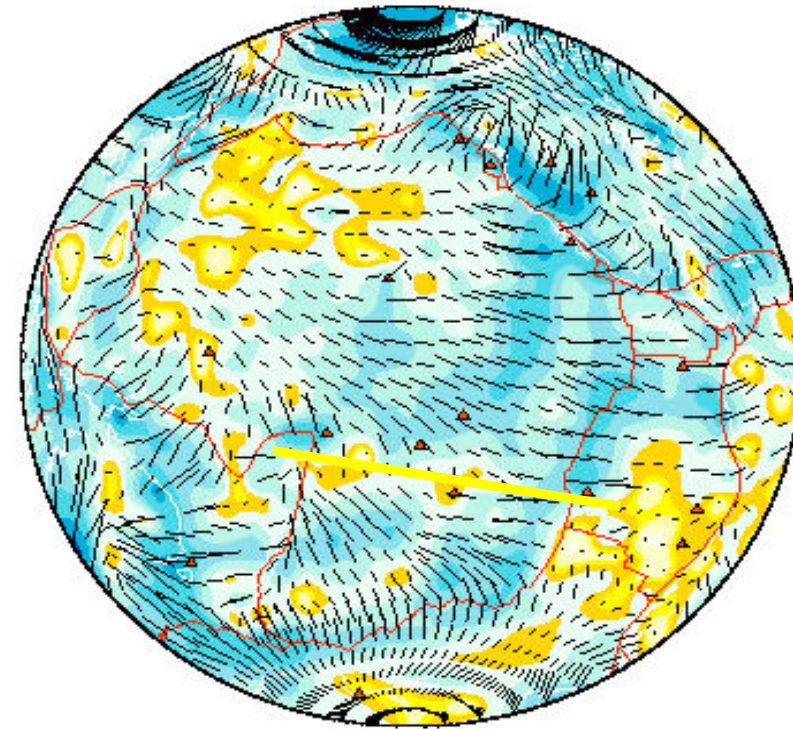


Future ridge between North and South Pacific ?

PREM (3SMAC) 2002 model - 140 km



(a) Radial anisotropy

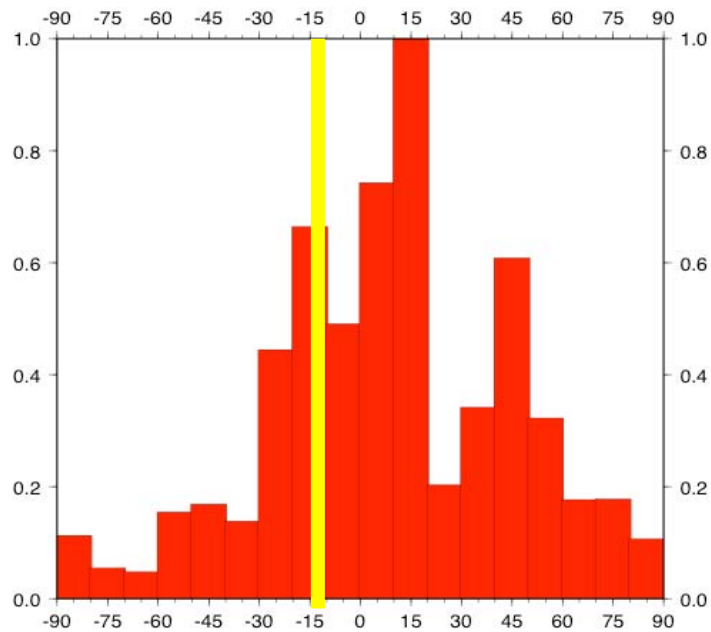


(b) Azimutal Anisotropy

Future Plate boundary within the Pacific plate?

Pacific Plate

Histogram Plate velocities - Seismic anisotropy

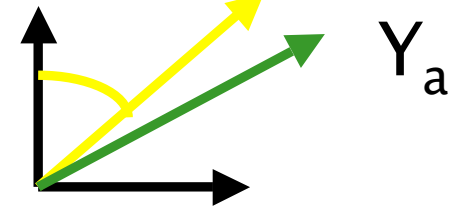


$Y_a - Y_{PL}$
Angular difference (in degrees)

$$\mathbf{V}_{PL} = \mathbf{W}_{PL} \times \mathbf{OM}$$



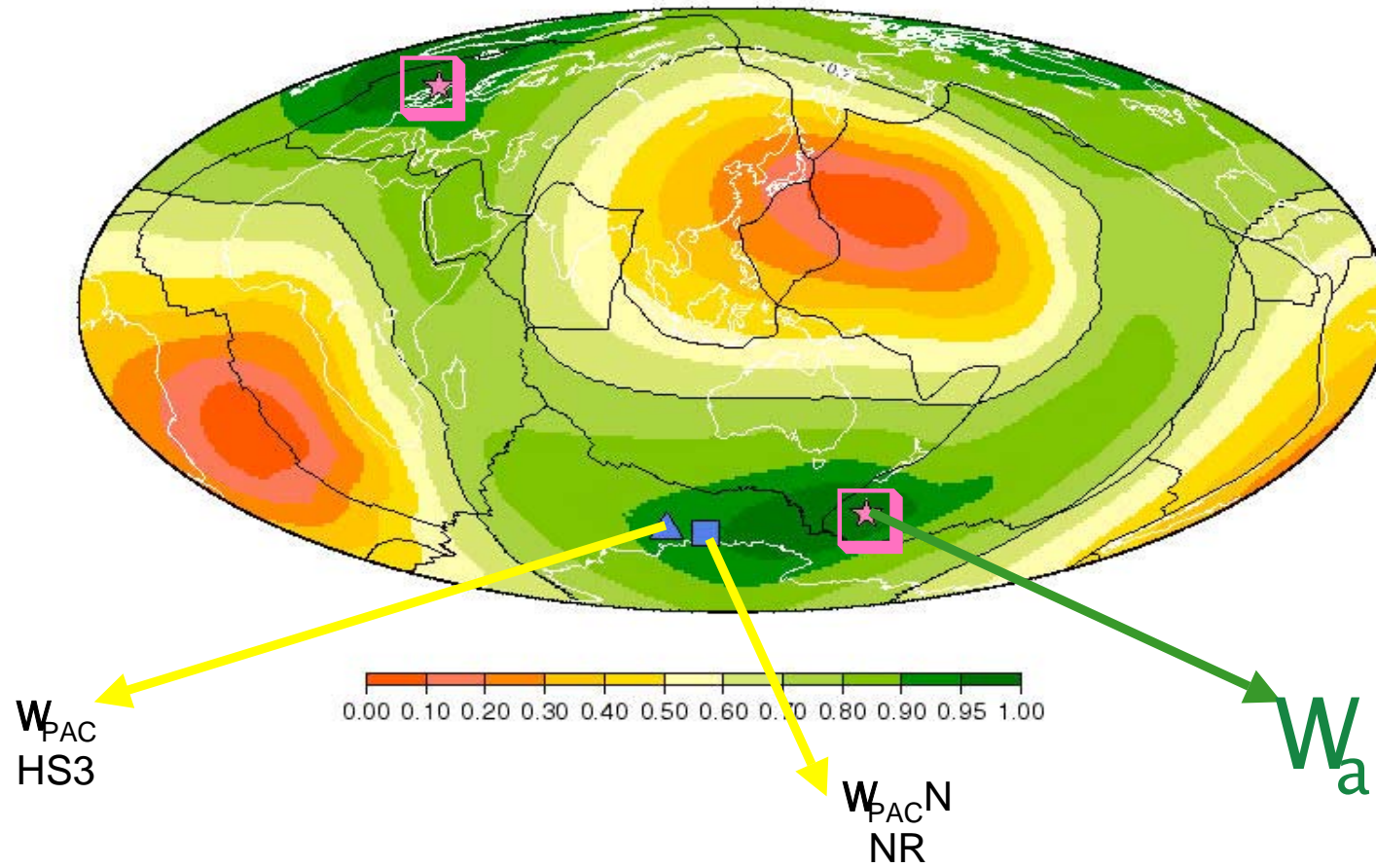
Y_{PL}



$$Y_a \longrightarrow (W_a, W_a^{\text{antip}})$$

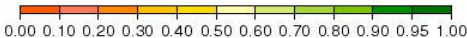
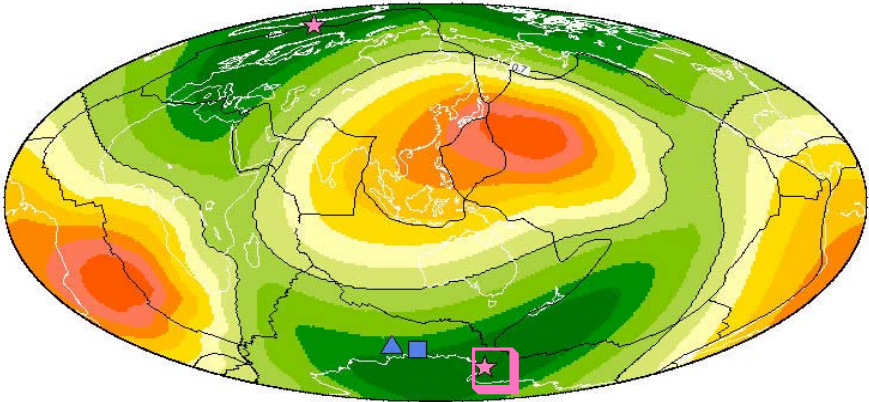
Cost function global Pacific Plate G

SKS-PREM-3SMAC-2002 model (threshold = 0.1)



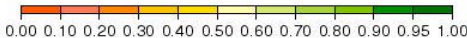
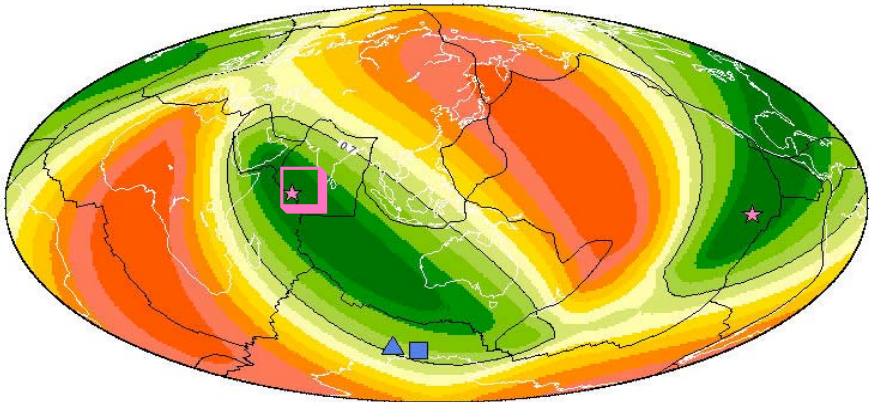
Cost funtion North Pacific Plate G

SKS-PREM-3SMAC-2002 model (threshold = 0.1)



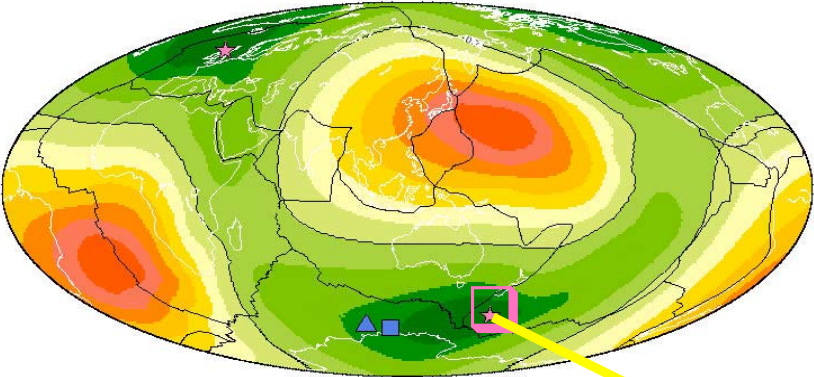
Cost funtion South Pacific Plate G

SKS-PREM-3SMAC-2002 model (threshold = 0.1)



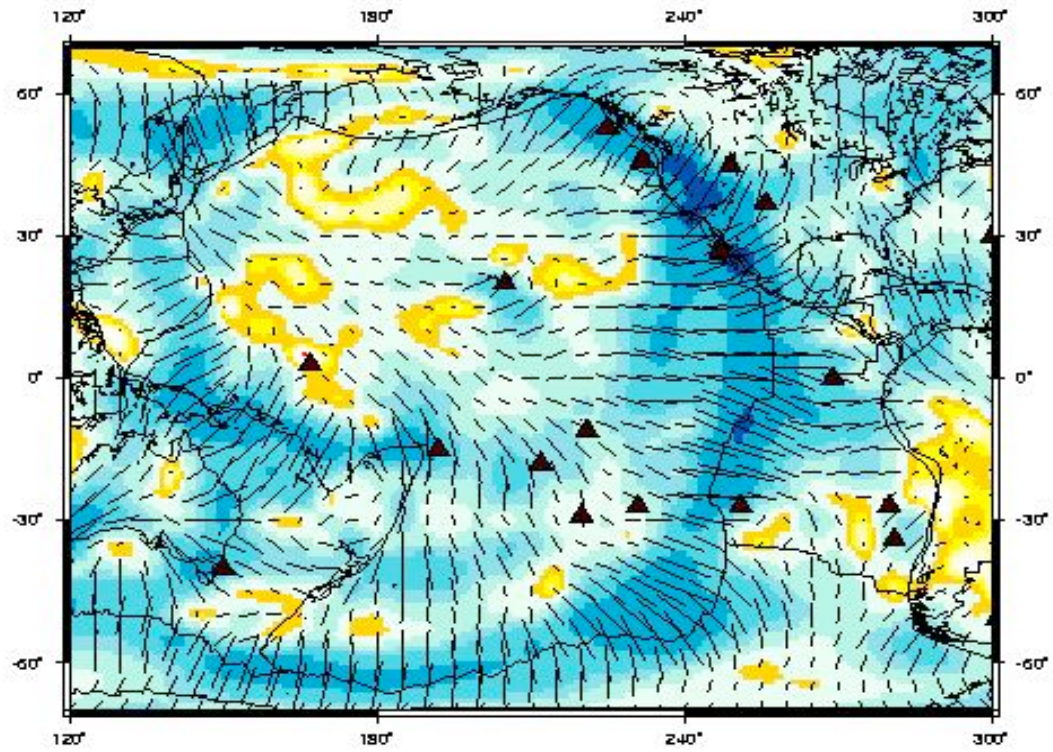
Cost funtion global Pacific Plate G

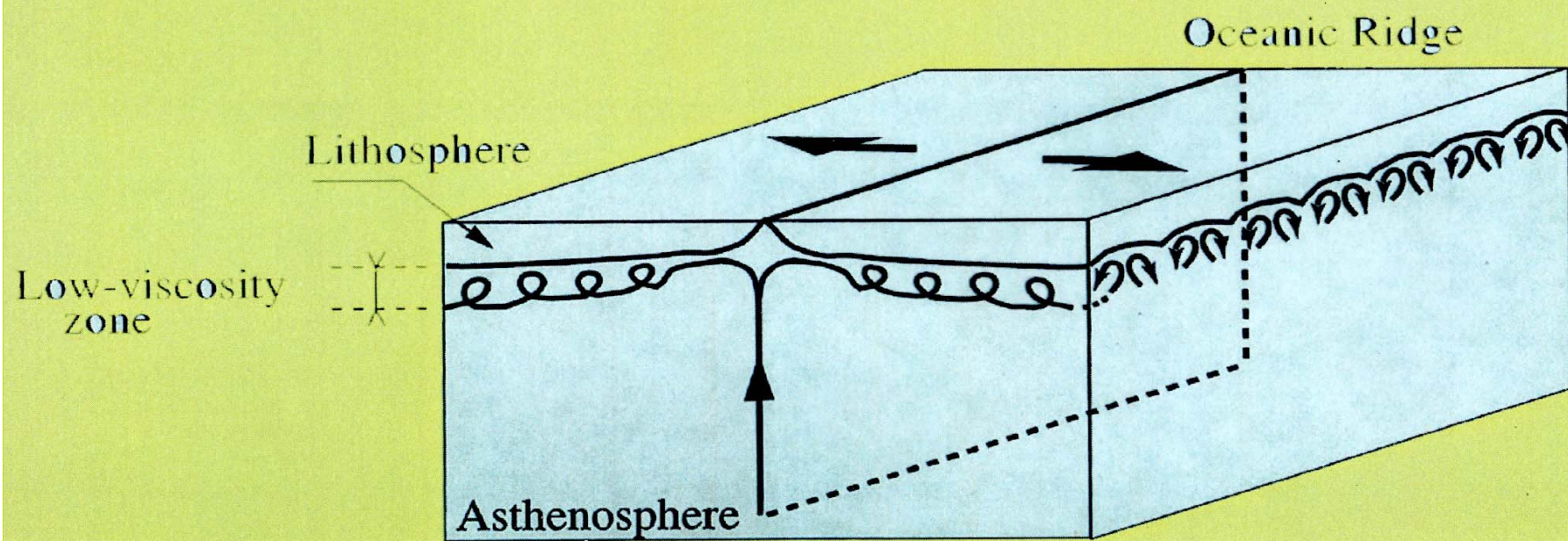
SKS-PREM-3SMAC-2002 model (threshold = 0.1)



W_a

G:Azim. Anis. Depth=100km

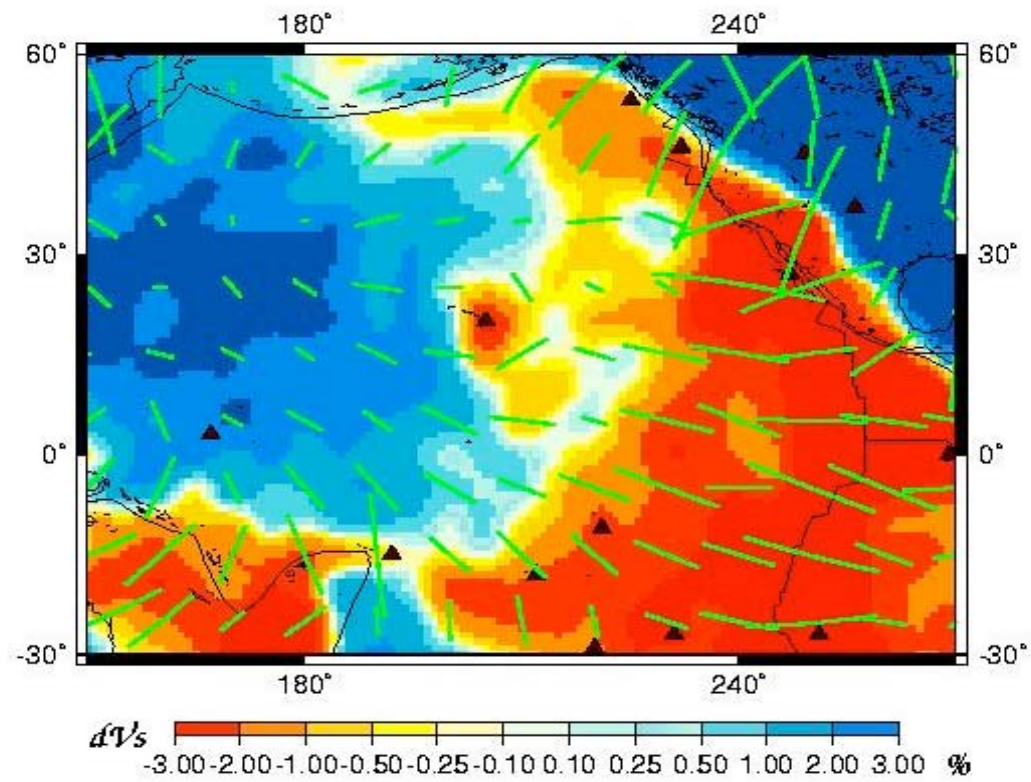


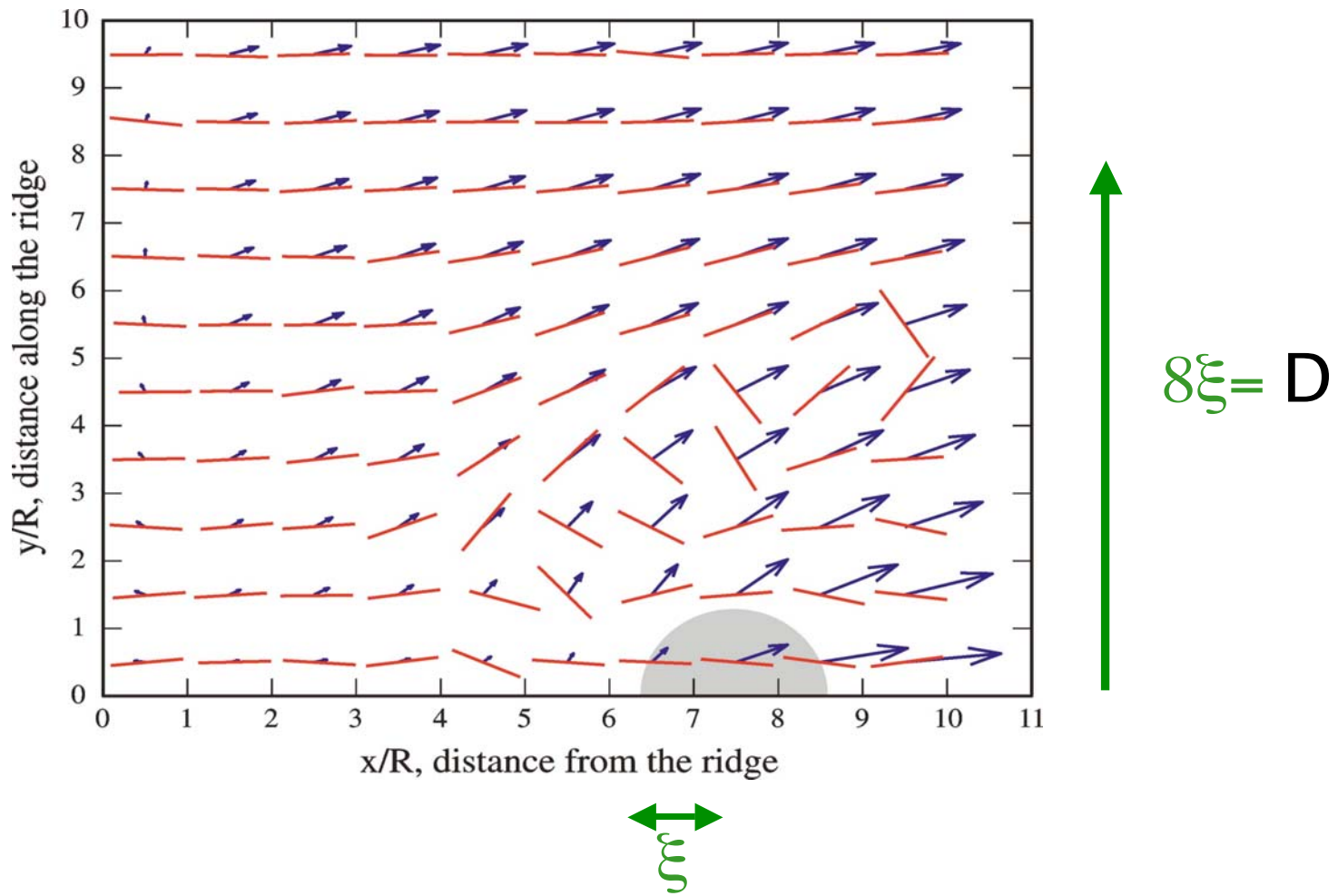


(Crambes and Davaille, 2002)

S-wave velocity + Azimuthal Anisotropy

Depth=120 km





(Kaminski and Ribe, 2001)

$$D \approx 2000\text{km} \Rightarrow d \approx 250\text{km}$$

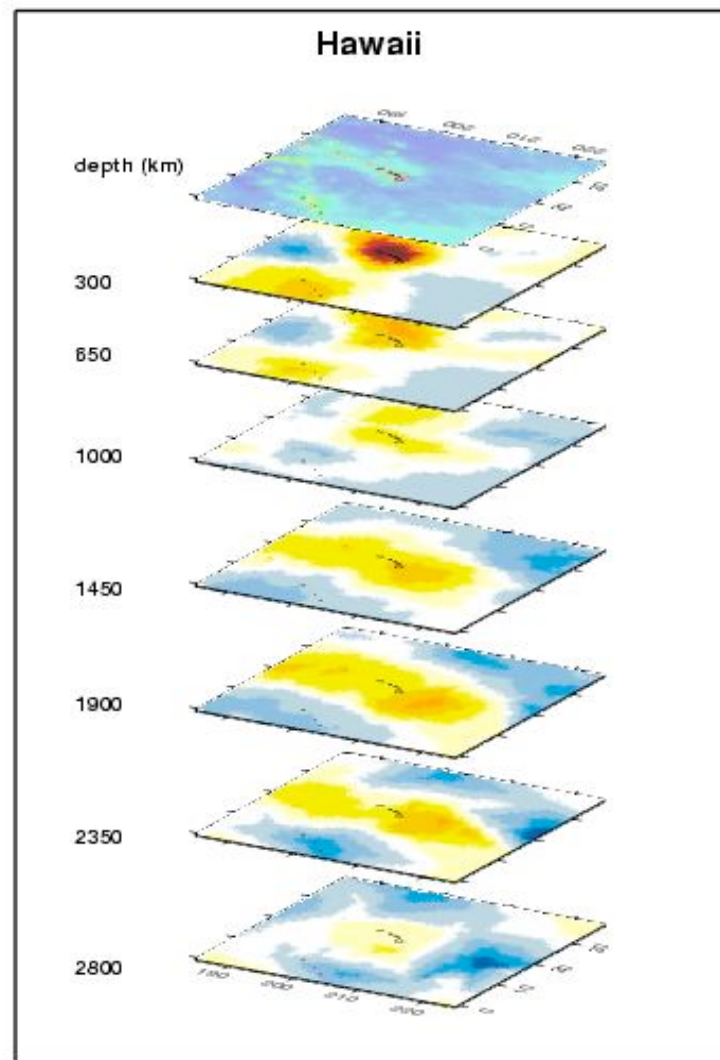


Plume Detection

- ❑ Indirect detection of plumes through Azimuthal and Radial anisotropies.
- ❑ Two families of plumes have been detected:
 - 1st kind is a consequence of small scale convection (<300km).
 - 2nd kind originates from deep in the mantle: transition zone (410-660km).
- ❑ Complex interaction Plume-lithosphere-asthenosphere:secondary scale of convection.
- ❑ Active hotspots in central Pacific and Africa participate to the reorganization of plate boundaries (New Plate boundaries).
- ❑ Lower Mantle plume not yet clearly detected because it cannot be detected with present seismic data
- ❑ Theoretical and Observational challenges

Banana-Doughnut Theory (Dahlen et al.)

Application to
global tomography
(Montelli et al.,
Science, 2004)



Overview

Large scale Seismology:

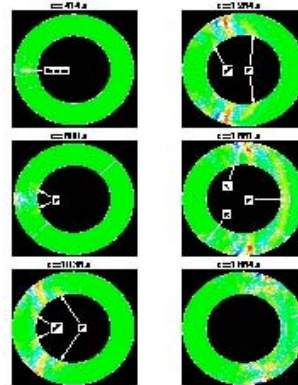
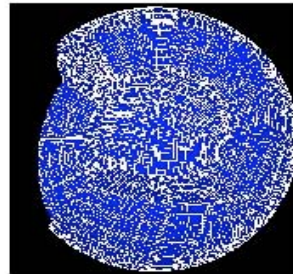
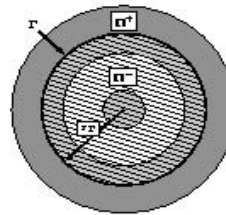
- Data (Seismic source) + Instrument (Seismometer) -> Observations (seismograms)
- Historical evolution: Ray theory, Normal mode theory, Numerical techniques (SEM, NM-SEM)
- Scientific Issues: earthquakes, structure of the Earth and planets
- Seismic Experiment: Plume detection
- NM-SEM and time reversal



Coupled method of Spectral Elements and Modal Solution

Principle:

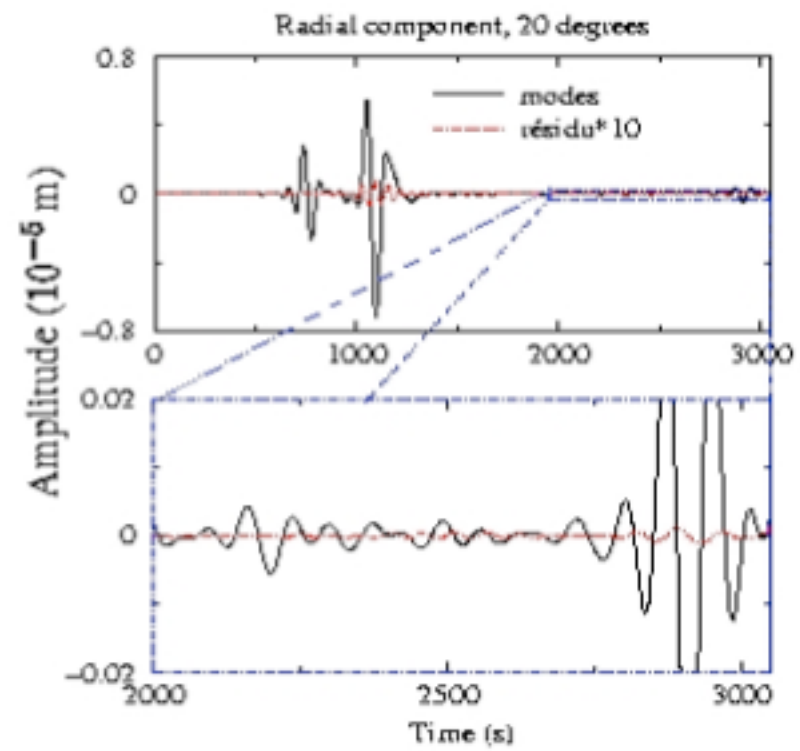
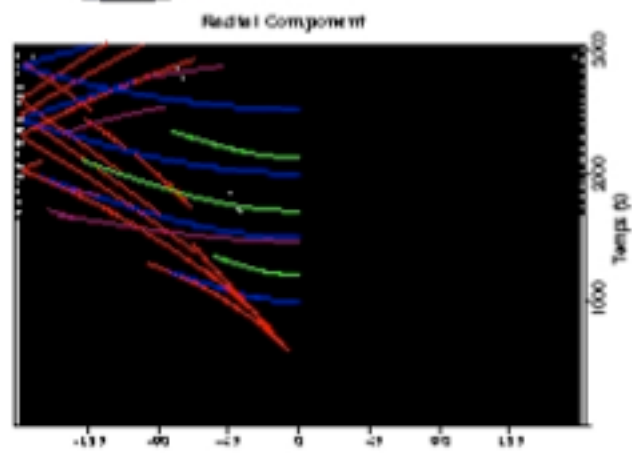
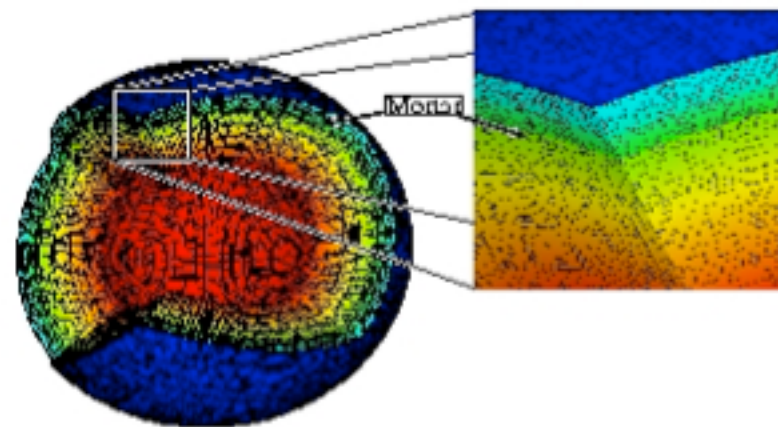
- Ω^+ : Spectral Element area:
3D model
- Ω^- : Modal Solution area:
1D model



Capdeville et al., 2003



Example: PREM



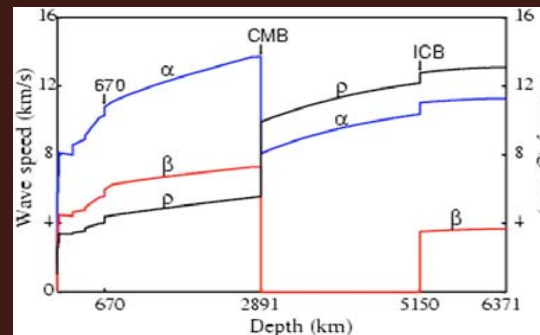
Time Reversal

1. Seismic displacement field $u(r,t)$ can be calculated everywhere by SEM-NM method

$$\partial^2 u / \partial t^2 = H \cdot u$$

2. In the absence of attenuation, if $u(t)$ is solution, $u(-t)$ is also solution.
3. It is possible to backpropagate $u(r,-t)$

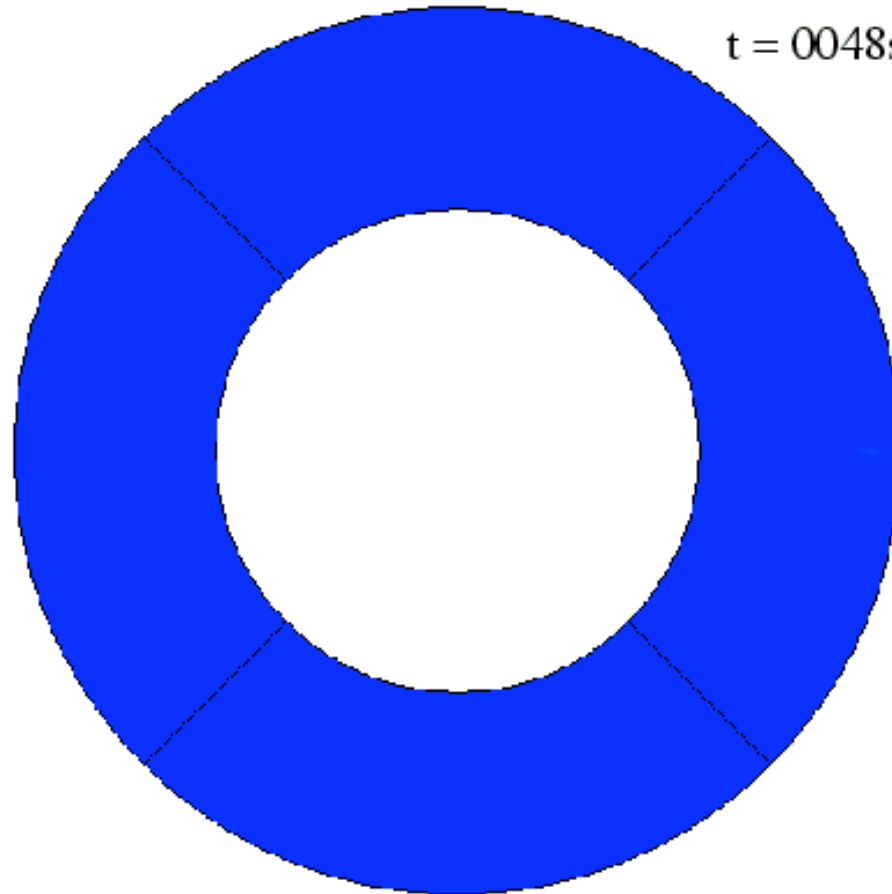
1D PREM



Larmat et al., 2004



Forward Problem

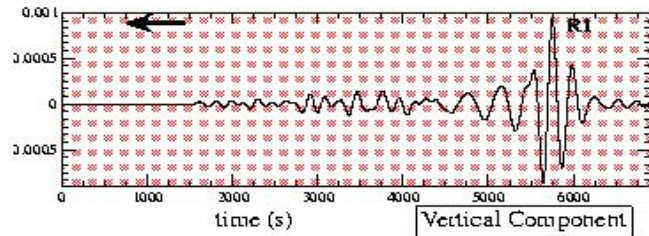


$t = 0.048s$

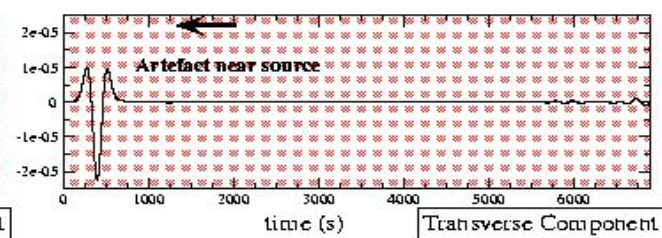
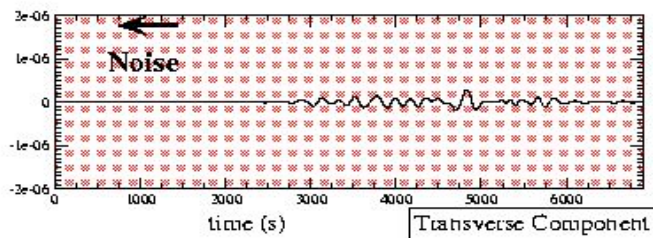
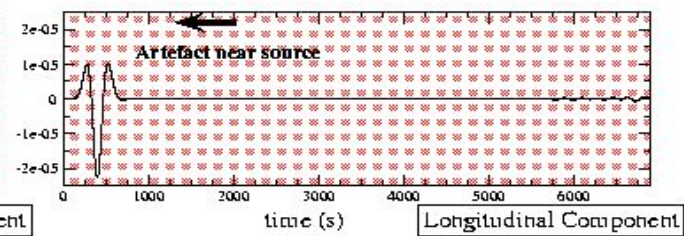
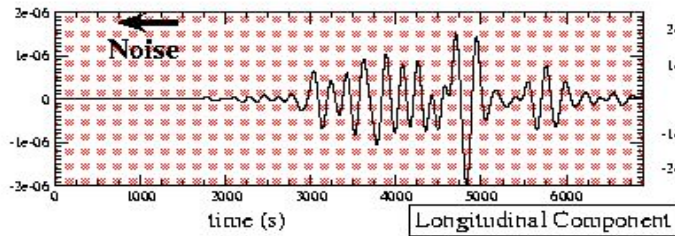
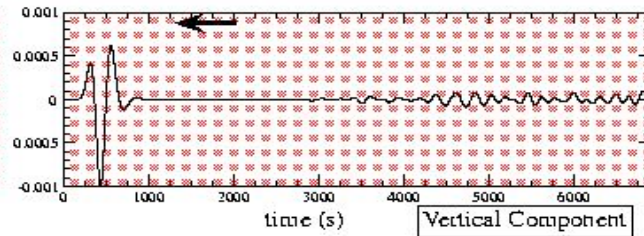


How much Information is backpropagated (PREM exp.)?

Antipode :



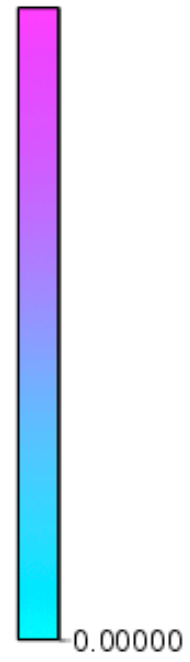
Epicentre :



$\varphi = 270^\circ$

$\varphi = 90^\circ$

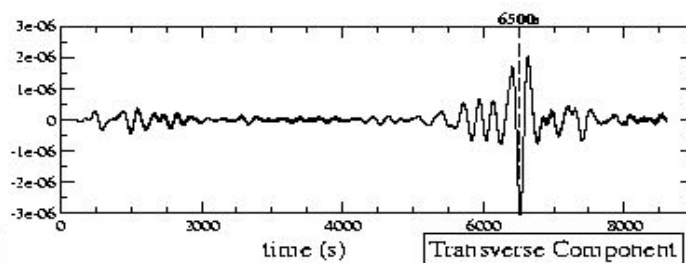
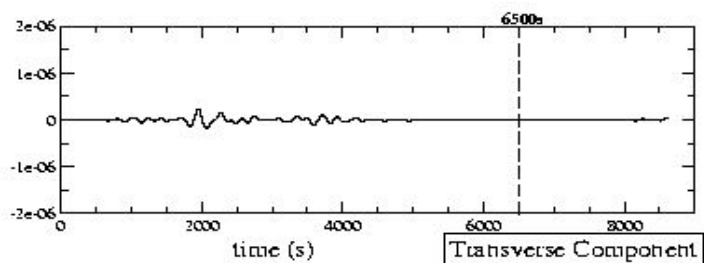
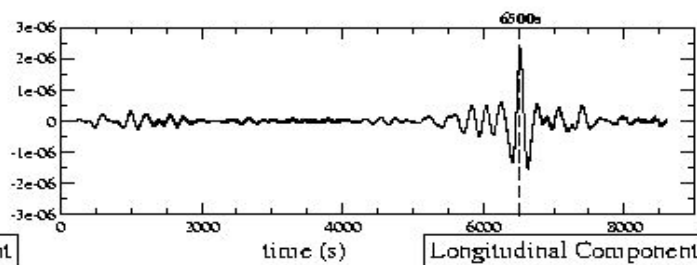
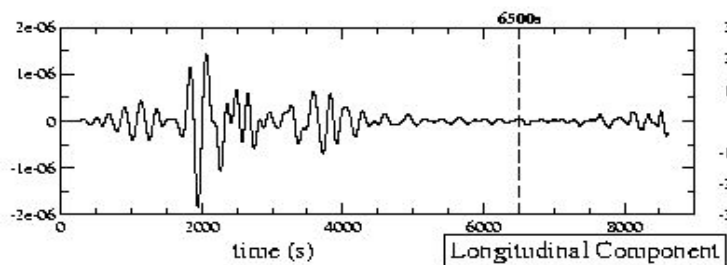
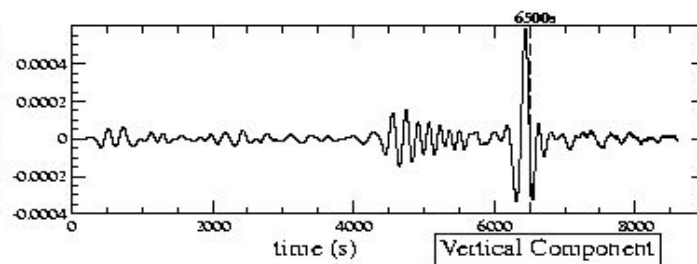
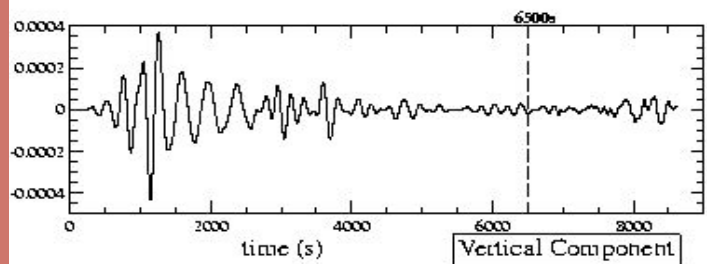
t = 00049 s



Time-reversed wave measurements – from all the points of the mesh (PREM)

Antipode ($p=398$ km):

Source Point ($p=398$ km):

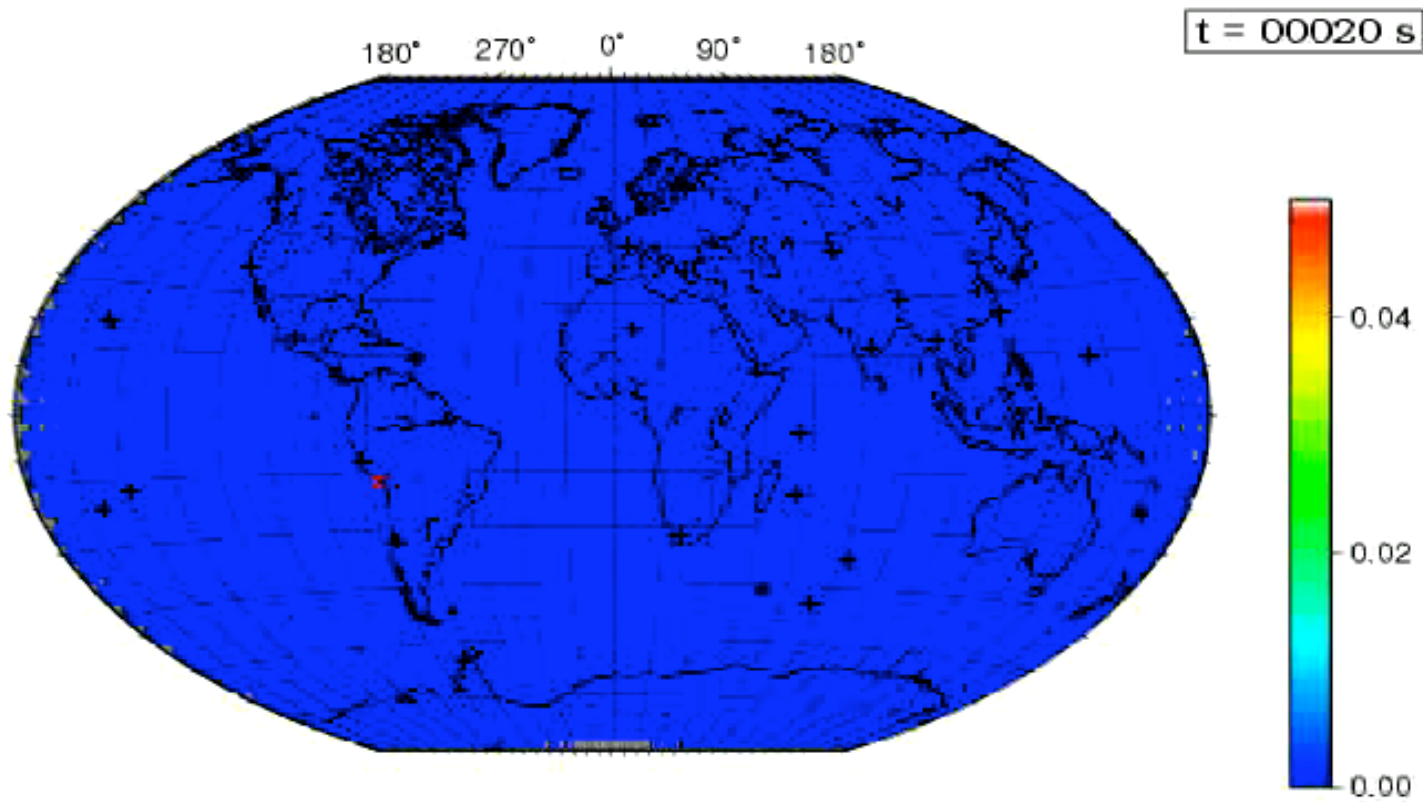


Time Reversal

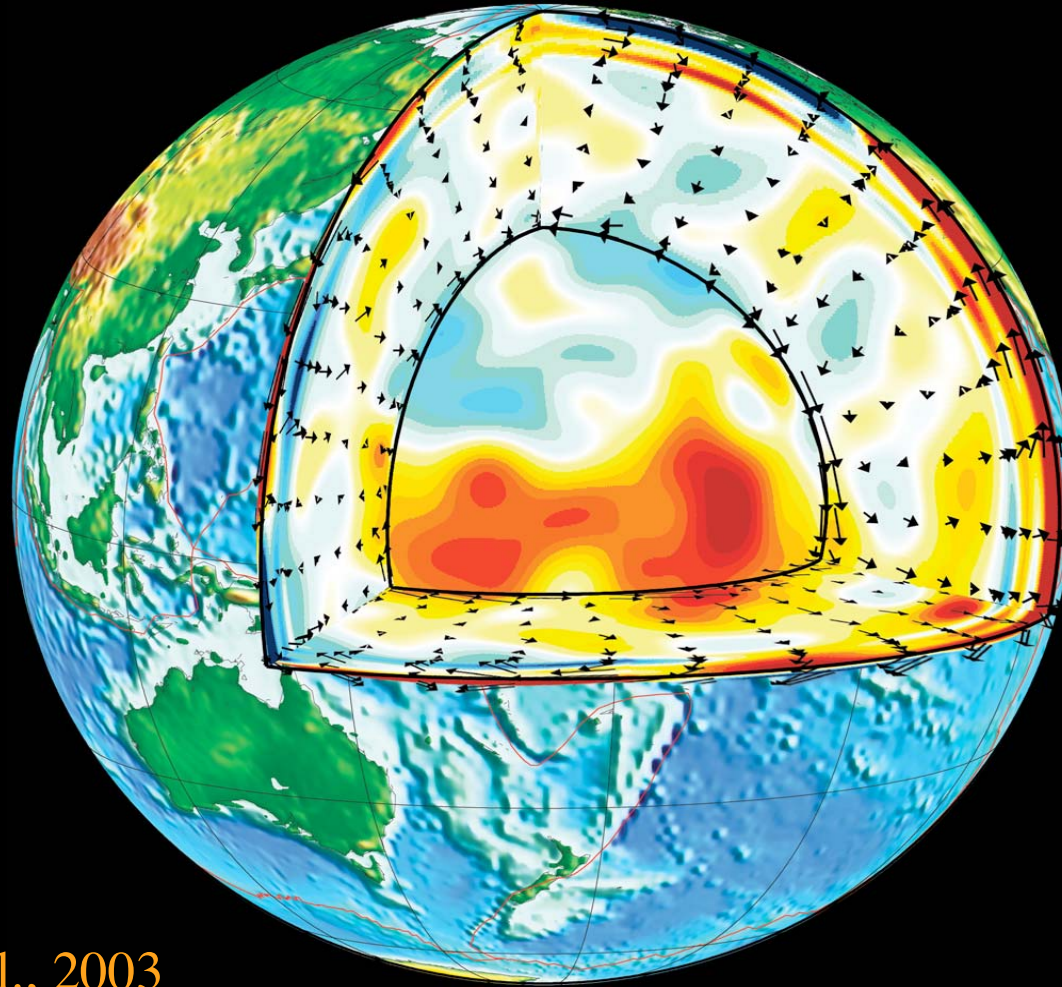
- Application to real seismograms with a real earthquake with a distribution of present seismic stations
- Detection of unknown seismic sources (quiet earthquakes, origin of “seismic hum”)
- Detection of mantle plume



Peru Earthquake (2002)



Anisotropy- Geodynamics Relationship

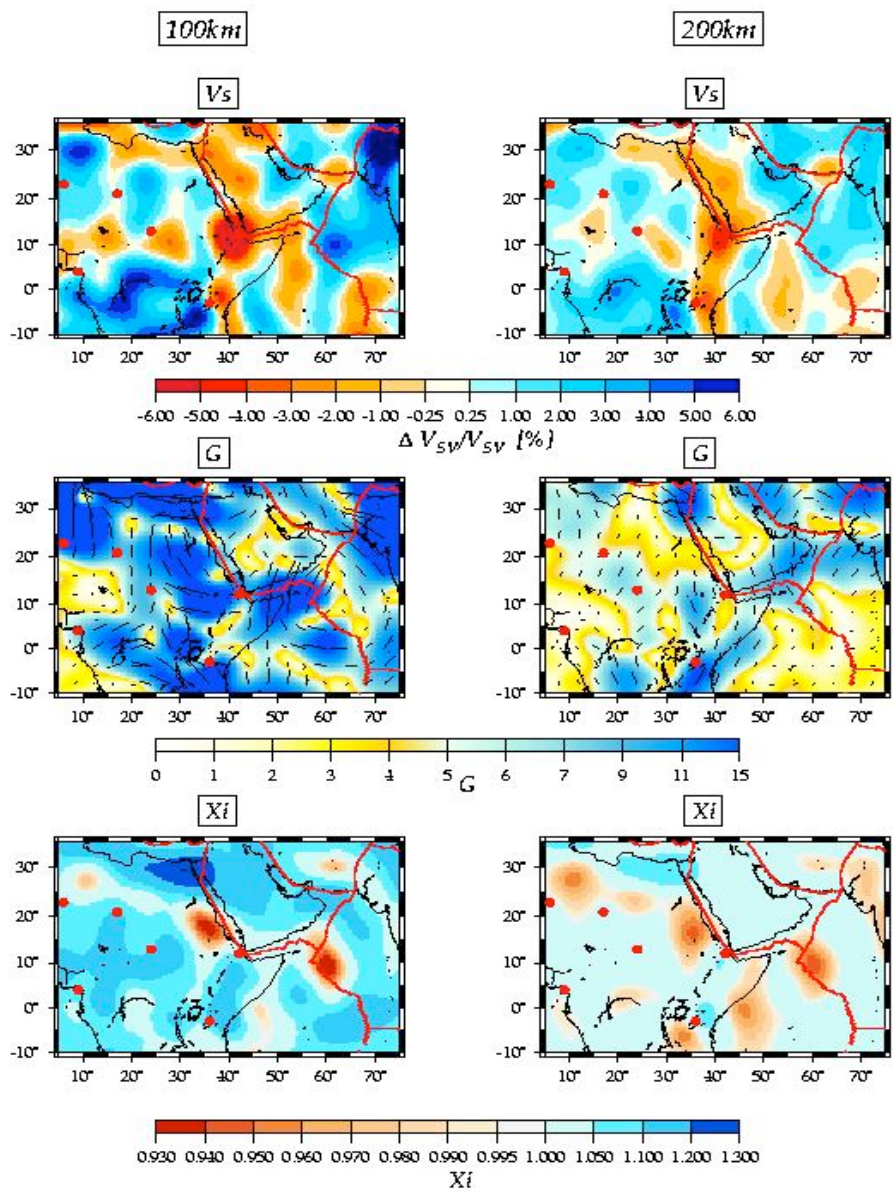


Gaboret et al., 2003



CONCLUSIONS

- Progress in instrumentation (Ocean bottom, Planet Mars; Spatial exploration)
- Ray Theory - Normal Modes -> Numerical Methods more and more powerful and accurate de by using more and more powerful computers.
- From Global scale towards regional scale- Incorporation of new parameters (anisotropy, anelasticity) in tomography
- Systematic Multidisciplinary Approach: Confrontation of seismological results with numerical and laboratory experiments



S-wave velocity

Azimuthal
anisotropy

Radial
Anisotropy
 $D = 1 - (dV_{SH}/V_{SV})^2$